APPLICATIONS OF TRANSITION METAL DOPED ZEOLITES

By

JOHN PHILLIP HAGE

A DISSERTATION PRESENTED TO THE GRADUATE SCHOOL
OF THE UNIVERSITY OF FLORIDA IN PARTIAL FULFILLMENT
OF THE REQUIREMENTS FOR THE DEGREE OF
DOCTOR OF PHILOSOPHY

UNIVERSITY OF FLORIDA

1994

ACKNOWLEDGEMENTS

I would like to thank the many people who have helped me throughout my career here at the University of Florida. I would first like to thank Dr. Russell S. Drago for his encouragement, his guidance, and support throughout the years. I would also like to thank his wife, Ruth, for her kindness and hospitality these many years.

I would also like to thank the people who were my co-workers. Past group members Dr. Mike Naughton, Dr. Steven Petrosius and Dr. Douglas Patton were always there as good friends. Present group members Dr. Doug Burns (and Imogene Burns), Dr. David Singh, Dr. Phillip Kaufman, Mike McGilvray, Donald Ferris, Chris Chronister, Jon Stack, Ken Lo, Mike Gonzalez, Mike Robbins, and Andy Dadmun have been a valuable source of knowledge and advice throughout these years. I am proud to call them my friends.

I would like to acknowledge people within the department who helped make things easier. Charlie Cromwell, Glennis Bryant, and Jeanne Zachary helped ease a lot of bureaucratic red tape. Maureen Abdalla, Kim Maxwell, and Kalée Gregory were very supportive of my efforts and helped me to get through what were some very difficult moments.

Most importantly, I would like to acknowledge and thank my family. My mother and father, Roxann and Thomas Hage, never faltered in their support. They gave up and did without so much so that I could have and attain the best. They taught me by example that I could do anything with hard work, determination and confidence. Most of all they taught me to never give up trying.

I would like to acknowledge Air Products for three years of financial support for this research.

TABLE OF CONTENTS

LIST OF TABLES

LIST OF FIGURES

Abstract of Dissertation Presented to the Graduate School
of the University of Florida in Partial Fulfillment of the
Requirements for the Degree of Doctor of Philosophy

APPLICATIONS OF TRANSITION METAL DOPED ZEOLITES

By

John Phillip Hage

April, 1994

Chairperson: Russell S. Drago
Major Department: Chemistry

Zeolites provide an interesting medium for carrying out numerous chemical reactions. The focus of this work is the employment of transition metal doped zeolites for the reversible binding of oxygen and as catalysts in hydrocarbon oxidation.

A large number of cobalt complexes consisting of a variety of ligands are known that reversibly bind oxygen. The main drawback to using these materials in catalysis or oxygen enrichment from air is that, in solution, dimerization and irreversible oxidation of the complexes occur. By synthesizing these complexes within the pores of a zeolite, these undesirable properties are eliminated. In this work, stable anionic cobalt(II)-cyanide complexes that reversibly bind oxygen have been synthesized inside zeolite Y. Synthetic methods developed to produce the maximum amount of these cobalt(II)-cyanide complexes inside zeolite Y are presented.

Industrial oxidation of hydrocarbons to useful oxygenated compounds is commercially important and carried out on a large scale. Often these oxidations involve high temperatures and pressures and lack selectivity. In this study, the oxidation of hydrocarbons with transition metal and transition metal complexes in various zeolites is investigated using hydroperoxides (hydrogen peroxide and t-butyl hydroperoxide) or oxygen. These reactions are carried out at a relatively low temperatures between 50-75^{o}C and at pressures of between one and three atmospheres.

CHAPTER 1
INTRODUCTION TO ZEOLITES

The properties and uses of zeolites are being explored in many scientific disciplines, including inorganic chemistry, physical chemistry, surface chemistry, crystallography, catalysis and chemical engineering process technology. There are a vast number of applications for zeolites, including catalysis of hydrocarbon reactions, separation of air components and oxygen enrichment of air, removing carbon dioxide from natural gas, and removal of atmospheric pollutants such as sulfur dioxide.[1] In the petroleum refining industry, by the mid-1980s, there was a clear trend worldwide to shift away from primarily gasoline oriented catalysis in favor of high octane fluid cracking catalysis using zeolites.[2]

The word zeolite is derived from two Greek words: zein, meaning to boil; and lithos, meaning stone. Zeolite minerals were first discovered and named in 1756 by Baron A. F. Cronstedt, a Swedish mineralogist.[3] He noted that the aluminosilicate mineral stilbite appeared to "boil" when heated in a blowpipe flame. This early water loss is described as intumescence. Since then, nearly 40 naturally occurring zeolite minerals and about 100 synthetic zeolites with no known natural counterparts have been identified and reported in the literature.[4]

Some dates of significance[5] in the history of zeolite technology are given in Table 1-1. Eichorn demonstrated as early as 1858 that chabazite and natrolite

Table 1-1. Important Achievements in Zeolite Technology.

Year	Accomplishment
1756	First zeolite recorded (stilbite).
1852	Nature of ion exchange soils clarified.
1858	Action of salt solutions on silicates investigated.
1862	First synthesis of a named zeolite (levynite) claimed.
1870-88	Various qualitative ion exchange studies on zeolites.
1875	A sedimentary zeolite deposit is reported.
1898	Quantitative studies of water-zeolite equilibria.
1899	Ion exchange by vapor phase using NH_4Cl.
1902-5	Ion exchange using salt melts.
1910	Heavy vapor sorption studies (I_2, Br_2, S, Hg, HgS)
1932	"Molecular sieve" term introduced.
1941-4	Quantitative separation by molecular sieves demonstrated.
1946	First synthesis of a zeolite not found in nature.
1949	Hydrogen zeolites first made by heating NH_4-zeolite.
1956 onward	Zeolite A, X, Y and L discovered.
1961	First direct synthesis with only organic bases.
1962	Zeolite catalytic cracking introduced.
1967	Preparation of ultrastable Y reported.
1971 onward	Very siliceous zeolites introduced.

exhibited reversible ion exchange. The first claim to synthesis of a zeolite dates from 1862 when Deville reported the production of levyne (levynite) by heating a potassium silicate with sodium aluminate in a sealed glass tube. Weigel and Steinhoff described molecular sieve attributes of chabazite in 1925.

Many scientists attempted to prepare synthetic forms of zeolite crystals, attracted to the properties which have made zeolites of significant importance: ion exchange and ion sieve behavior; selectivity as sorbents and molecular sieves; and shape selective catalytic functions.[6] With the development of X-ray diffraction techniques in the early 1930s, a more positive identification of the complex structures found in zeolites became available.

In 1938, R. M. Barrer, a physical chemist, began his pioneering work with zeolites. He began by furnishing quantitative and theoretical descriptions of the ion exchange, dehydration and gas-sorptive behavior of natural zeolites.[7] Barrer also demonstrated that some zeolites could be synthesized in a form identical to their natural counterparts and that new zeolite phases, unknown in nature, could be synthesized under mild laboratory conditions.[8-10] At the time, many scientists attempted to mimic the conditions under which zeolites of volcanic origin were formed: high pressure, high temperature, and high salt concentration.

This way of thinking changed dramatically in 1949. Attracted to the application potential of zeolites (especially in the separation of gases), R. M. Milton and his co-workers at Union Carbide Corporation's Linde Division initiated a study of zeolite synthesis by low-temperature hydrothermal processes. By 1952, many

different species of synthetic zeolites had been prepared in the research laboratory at Linde.[11-12] Some were analogues of natural zeolite minerals, such as zeolite X and Y (analogues of faujasite) while others were not found in nature (such as zeolite A and L).

Zeolites as synthesized or found in nature are crystalline, hydrated aluminosilicates of Group I and II elements especially sodium, potassium, magnesium, calcium, strontium and barium. Structurally, zeolites are tectosilicates, meaning they have framework structures that are constructed from SiO_2 and AlO_2^- tetrahedra linked to each other by sharing all the oxygens. This creates infinite lattices comprised of identical building blocks (unit cells) in a manner common to all crystalline materials. The individual tetrahedra are always close to regular, but because the shared oxygen linkage can accommodate T-O-T angles [T, tetrahedral species (silicon or aluminum)] from 130-180^0, they can be combined into a variety of framework structures.[13]

Extensive research has been performed on zeolites, trying to explain their properties in the areas of ion exchange, molecular sieve properties, and catalysis. Interpretation of their properties relies heavily on a precise description of structural features, such as framework composition, pore size, cation location, site occupancy and location of water molecules.[6] The structural formula of a zeolite is best described for the crystallographic unit cell as

$$M_{x/n}[(AlO_2)_n(SiO_2)_y]\cdot wH_2O$$

where M represents the cation of valence n, w is the number of water molecules and the ratio of x/y varies between 1 and 5 depending on the structure. The sum (x+y) is the total number of tetrahedra in the unit cell.

The portion of the formula within the brackets gives the composition of the framework. The AlO_2^- tetrahedra in the structure determine the framework's overall negative charge. This charge is balanced by cations that occupy non-framework positions. The crystalline framework contains channels and interconnected voids of discrete size occupied by these charge balancing cations and water molecules. The cations are quite mobile and may usually be exchanged, to varying degrees, by other cations. The extent and location of water molecules depend upon a) the overall size and shape of the zeolite cavities and channels present, and b) the number and nature of the cations in the structure.[7]

The need to comprehend the large number of complex zeolite structures and to try and compare structural properties has led to a number of classification systems. One way to classify zeolites is by pore size. In this system, grouping depends on the number of tetrahedral atoms (Si or Al) that define the pore opening. There are only three pore openings known to date in the aluminosilicate structures.[14] They are referred to as 8, 10, and 12-member ring openings. Zeolites containing these pore openings are also referred to as small (8-member ring), medium (10-member ring), and large (12-member ring) pore zeolites.

A representative list of zeolites whose pore structures are known[5] is given in Table 1-2. Chabazite, zeolite rho and A have 8-member ring windows to the

Table 1-2. Zeolite Pore Structures and Dimensionalities.

Zeolite	Window	Dimensions (Å)	Channel System
(Small pore)			
Levynite	8-ring	3.3 x 5.3	2-D
Chabazite	8-ring	3.6 x 3.7	3-D
Erionite	8-ring	3.6 x 5.2	3-D
ZK-5	8-ring	3.9	3-D
Paulingite	Double 8-ring	3.9	3-D
Rho	8-ring	3.9 x 5.1	3-D
Laumontite	10-ring	4.0 x 5.6	1-D
A	8-ring	4.2	3-D
(Medium pore)			
Dachiardite	10-ring 8-ring	3.7 x 6.7 3.4 x 4.8	2-D
Ferrierite	10-ring 8-ring	4.3 x 5.5 3.4 x 4.8	2-D
ZSM-5	10-ring	5.1 x 5.6	3-D
ZSM-11	10-ring	5.1 x 5.5	3-D
(Large pore)			
ZSM-12	12-ring	5.7 x 6.1	1-D
Cancrinite	12-ring	6.2	1-D
Mordenite	12-ring 8-ring	6.7 x 7.0 2.9 x 5.7	2-D
L	12-ring	7.1	1-D
Mazzite	12-ring	7.4	1-D
Faujasite	12-ring	7.4	3-D

micropore volume. The pentasil zeolites ZSM-5 and ZSM-11 have 10-member ring windows and are considered medium pore zeolites. Mordenite, faujasite, and zeolite L are classified as large pore zeolites with 12-member ring windows.

Typically, pore size is obtained by selecting the proper molecular probes and examining the zeolite's ability to adsorb them. Molecular probes commonly applied to pore size determination include n-hexane, 2-methylpentane, cyclohexane, o-xylene, and mesitylene.[14] Linear alkanes adsorb into 8, 10, and 12-member ring openings of a zeolite channel system. 2-Methylpentane, cyclohexane, and o-xylene, larger in size at 6.5- 7.4 Å, will be too large to enter an 8-member ring channel system, but may enter a 10-member ring and readily enter a 12-member ring channel system. The large mesitylene molecule will be excluded from all but the large 12-member ring pores.

After considering the pore size of a zeolite, it is also important to consider a finer detail of the channel system- the number of dimensions encompassed by the pores. Laumonite (Table 1-2), a medium pore zeolite, contains a channel system consisting of non-intersecting, one dimensional channels. In mordenite, the channel system is two dimensional, with intersecting 12 and 8-member ring channels. Both ZSM-5 and ZSM-11 contain interconnecting, three dimensional, 10-member ring channel systems. The ZSM-5 zeolite contains a zigzag channel system intersecting a straight 10-member ring channel to produce the three dimensional pore system. ZSM-11 has two 10-member ring linear channels that intersect and form a three dimensional pore system.[14]

Another way to classify zeolite structures is to relate them by the symmetry of their unit cells. This, however, is extremely cumbersome. It is much easier to classify them if the observation is made that zeolite structures are often made up of identical (or very similar) repeating sub-units. These sub-units are less complex than the repeating unit cells. These recurring sub-units are known as secondary building units (or SBUS). There are nine such building units which can be used to describe all known zeolite structures.[15] The secondary building units (Figure 1-1) consist of 4, 6, and 8-member single rings, 4-4, 6-6, and 8-8-member double rings, as well as 4-1, 5-1, and 4-4-1 branched rings.

These representations (Figure 1-1), as well as most zeolite representations, are often presented for simplicity as a line drawing. In a line drawing, a tetrahedral atom (Si or Al) is located at each vertex. Oxygen atoms are located between the tetrahedral atoms, but not necessarily on the edges. Edges do not portray bonds, merely geometry. Also listed with each secondary building unit in Figure 1-1 are the symbols used to describe them.

ZSM-5, ZSM-11, and mordenite are composed (Table 1-3) of only the complex 5-1 building unit. Often, appropriately, ZSM-5 and ZSM-11 are referred to as pentasil zeolites. Stilbite is composed solely of the 4-4-1 secondary building unit, while cancrinite, erionite, offretite, and zeolite L are generated using only single 6-member rings (S6R). Often structures are generated using more than one secondary building unit. Faujasite and zeolite A are both examples of this.

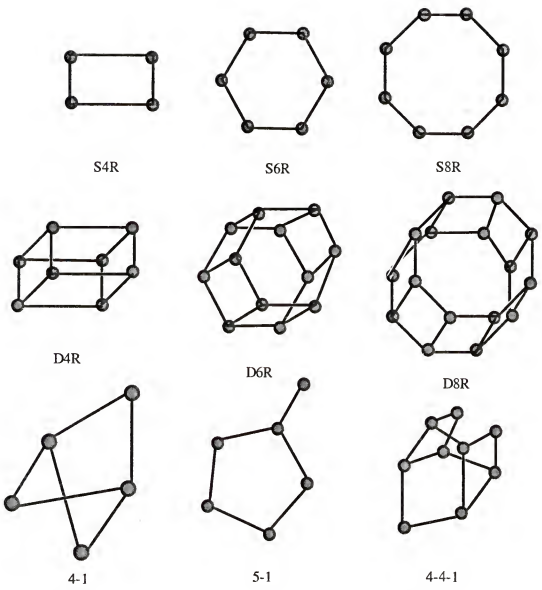

Figure 1-1. Zeolite Secondary Building Units.

Table 1-3. Zeolite Secondary Sub-Unit Composition.

	Secondary Building Units							
Zeolite	S4R	S6R	S8R	D4R	D6R	D8R	4-1	5-1
ZSM-5								X
ZSM-11								X
Laumontite		X						
Mordenite								X
Offretite		X						
Natrolite							X	
Cancrinite		X						
Zeolite L		X						
Mazzite	X							
Erionite		X						
Paulingite	X							
ZK-5	X	X	X		X			
Chabazite	X	X			X			
Rho	X	X	X			X		
Zeolite A	X	X	X	X				
Faujasite	X	X			X			

Although faujasite and zeolite A are not made up of identical secondary building units, they do have very similar polyhedral cavities. Faujasite and zeolite A both have frameworks consisting of a single geometric unit. By taking six single-4-ring units and eight single-6-ring units, a polyhedron is formed which has 36 edges and 24 vertices. This unit is referred to as a cubo-octahedron, a Type I-26-hedron or a sodalite unit (Figure 1-2(b) and 1-2(c)).

The difference between zeolite A and faujasite is how the sodalite units are connected to one another. In zeolite A, the sodalite units are linked via the single-4-ring(S4R) faces to propagate cubic symmetry. In the faujasite zeolite framework, shared by the synthetic zeolites X and Y, sodalite units are linked through the hexagonal (S6R) faces (Figure 1-2(d)). In either case, the linking of the sodalite units often referred to as β cages, creates another type of polyhedron cavity. It is referred to as a Type II-26 hedron, a supercage, or as an α cage.

Both zeolite X and Y have a unit cell which contains 192 $(Si,Al)O_4$ tetrahedra. The only difference between zeolite X and Y is the ratio of silicon to aluminum present in the framework. Zeolite X has a Si/Al ratio of nearly 1, while zeolite Y has a Si/Al ratio between 2 and 3. Much of the work described in this dissertation involves the use of zeolite Y. It was chosen because of its large pore openings, large cavities and three-dimensional pore structure. Y was chosen over X because of the smaller charge density on the framework. The metal cations are therefore more mobile and available to coordinate with ligands other than the oxygen ions of the framework.[16]

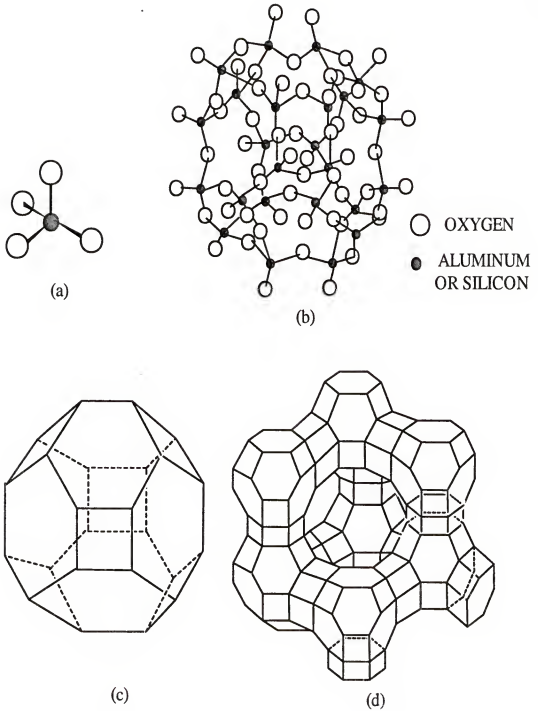

Figure 1-2. Structural Representation of Zeolites (a) Silicon or Aluminum Tetrahedral Units; (b) Ball and Stick Representation of Sodalite Unit; (c) Line Drawing of Sodalite Unit; (d) Line Drawing of Faujasite.

Zeolite Y, with a Si/Al ratio of 2.4, has a molecular formula of $Na_{56}[(AlO_2)_{56}(SiO_2)_{136}]$. Due to the polar nature of the covalent bonds between silicon or aluminum and oxygen, as well as the overall negative charge of the framework, zeolites are very hydrophilic. Typically, the unit cell of zeolite Y contains 264 water molecules.[6]

As stated previously, by having aluminum atoms in place of silicon, the zeolite framework has an overall negative charge. This negative charge is balanced by the presence of cations located in non-framework positions. These cations can be located in many different sites (Figure 1-3). The smallest of these sites (Site I) are located in the hexagonal prisms (the double-6-rings). The opening to the site is 2.2 Å with an internal free diameter of 2.4 Å. This site is only accessible to non-solvated cations. There are 16 of these Site I positions available per unit cell in zeolite Y.

The sodalite cage or β cage is next in size. It has a pore opening of 2.2 Å with an internal free diameter of 6.6 Å. With such a small pore opening, only small ligands such as water or ammonia can enter. Three cation sites (Figure 1-3) are present in the sodalite cages. Site I' is located near the hexagonal prism entrance in the β cage, Site II' is in the β cage near the single-6-ring leading to the supercage. Site U is located at the center of the sodalite cage. In the unit cell, there are 32 Site I', 32 Site II', and 8 Site U cation positions available.

The large cavities, formed when the sodalite units are joined together, have four dodecahedral openings which are 7.4 Å in diameter, while the free diameter of the α-cage is 13 Å. This allows for entrance of large ligands and formation of

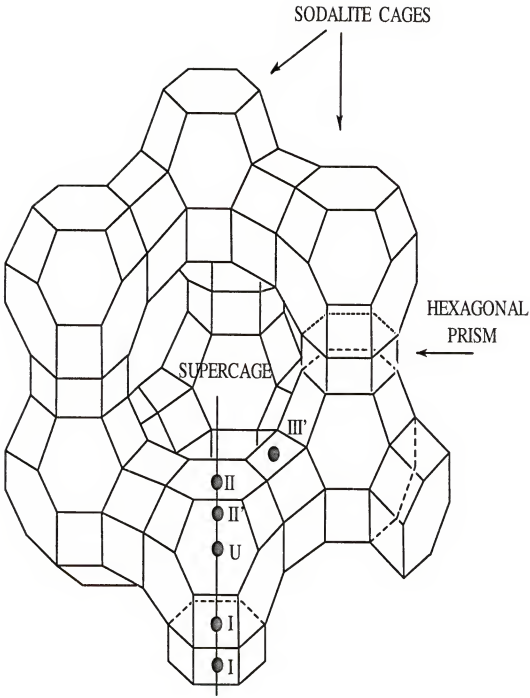

Figure 1-3. Cation Sites Available in Zeolite Y.

complexes which are of substantial size. Within the α cages, there are four types of cation sites available. Site II approaches the single-6-ring outside the β cage and lies within the α cage opposite Site II'. Site III and Site III' lie within the twelve-member aperture to the α cage: Site III above the hexagonal prism, Site III' above a square face of a sodalite unit. Within the α cage lies Site IV. There are 32 Site II', 48 Site III, 32 Site III' and 8 Site IV cation positions available per unit cell in zeolite Y.

These cations are only electrostatically bound to the framework and can migrate within the structure. Their distribution among the sites depends on several factors,[6] which include a) size of the cation, b) extent of hydration of the zeolite, c) the presence of molecules or ions that can serve as ligands, and d) the nature of other cations present. Lunsford has proposed[16] that a cation which might be in an inaccessible site (e.g. Site I) at one moment would be available for coordination with a ligand in the α cage at a later time, provided the energetics for coordination are favorable.

For example, rubidium and cesium are unable to enter Site I positions in the hydrated zeolite Y at room temperature due to the 2.2 Å pore openings. In fact, for rubidium and cesium, Site III is preferred.[17] Only when zeolite Y exchanged with cesium or rubidium is dehydrated above 400°C do Cs^+ and Rb^+ begin to occupy Site I.[18] Multivalent cations, such as Ba^{2+}, Mg^{2+} and Ca^{2+}, prefer Site I due to the strong solvation provided by the lattice oxygens in this site.

As stated earlier, there have been a vast number of applications for zeolites. The work presented in this dissertation is concerned with two applications of zeolites.

The first application deals with the preparation of a new adsorbent which can separate oxygen from nitrogen. The goal is to maximize the formation of a transition metal complex inside zeolite Y that reversibly binds oxygen. The second application deals with transition metals and transition metal complexes inside zeolites. The goal here is to use these as heterogeneous catalysts for alkane oxidations.

CHAPTER 2
REVERSIBLE OXYGEN BINDER INSIDE ZEOLITE Y

Background

Introduction

Oxygen is the most abundant element on the earth, occurring both as the free element and combined in countless compounds. It comprises 23% of the atmosphere by weight, 46% of the lithosphere (450000 ppm in crustal rocks), and greater than 85% of the hydrosphere (85.8 of the oceans, 88.1% of pure water).[19] Most of the oxygen is produced in the biosphere, due to photosynthesis of land and sea plants. Oxygen removed from the air by combustion and respiration processes is restored by photosynthesis in which carbon dioxide and water (Equation 2-1) with light, react

$$CO_2 + H_2O + h\nu \xrightarrow{\text{chlorophyll}} O_2 + [CH_2O] \qquad (2\text{-}1)$$

in the presence of chlorophyll to form nutrients and liberate oxygen.

Oxygen is currently the third largest volume chemical produced in the United States. It is currently ranked after only sulfuric acid and nitrogen and ahead of ethylene, ammonia, and lime.[20] Since 1987, it has held this ranking with oxygen production that year of 32.28 billion pounds.[21] Current figures report that 42.38 billion pounds of oxygen was produced in this country in 1992.[20]

Uses of Oxygen

The large scale production of oxygen is necessary to provide for the demands from the numerous industrial applications of oxygen. One of the main uses of oxygen is for metal and steel manufacturing (Table 2-1). Oxygen is added to enrich the combustion air in melting furnaces. This results in more efficient use of fuel, higher temperatures, longer furnace life and greater productivity.[22] By using high-purity oxygen (>99%) for the conversion of hot metal into steel, nitrogen occurrence in the resulting steel is avoided, an inconvenience resulting from the use of air.[23] Related smaller-scale applications include steel cutting, oxyhydrogen and oxyacetylene welding, as well as oxygen lancing.

Another large single user of oxygen is coal gasification. Technologies have developed to convert coal into electric power, fuel, and natural gas. When coal is gasified using oxygen and steam, the resulting gas mixture consists mainly of hydrogen and carbon monoxide (synthesis gas).[24] The Lurgi process,[25] for example, utilizes lumpy coal or briquets degassed at 20-30 bar and 600-700^{o}C fed downward against an upward stream of oxygen. Using the Winkler process,[25] fine grain coal, steam, and oxygen at atmospheric pressure in the temperature range of 800-1100^{o}C yields a product with a H_2:CO ratio of 1:4:1. The hydrogen from these processes can be used to turn coal into liquid hydrocarbon fuels. Ultimately, water, coal, and oxygen form the starting point for automotive fuels.

Table 2-1. Uses of Oxygen.

Description	Proportion (%)
Primary metals and steel manufacturing	55
Chemical manufacturing	20
Partial oxidation processes	10
Metal fabrication	5
Others: pollution control, medicine, wielding, glass manufacture	10

Chemical manufacture is another large scale consumer of oxygen. Oxygen used in these processes comes from two sources- air and pure oxygen. The chemical processes which utilize oxygen are numerous and beyond the scope to be adequately covered here. However, there are a few large scale processes that utilize pure oxygen which are worth noting here.

The reaction of ethylene and oxygen leads to numerous industrial products. The first of these is ethylene oxide. Ethylene oxide (Equation 2-2) is mainly produced by the direct, vapor phase oxidation of ethylene over a silver catalyst at

$$CH_2{=}CH_2 + 1/2O_2 \xrightarrow{Ag} H_2C(O)CH_2 \qquad (2\text{-}2)$$

10- 30 atmospheres of pressure and 200-300^{o}C.[26] Most ethylene oxide is converted into other products. Products derived from ethylene oxide have many different uses. Some of these include monoethylene glycol[27] (antifreeze), diethylene glycol and triethylene glycol (plasticizers), poly(ethylene glycols)[28] (cosmetics and solvents), ethylene glycol ethers (brake fluids), and ethanolamine (soap and detergents).[29]

Another major industrial process involves ethylene and oxygen at 130^{o}C and 3 atmospheres of pressure is the Wacker process for production of acetaldehyde.[30] Direct oxidation of ethylene to acetaldehyde, represented by the overall Equation 2-3,

$$C_2H_4 + PdCl_2 + H_2O \longrightarrow CH_3CHO + Pd + 2HCl \qquad (2\text{-}3)$$

is based on the oxidation of ethylene by palladium chloride in the presence of water (Equation 2-6). Palladium chloride is reduced to the metallic state and is reoxidized

$$Pd + 2CuCl_2 \longrightarrow PdCl_2 + 2CuCl \qquad (2\text{-}4)$$

$$2CuCl + 2HCl + 1/2O_2 \longrightarrow 2CuCl_2 + H_2O \qquad (2\text{-}5)$$

$$C_2H_4 + 1/2O_2 \xrightarrow{PdCl_2,\ CuCl_2,\ H_2O} CH_3CHO \qquad (2\text{-}6)$$

chloride is reduced to the metallic state and is reoxidized to the active oxidation state (Equation 2-4). Cuprous chloride is then oxidized by oxygen (Equation 2-5). the reaction is carried out in aqueous solution employing a catalyst solution of copper chloride containing small quantities of palladium chloride. By using oxygen, the process is conducted at lower pressures and a single step, as opposed to a two step process when air is used to regenerate the catalyst.[29] Acetaldehyde and oxygen also serve as the feedstock for the production of acetic acid. Acetaldehyde is oxidized into acetic acid by oxygen in the presence of a manganese acetate catalyst.[31]

A final industrial process involving ethylene and oxygen is the production of vinyl chloride. The conventional route to vinyl chloride monomer (VCM) is the balanced oxychlorination process in which ethylene and chlorine are converted to vinyl chloride monomer.[32] In one step, chlorine is combined with ethylene in the liquid phase (Equation 2-7) to form ethylene dichloride (EDC). The heart of the

$$2C_2H_4 \longrightarrow 2C_2H_3Cl + 2HCl \quad (VCM) \qquad (2\text{-}7)$$

$$C_2H_4 + 2HCl + 1/2O_2 \longrightarrow C_2H_4Cl_2 + H_2O \qquad (2\text{-}8)$$

$$C_2H_4 + 2HCl + 1/2O_2 \longrightarrow C_2H_4Cl_2 + H_2O \qquad (2\text{-}9)$$

process is the oxychlorination step (Equation 2-9) in which hydrogen chloride, the by-

product from the EDC dehydrochlorination reaction is reacted with ethylene and oxygen to produce EDC and water. Resultant EDC is recycled to the dehydrochlorination step and converted to vinyl chloride.[31,32] By using oxygen in this process relative to air, increased ethylene selectivities and Hcl conversions are attained, while atmospheric emissions are significantly reduced.[33]

Another industrial chemical process which utilizes oxygen is the production of acrylonitrile. Acrylonitrile is very useful because of its two reactive groups, the olefinic bond and the nitrile group. It is used for the production of acrylic fibers (most notably nylon 66), nitrile rubber and plastics.[34] Acrylonitrile is produced using the Sohio process[31,35](Equation 2-10), which involves ammoxidation of propene typically below 500°C and 3 atmospheres pressure. This ammoxidation process is more commercially attractive than the synthesis of acrylonitrile from acetylene and HCN,[36] because of the cheaper costs of NH_3 relative to HCN and the recoverable by-product quantities from Equation 2-10. By-products from the Sohio process

$$H_2C{=}CHCH_3 + NH_3 + 3/2O_2 \xrightarrow[425^oC]{Bi_2Mo_3O_3} H_2C{=}CHCN \qquad (2\text{-}10)$$

include acetonitrile and HCN.[37]

One final industrial chemical process which utilizes oxygen is the production of phenol and acetone from the formation and decomposition of cumene hydroperoxide (Equation 2-11). This involves rearrangement of cumene hydroperoxide where a phenyl group migrates from carbon to an electron- deficient oxygen atom. The hydroperoxide (Equation 2-11) is made by the reaction of oxygen

$$C_6H_5CH(CH_3)_2 + O_2 \xrightarrow[(2)\,H_2SO_4,\,70\text{-}80^{o}]{(1)\,110\text{-}115^{o}C} C_6H_5OH + (CH_3)_2C{=}O \quad (2\text{-}11)$$

with cumene at 110-115°C until 20-25% of the hydroperoxide is formed.[25,38] Concentration of the hydroperoxide to 80% is followed by acid catalyzed rearrangement at 70-80°C. A side product of this reaction, α-methylstyrene, can be hydrogenated back to cumene, and reused.[39]

Two smaller scale applications of oxygen are finding increased use due to growing environmental awareness. The first of these is the use of oxygen in wastewater treatment. One such treatment, UNOX[40] (developed by Union Carbide) uses a covered, multistage oxygenation and reaction system, operated at atmospheric pressure. Wastewater and sludge are contacted in a series of gas-liquid mixing stages. One main advantage of these types of oxygen aeration systems is that as increased demand is placed on a system (through larger populations), the system can handle the increased workload. Furthermore, the waste gas quantity from these systems is 1% of that produced in conventional air-aerated systems (lower specific odor problems).[40] Currently in the state of Florida, there are wastewater treatment plants utilizing oxygen in Miami, Hollywood, and Jacksonville.[41]

A second smaller application of oxygen with environmental benefits is in the bleaching of wood pulp. Pulp and paper firms are having to change their processes to reduce or eliminate chlorinated organics as fears of carcinogenic chemicals and environmental pollution spread. Topping these concerns is dioxin- 2,3,7,8-tetrachlorodibenzo-p-dioxin and other adsorbable organic halides, carried into the

environment by wastewater from paper mills. Before bleaching, pulp-washing and cooking methods can remove lignin which holds wood together. The amount of leftover lignin, which turns brown during the pulp-making process, determines the amount of bleach needed to whiten the pulp.[42]

The technology has existed since 1974 to delignify and bleach cellulose pulp with oxygen.[43] International Paper[44] debuted its Ticonderoga, New York mill in 1975. This plant made use of alkali and oxygen to delignify and bleach pulp. In 1991, Sweden installed an oxygen delignification plant in Columbus, Mississippi. Chlorine dioxide is another oxidant replacing chlorine. However, oxygen is replacing even ClO_2 due to lower cost and the potential for less environmentally hazardous organochlorine effluents.[45]

Production of Oxygen and Oxygen-Rich Air

The previous examples all show how important oxygen production is to various industries. The search for ways to improve the separation of oxygen from air is worthy of further study. Pure oxygen and oxygen-rich streams from air are produced mainly using three methods: membrane separation, cryogenic fractional distillation, and pressure swing adsorption (PSA). Cryogenic separation yields extremely pure gases: 99.9999+%-pure nitrogen and 99.5-99.9%-pure oxygen. In contrast, PSA and membrane separation methods produce gases that are 95-99.9% pure. As of 1991, of the 57.3 billion pounds of nitrogen and 39 billion pounds of oxygen produced, only 2-5% of this came from PSA and membrane separation.[46]

Gas separation by membranes is based on the principal that some gases permeate more rapidly than others due to differences in their mobilities or solubilities in a membrane material. To be useful for industrial gas separations, a membrane must have a reasonable separation efficiency (selectivity or separation factor) and a high flow rate through the membrane of the more permeable gas.[47] Membrane systems are compact, lightweight and have few moving parts. They are ideal for remote locations use where their onsite generation capabilities, reliability and ease of maintenance are useful.

Oxygen concentration via membranes is still in its beginning stages with most units on the market used for making enriched air with oxygen levels of 35-40%.[48] The difficulty encountered with separating oxygen from air is that oxygen diffuses through the membrane at a rate inversely proportional to its partial pressure. Even with a highly selective membrane, the diffusion rate of oxygen approaches that of nitrogen as the concentration and partial pressure of oxygen approaches zero. Currently, membrane technology is being used more for nitrogen recoveries from air instead of oxygen. Membranes can currently produce nitrogen in the 95-99.9%-pure range.[46]

Cryogenic distillation has been the workhorse of the air separation industry for many years now. Cryogenic separation can yield extremely pure gases- 99.999+%-pure nitrogen and 99.9%-pure oxygen. During this process, air is compressed and chilled to a liquid. Because each of the member gases vaporizes at a different boiling point, the air is fractionally distilled.

Cryogenic separation is performed using a number of different methods, one of which is the contemporary double column system which is employed by Linde.[49-51] Using this method (Figure 2-1), the air is compressed to about 6 atmospheres after which the water vapor and carbon dioxide are removed. The air then passes through a precooling heat exchanger. The partially liquified compressed air is admitted to the lower column, which is operated at 5-6 atmospheres, while the upper column is operated at a pressure of approximately 1 atmosphere. At 5 atmospheres, the boiling point of pure nitrogen (94.2 K) is higher than the boiling point of pure oxygen at 1 atmosphere (90.2 K). Therefore, the refrigeration required by the nitrogen at the top of the lower column is supplied by boiling oxygen in the boiler of the upper column, also furnishing the upgoing vapor for the upper column.[50] The oxygen-rich stream from the bottom of the lower column serves as a feed to the upper column, while cooled gaseous air from an expansion turbine provides the other.

In the past two decades, there has been a tremendous growth of gas adsorption processes that have made adsorption systems a key separation tool in chemical and petrochemical industries.[52] This growth is a result of the introduction of many new adsorbents, new separation strategies and new applications. Pressure swing adsorption now finds widespread use in bulk separation of industrial gases. Pressure swing technology has various industrial applications. These include air drying,[53] purification of hydrogen rich mixtures,[54] efficient separation of paraffins (normal and iso),[55] and oxygen or nitrogen production from air.

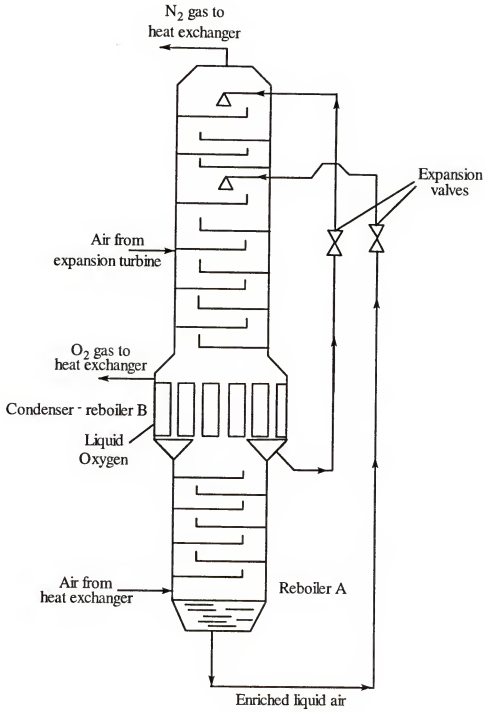

Figure 2-1. Contemporary Double Column Gas-Separation System.[50]

In applications with oxygen where a high purity is not required and daily requirement is not large, PSA processes have been shown to be more economical than cryogenic processes. PSA-based oxygen systems are competitive with cryogenic processes at oxygen purity levels of 80-95% and oxygen capacities approximately below 40 metric tons per day.[52] This is especially true in the low capacity ranges where PSA units allow for on site production of gases as a replacement for bottles or liquefied gases. Advantages which pressure swing adsorption processes have over cryogenic processes include (1) easy, trouble free separation; (2) quick startup; and (3) flexibility in production capacity as oxygen purity.[56]

Pressure swing adsorption processes separate gases in a mixture or purify a gas mixture by removal of gaseous impurities. A feed gas is passed through a solid adsorbent contained with a vessel with one or more components of the mixture being preferentially adsorbed. Unadsorbed gases flow through the adsorbent vessel. At some point, the adsorbent bed becomes saturated with one or more of the adsorbed gases. The adsorbent bed must then be regenerated, either by evacuation, controlled pressure release, or by passing a gas which is not adsorbed through the bed so that adsorbed gases are desorbed.[57] If the regenerating desorption pressure is substantially different from the operating adsorption pressure, this is known as a PSA process. More often, PSA processes use three beds or more in parallel. The advantages include (1) energy savings, which accrue from using gas from a high pressure bed to partially repressurize a low bed following desorption, and (2) higher

product recoveries which occur from using a combination of purging steps in the cycle.[58]

The original idea of using pressure swing to separate air was disclosed in a patent by Skarstrom from Esso Research and Engineering in 1958.[59] The Skarstrom process,[9,40,59] which employs two adsorbent beds is shown in Figure 2-2. A compressed feed gas is introduced to the first bed while the product gas is withdrawn at the same time from the other end of the bed. After the adsorption step, the first bed is reduced to atmospheric pressure. Simultaneously, the compressed feed mixture is switched to the second bed to repressurize and start its adsorption step. Following the depressurization, part of the product gas from the second bed is passed through the first bed, opposite to the feed direction in order to purge the bed at atmospheric pressure.

After the purge, the system is ready for another cycle. The second bed is a half-cycle off phase from the first bed to ensure a steady and continuous flow of both feed and product gas systems. Skarstrom's cycle has been used mainly for air drying. For oxygen production from air, however, the oxygen recovery is too low and hence the energy requirement too high to be economical.[52] To a limited extent, it was used to produce a low concentration of O_2 (30-40%) for medical applications.[40]

One important element of any PSA air separation process is the adsorbent used for the nitrogen-oxygen separation. All commercial processes use either zeolites or carbon molecular sieve adsorbents. Zeolites are polar and selectively adsorb nitrogen from air because it has a larger permanent quadrupole (1.52×10^{-26} esu•cm^2)

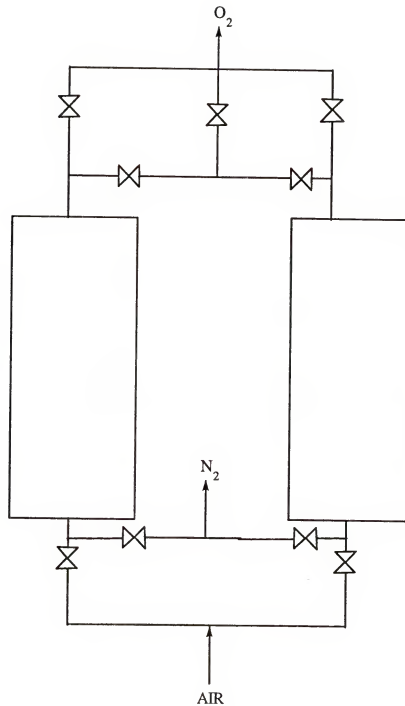

Figure 2-2. Skarstrom Process.[58]

than that for oxygen ($0.30x10^{-26}$) or argon ($0.0x10^{-26}$).[60] The capacity, selectivity and heats of heats of adsorption of nitrogen, oxygen, and argon vary significantly depending on the zeolite structure and the cations present within them.

Zeolite types A, X, and mordenite ion exchanged with metals of Group I and II are typically used for air separation.[57] The selectivity of N_2/O_2 on these zeolites is between 2 and 3 in the pressure range of practical application (1-3 atmospheres), and declines to less than 2 as the pressure is increased to 8 atmospheres.[40] Because the selectivity of O_2 and argon on zeolites is nearly identical, argon is also obtained as a product. The limiting purity for O_2 production is approximately 96% because air contains approximately 1% argon.

Carbon molecular sieves (CMS) for air separation, on the other hand, are made by further narrowing the pore mouths of a small pore activated carbon by depositing coke produced by thermally cracking hydrocarbons.[61] This molecular sieve was invented at Bergbau-Forshchung GmbH (Essen, West Germany) in the late 1970's. In contrast with zeolites, the selectivity in this system depends on the faster diffusion of oxygen within the micropores of the carbon sieve. The CMS allows faster diffusion of relatively smaller O_2 molecules (3.46 Å) into its pore structure than N_2 (3.64 Å).[62,63] Air contact time on the CMS becomes an important variable because there is no thermodynamic selectivity for O_2 over N_2 The kinetic O_2 capacity of the CMS increases with increased contact time, but its kinetic selectivity decreases.[61]

Two commercial PSA processes for air separation are worth noting here. The first process is patented by Union Carbide[64] and uses zeolitic adsorbents. The

schematic for the Union Carbide PSA Process (see Figure 2-3) follows six steps in the cycle:[60]

(a). Pressurization of an adsorbent bed by compressed air fed through one end of the adsorber and with an oxygen-rich gas recovered from the other end.

(b). Further pressurization by compressed feed air alone.

(c). Depressurization of the adsorber in the direction of the feed flow and withdrawal of oxygen-rich gas through the product end. Part of the recovered gas is used to pressurize another adsorber undergoing Step (a) and the remainder is withdrawn as product.

(d). Further depressurization of the adsorber and withdrawal of oxygen-enriched gas through the product end. Part of this gas is used as the desorption gas (purge) for another adsorber undergoing Step (f) below while the remainder is withdrawn as product.

(e). Depressurization of the adsorber in the opposite direction of air feed flow (countercurrent). This effluent is part of the nitrogen-rich desorbed gas.

(f). Further desorption of the adsorbed nitrogen by flowing oxygen-rich gas through the bed in a countercurrent direction near atmospheric pressure. The purge gas comes from Step (d). The exit gas (nitrogen-rich) proceeds through the feed end of the adsorber.

(g). Repeat from Step (a).

Using a 5A zeolite and operating between one and three atmospheres, the process can produce a 90% O_2 product gas (dry and CO_2 free) with an oxygen recovery of 38.0%[64]

Another PSA-oxygen process has been patented by Air Products and Chemicals. This system,[65] which operates at a temperature of between 30-65° C, can produce a 90.3-92% O_2 product gas (dry and CO_2 free) with an oxygen recovery of 35.8-42.9%. The schematic for the Air Products PSA Process is shown in Figure 2-4

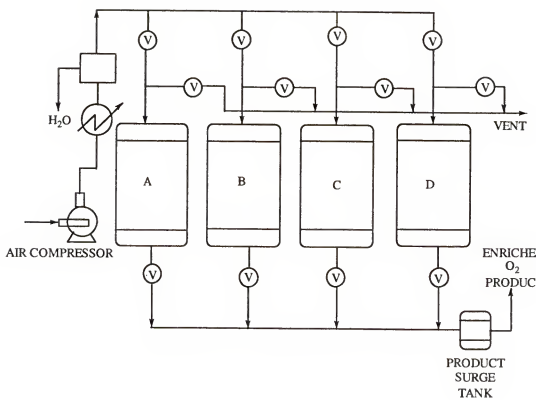

Figure 2-3. Union Carbide PSA-Oxygen Process.[60]

and consists of the following cyclic steps:[66]

(a). Feed air is passed through an adsorption column at highest pressure level (P_A) of the PSA cycle with removal of an oxygen-rich gas at the feed air pressure.

(b). When the oxygen concentration of the product stream starts to deviate from the preset concentration product gas composition, the adsorber is connected with an adsorber which has just concluded Step (f) below. After this step, both columns are at the same pressure, P_I, which is less than P_A.

(c). The adsorber is connected to another adsorber which has just concluded Step (e). Both adsorbers are pressure equalized to P_{II}, which is greater than P_I.

(d). The adsorber is reduced from P_{II} to atmospheric pressure in a concurrent flow direction.

(e). After Step (d), the adsorber is countercurrently purged at one atmosphere with part of the product gas from an adsorber undergoing Step (a).

(f). After purging, the adsorber is connected with another adsorber undergoing Step (c). The two adsorbers are pressure equalized to P_{II}.

(g). The adsorber is connected with another adsorber undergoing Step (b) and the pressure is raised to P_I.

(h). The adsorber is brought back to the pressure level (P_A) by concurrent introduction of oxygen-enriched product from another adsorber undergoing Step (a). A new cycle begins from Step (a).

Zeolite adsorbents in these pressure swing processes have inherent problems in the amount of optimum attainable oxygen from air because oxygen cannot be separated from contaminants such as argon. This results in a higher contaminant concentration in the oxygen product stream than in the inlet air. The advantage of an oxygen selective system is that oxygen is adsorbed while nitrogen and other contaminants are left in the gas stream. The contaminants pass through along with

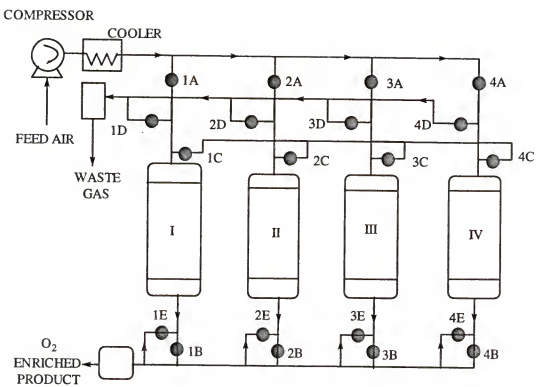

Figure 2-4. Air Products PSA-Oxygen Process.[65]

N_2, while a pure oxygen stream is recovered through desorption. Because such an adsorbent would adsorb oxygen (21% in air) instead of nitrogen (78% in air) bed size would be reduced. This would result in savings at a time when smaller, more portable systems are desired.

Oxygen selective systems have been sought after because of renewed interest in separating oxygen from air with a minimum expenditure of energy.[67] In nearly all these systems, the substances that reversibly bind oxygen decompose upon repeated oxygenation and deoxygenation cycling. Those systems with better stability are very moisture sensitive and easily deactivated by water. This work reports the preparation and characterization of a material that overcomes both of these drawbacks by entrapping a stable, moisture resistant cobalt(II)-cyanide complex that reversibly binds oxygen inside a zeolite cavity. This zeolite entrapped cobalt(II)-cyanide complex has a high affinity for O_2 and is stable to repeated cycling of oxygenation and deoxygenation. This work is also concerned with what the effect of these entrapped complexes have on the gas uptake characteristics of the zeolite material. Single component gas adsorption isotherms are measured here.

Transition Metal Complexes inside Zeolites

The synthesis and characterization of transition metal complexes inside zeolites have been the subject of much research.[68-71] Zeolites provide an interesting medium for carrying out coordination and transition metal chemistry,[72] functioning not only

as solid supports for complexes, but also as solvents or ligands. In many cases, they serve one or more of these functions simultaneously.

The three dimensional pore structure of zeolites offers the opportunity of preparing complexes that are unstable in solution. Using zeolites with the faujasite type structure, such as zeolite X and Y, has allowed the formation of complexes in the large α cages that would otherwise dimerize in solution. The formation of these "ship in the bottle" complexes[73] occurs because the α cages are larger than the connecting channels. Besides possessing the ability to physically entrap or isolate complexes, zeolites may also stabilize complexes through their unique solvating and ligating properties. This can result in the formation of complexes with unique coordination numbers[72] or oxidation states that cannot otherwise be prepared in solution.[74] In its ability to act as a ligand, a zeolite may also stabilize complexes through anchoring to the lattice through framework oxygens.[75-76]

This work is concerned with the preparation of a zeolite entrapped transition metal complex that reversibly binds oxygen. However, this is not a new idea because Lunsford and co-workers have been working in this area for some time.[75-77] The main focus of his research in this area deals with the investigation of oxygen adducts formed in cobalt(II)-exchanged X and Y zeolites with various ligands. His early work in this area dealt with the formation of cobalt(II) amine complexes. He was able to synthesize and characterize a series of cobalt amine oxygen adducts with the formula $CoL_5O_2^{2+}$ where L= NH_3, CH_3NH_2, and n-$CH_3CH_2CH_2NH_2$.[77]

EPR characterization of the 1:1 adducts yielded similar results to the analogous complexes in solution. Much like in solution, these zeolite entrapped complexes have a tendency to dimerize. When the ligand is NH_3 or CH_3NH_2, prolonged exposure to oxygen resulted in the formation of dimeric $[L_5CoO_2CoL_5]^{5+}$. However, when n-propylamine is used only the 1:1 oxygen adduct is observed. This was the first report of using a zeolite cavity in relationship to ligand size to sterically inhibit dimerization.

Another interesting zeolite entrapped complex which came out of early work of Howe and Lunsford was the square planar $Co(en)_2^{2+}$ (en= ethylenediamine) complex[75] seen in Figure 2-5. The proposed structure is similar to 1:1 cobalt oxygen adducts formed in solution where the in-plane ligand is a Schiff base[78] or porphyrin[79] and the sixth axial coordination site is occupied by a coordinating base such as pyridine. It is stable toward binding O_2 up to 70°C, with no evidence of dimer formation which occurs in solution.[80] The stability of the monomer was attributed not to the steric restraints of the cavity, which would allow formation of the dimer, but instead to immobilization of the complex through coordination to the zeolitic framework.

The most recent zeolite entrapped cobalt complex that reversibly binds oxygen reported by Vansant and Lunsford is $[Co(bpy)(terpy)]^{2+}$ (bpy= bipyridine; terpy= terpyridine).[81] The oxygen adduct was shown to be completely reversible at 25° C and thermally stable in the presence of O_2 up to 70° C. This

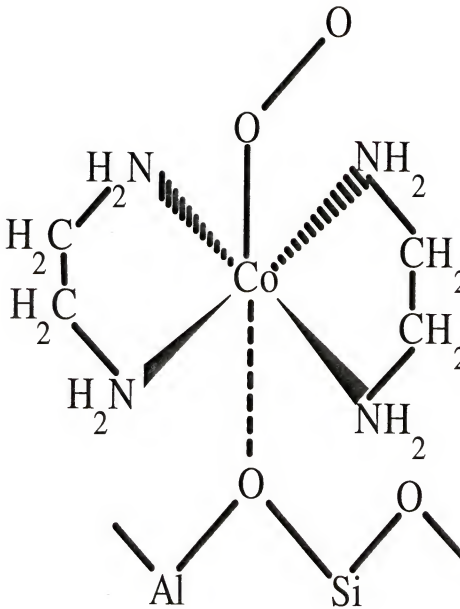

Figure 2-5. $Co(en)_2^{2+}$ in Zeolite Y.

complex was also found to be very effective for separating oxygen from air, with a mean separation factor (O_2/N_2) of 12.3.

This $[Co(bpy)(terpy)]^{2+}$-Y material did have a few disadvantages as a heterogeneous, reversible oxygen binder. Its synthesis was not trivial. CoY had to be exposed to bipyridine and terpyridine vapors simultaneously, leading to the formation of $Co(bpy)_3^{2+}$ and $Co(terpy)_2^{2+}$ as the major products, with $[Co(bpy)(terpy)]^{2+}$ being formed only in very low concentrations. Furthermore, the $[Co(bpy)(terpy)]^{2+}$-Y material was extremely sensitive to moisture. Water can occupy the sixth axial coordination site of the complex and prevent oxygen from binding. In the presence of water and oxygen, $[Co^{III}(bpy)(terpy)O_2^-]^{2+}$ is converted to a hydroperoxy radical, which then tends to oxidize the bipyridine and terpyridine ligands.[81] The effect is irreversible with complete deactivation of the complex towards further oxygen binding.

One of the most recent zeolite entrapped cobalt complexes that reversibly binds oxygen reported in the literature was CoSALEN (SALEN= 1,6-bis(hydroxyphenyl)-2,5-diaza-1,5-hexadiene). This complex became known as Herron's "ship in a bottle" complex.[82] It received this name because the complex is so rigid and so large that it is physically entrapped inside the zeolite supercages (see Figure 2-6). The complex, as its pyridine adduct, showed affinity for O_2 binding and formed monomeric adducts. Also, $[CoSALEN \cdot py]O_2$ showed excellent resistance to autoxidation of the ligand even at elevated temperatures. However, the O_2 binding

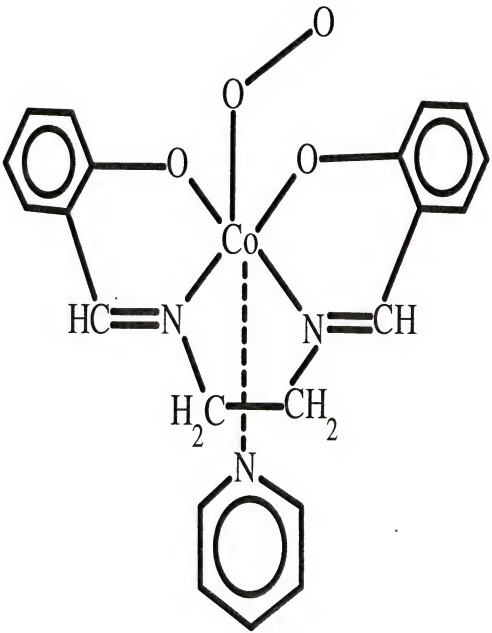

Figure 2-6. CoSALEN in Zeolite Y.

equilibria were found to be less favorable,[74] (K_{O_2} = 0.0033 $torr^{-1}$ at 293 K) especially when compared to Lunsford's earlier work.

These examples point out the importance of entrapping oxygen binding transition metal complexes inside zeolite Y. The major advantages of these complexes are the stability of the monomeric oxygen adducts as compared to their solution counterparts which tend to dimerize. However, as was seen in the example of $[Co(bpy)(terpy)]^{2+}$-Y, none of these complexes are stable under the conditions needed to be useful in practical applications. There is a need for a new ligand system not based on nitrogen donors (oxidatively stable) which is not as sensitive to moisture. This ligand system was found using cyanide ion.

Cobalt Cyanide Complexes

Cyanide is known to form low spin complexes with cobalt(II)[83] and is very stable towards oxidation. The chemistry of cobalt(II) cyanide complexes in solution is very well known,[84] as seen in Equations 2-12 through 2-15:

$$Co^{2+}_{(aq)} + 5CN^{-}_{(aq)} \longrightarrow Co(CN)^{3-}_{5\,(aq)} \qquad (2\text{-}12)$$

$$2Co(CN)^{3-}_{5\,(aq)} \longrightarrow Co_2(CN)^{6-}_{10\,(aq)} \qquad (2\text{-}13)$$

$$Co(CN)^{3-}_{5\,(aq)} + O_{2\,(g)} \longrightarrow Co(CN)_5O^{3-}_{2\,(aq)} \qquad (2\text{-}14)$$

$$Co(CN)^{3-}_{5(aq)} + Co(CN)_5O^{3-}_{2(aq)} \longrightarrow (CN)_5Co\text{-}O_2\text{-}Co(CN)^{6-}_{5\,(aq)} \qquad (2\text{-}15)$$

Pentacyanocobaltate(II) anion can be formed in solution (Equation 2-12), and is stable in low concentrations in the absence of oxygen. At higher concentrations,

dimerization (Equation 2-12) occurs. The purple potassium salt of the dimer, $K_6[Co_2(CN)_{10}]$, also known as Adamson's salt,[85] can be precipitated out of solution. In the presence of oxygen (Equations 2-14 and 2-15), a μ-peroxy dimer is formed irreversibly.[86] Whether the dimer or μ-peroxy dimer is formed, pentacyanocobaltate(II) is deactivated toward further oxygen binding.

Pentacyanocobaltate(II)[87] and its monomeric oxygen adduct[88] have been isolated from dimethylformamide solutions using bulky tetraalkylammonium counterions. It becomes evident that under the right conditions, dimerization can be prevented. Perhaps, dimerization could be inhibited by using a zeolite to entrap the transition metal complex.

In our laboratory, we reported the formation of an anionic cobalt(II) cyanide complex inside zeolite Y,[89-90] which represented the first case in which an anionic complex had ever been synthesized inside a zeolite cavity. All other complexes were either cationic or neutral. When Co(II)Y is reacted with a methanolic solution of sodium cyanide, the major species formed is $Co(CN)_6^{3-}$ which is characterized by an infrared stretching frequency[90] at 2129 cm^{-1}. The most interesting species formed in the reaction of CoY and cyanide is a low spin cobalt(II) complex capable of reversibly binding oxygen. However, it represented less than 1% of the total cobalt present. The EPR parameters[89] for this active complex (see Figure 2-7) suggested that this active species is the square planar tetracyanocobaltate(II), $Co(CN)_4^{2-}$ which may be five coordinate by anchoring to the lattice oxygen of the zeolite framework. This complex was stable to repeated recycling, and even in low concentration,

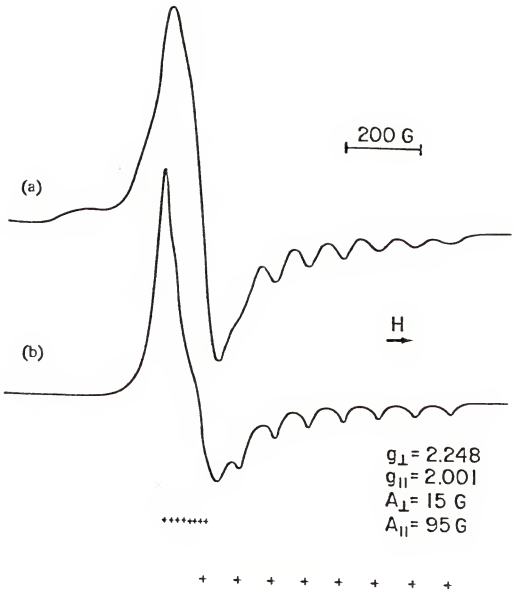

Figure 2-7. EPR Spectra of $Co(CN)_4^{2-}$ (a) Experimental; (b) Simulated.

increases the amount of oxygen adsorbed by NaY at 100 torr by 100%. In view of the unique stability of this entrapped cobalt(II) cyanide complex in reversible oxygen binding, attempts were made to increase the amount of $Co(CN)_4^{2-}$ formed in Co(CN)-Y. In an attempt to increase the amount of $Co(CN)_4^{2-}$ present, it was found that by exchanging cesium into CoY prior to the addition of cyanide, less oxidation of the cobalt was observed and a new cobalt complex that reversibly binds oxygen, pentacyanocobaltate, $Co(CN)_5^{3-}$, was formed inside the zeolite at higher concentrations than the previously reported $Co(CN)_4^{2-}$ complex. The main focus of this research has been to develop a synthetic method which will maximize the amount of active cobalt complex, $Co(CN)_5^{3-}$, inside zeolite Y.

Experimental

Solvents and Reagents

Methanol used was spectral grade and dried over activated 3A molecular sieves. Acetonitrile was distilled over P_2O_5 and stored over 4A molecular sieves. NaY used was LZY-54 powder (lot no. 955087001010-S) obtained from UOP. Ultrastable Y powder (USY) was obtained from Amoco (lot no. 26-89-001). Benzene and N,N-dimethylformamide used were reagent grade and purchased from Fischer Scientific. All chemicals were used as obtained without further purification. Cobalt(II) chloride hexahydrate was obtained from Mallinckrodt. Potassium cyanide and sodium cyanide were A.C.S. certified from Fischer Scientific. Tetraethylammonium cyanide, cesium chloride (99.999%), ethylenediamine tetraacetic

acid, tetrasodium salt 98% (Na_4EDTA), sodium fluoride, dimethylglyoxime, tetraethylphosphate, and calcium chloride were obtained from Aldrich Chemical Company. Argon, helium, hydrogen, and oxygen were obtained from Liquid Air Corporation. All water used was distilled.

Sodium exchanged zeolites

Zeolite Y (20 g) was stirred in an aqueous 0.25M NaCl solution (400 mL) at room temperature for 24 hours. This was done to ensure that the exchangeable counter-cations present in the zeolite initially were Na^+. The solid was then collected by vacuum filtration and washed with deionized water until no precipitation was observed when the filtrate was tested with a 0.1M silver nitrate solution. The NaY was then dried at 150°C for 24 hours and stored in a desiccator prior to use.

Pretreatment of the Zeolite Prior to Metal Exchange

In some experimental studies, pretreatment of the zeolite occurred prior to exchange with aqueous metal chloride solutions. The pretreatment (typically performed on 20 grams of NaY) reagents included the following: (1) 400 mL of aqueous 0.1M NaF; (2) 400 mL of aqueous 0.1M N_2H_4; (3) 400 mL of triethylphosphate; (4) 400 mL of aqueous 0.1M NaOH; (5) 400 mL of 0.01 or 0.1M dimethylglyoxime (in ethanol); and (6) 400 mL of aqueous 0.1M $CaCl_2$, followed by 400 mL of aqueous 0.2M NaOH. Each of these NaY solids were collected by filtration, washed with the exchange solvent, then dried at 150°C under vacuum for 24 hours.

Nomenclature for Metal Exchanged Zeolite Y

A shorthand notation system is used to identify the procedure for preparing metal exchanged zeolites containing more than one metal cation. Although not denoted in the shorthand formula, Na^+ is present in the zeolite. For example, CsCoY is the shorthand notation for $Cs_xCo_yNa_zY$ ($Y = [(AlO_2)_{56}(SiO_2)_{136}]$), where x, y, and z summed up total 56. Order of metal cation exchange is also given in the formula, where the order of exchange is noted from right to left. Therefore, CsCoY indicates Co^{2+} was exchanged first, followed by Cs^+, while CoCsY indicates Cs^+ was exchanged first, followed by Co^{2+}. When simultaneous exchange of Cs^+ and Co^{2+} occurred, this is denoted by (CsCo)Y. This order method also applies to any other metal cations exchanged into the zeolite, especially Ca^{2+}.

Metal Exchanged Zeolite Y

Cobalt exchange into sodium zeolite Y

CoY was prepared by exchange of Na^+ for Co^{2+} by adding NaY to an aqueous $CoCl_2$ solution (400-800 mL) at 70°C for 24 hours. Aqueous $CoCl_2$ solutions were within 0.03-0.10M concentrations. The resulting pink solid was collected by vacuum filtration, washed with water until no Cl^- was present in the filtrate, and dried at 150°C under vacuum overnight. The resulting CoY solid was a deep purple/blue color.

Cesium exchange into cobalt zeolite Y

Cesium exchanged CoY samples were prepared by stirring CoY in an aqueous solution of 0.1M CsCl (400-800 mL). These exchanges were done at room temperature and allowed to stir a minimum of 16 hours. The treatment was repeated three times to ensure maximum Cs^+ exchange. After the final exchange, the solid was washed with water until no Cl^- was present in the filtrate. The resulting pink solid was dried at 150°C under vacuum overnight. The resulting CsCoY solid was a deep blue color.

Synthetic variations for addition of cobalt and cesium

CoCsY variation. In some cases, the cesium exchange took place prior to the cobalt exchange. In this procedure, NaY was placed in an aqueous solution of 0.1M CsCl (400-800 mL) at room temperature and allowed to stir a minimum of 16 hours. Often the treatment was repeated three times to ensure maximum Cs^+ exchange. After the final exchange, the solid was collected by vacuum filtration and washed with water until no Cl^- was present in the filtrate.

The solid was then added to an aqueous $CoCl_2$ solution (400-800 mL) at 70°C for 24 hours. Aqueous $CoCl_2$ solutions were within 0.03-0.10M concentrations. The resulting pink solid was collected by vacuum filtration, washed with water until no Cl^- was present in the filtrate, and dried at 150°C under vacuum overnight. The final CoCsY material was a deep blue color.

(CsCo)Y variation. In some cases, exchange of cesium and cobalt was performed simultaneously. In this procedure, NaY was placed in an aqueous solution

of 0.01 M $CoCl_2$ and 0.05M CsCl (400-800 mL total volume) and allowed to stir at room temperature a minimum of 24 hours. The pink solid was collected by vacuum filtration and washed with water until no Cl^- was present in the filtrate. The solid was dried at 150°C under vacuum overnight. The final Cs/CoY material was a deep blue color.

Calcium exchange into sodium zeolite Y

CaY was prepared by exchange of Na^+ for Ca^{2+} by adding NaY to an aqueous $CaCl_2$ solution at room temperature a minimum of 24 hours. A typical reaction run utilized 10 grams of NaY. Aqueous $CaCl_2$ solutions used were 0.55M concentration. The resulting solid was collected by vacuum filtration and washed with water until no Cl^- was present in the filtrate. The solid was then dried in a tube furnace under flowing nitrogen for 24 hours at 500°C.

Cobalt exchange into calcium zeolite Y

Cobalt exchanged CaY was prepared by stirring CaY in an aqueous solution of 0.01M $CoCl_2$ a minimum of 24 hours at room temperature. The solid was collected by vacuum filtration and washed with water until no Cl^- was present in the filtrate. The resulting pink CoCaY solid was dried at 100°C under vacuum overnight. The dried CoCaY sample was a deep blue color.

Lithium exchange into sodium zeolite Y

Total exchange of lithium for sodium in NaY was accomplished using the following method. LiCl (14.90 g) was dissolved in 800 mL of methanol. NaY (40 g) was added into the solution and stirred at room temperature for 24 hours. The solid

was then filtered and washed. The procedure was repeated a total of five times to ensure the complete exchange of Li^+ for Na^+. After the final lithium exchange, the solid is filtered and exhaustively washed until no Cl^- is present in the filtrate. The solid was dried at 150°C under vacuum.

Cobalt exchange into lithium zeolite Y

Cobalt exchanged LiY samples were prepared by stirring LiY in a solution containing 20 grams of LiY and 3.20 grams of $CoCl_2$ in 400 mL of deionized H_2O. The exchange was done at 70°C and stirred for 24 hours. The pink solid was filtered and washed until no Cl^- was present in the filtrate. The solid was then stirred in a dry solution of DMF overnight. After filtration, this was repeated in fresh, dry DMF a total of three times. The solid was then dried under vacuum at 100°C.

Simultaneous cobalt and cesium exchange into calcium zeolite Y

In some cases, exchange of cesium and cobalt was performed simultaneously. In this procedure, CaY (20 g) was placed in an aqueous solution of 0.01M $CoCl_2$ and 0.05 M CsCl (400 mL total volume) and allowed to stir at room temperature a minimum of 24 hours. The pink solid was collected by vacuum filtration and washed with water until no Cl^- was present in the filtrate. The solid was dried at 100°C under vacuum overnight. The final Cs/CoCaY material was a deep blue color.

Aprotic Solvent/Azeotrope Drying Procedure

An alternative method of drying the metal exchanged zeolites besides vacuum drying at elevated temperatures involved using an aprotic solvent (either acetonitrile

or DMF) and benzene. After the final metal exchange and the final washing to remove all Cl^- present, the pink zeolite material (i.e. CsCoY, CoCsY, or CoCaY) was placed in either DMF or CH_3CN and slurried overnight. The solid material was then collected by vacuum filtration and added to new solvent. This process was repeated a total of three times. By visual inspection, the color of the solid starts out pink and by the third slurry, the solid is a purple color. The solid was then further dried by first refluxing in benzene and then distilling off the benzene. The azeotrope of benzene and water was observed distilling off at 69.4°C. The zeolite was then placed in fresh benzene and the procedure repeated. By the third distillation, only benzene was observed distilling off at 80.1°C. The final color of the solid was a violet blue.

General Cyanide Reaction Conditions

Unless otherwise specified, all reaction conditions were carried out in the presence of atmospheric oxygen and moisture. Flasks were stoppered during stirring but no precautions to exclude air were taken. Reactions done under inert atmosphere were carried out using Schlenk techniques under purging argon. In some instances, oxygen, argon, or hydrogen were bubbled into the reaction flask.

Cesium cobalt cyanide in zeolite Y

Dry cobalt exchanged zeolite samples (i.e. CsCoY, CoCsY, or CoCaY) were reacted with cyanide salts in various solvents at room temperature. Cyanide salts used included NaCN, KCN, and $(CH_3CH_2)_4NCN$. Solvents used included water, methanol, DMF, and CH_3CN. Reaction times ranged from one hour to 168 hours.

The ratio of cyanide in solution to cobalt in the zeolite from 5:1 to 10:1 (stoichiometric to two fold excess). A typical synthetic run involved the following procedure. The cyanide salt was dissolved in the appropriate solvent. 3-5 grams of CsCoY was added to the cyanide solution and stirred for the appropriate amount of time. The solid was then collected by vacuum filtration and washed using copious amounts of the reaction solvent until no CN^- was observed in the filtrate (i.e. gives a negative Prussian blue test toward Fe^{2+}). The zeolite sample, now identified as CsCo(CN)-Y was then dried under vacuum at 100°C overnight. Typically, the final CsCo(CN)-Y material was a tan to yellow brown color.

Lithium cobalt cyanide in zeolite Y

In a three necked round bottom flask equipped with an addition funnel, 5.00 grams of LiCoY was slurried in 170 mL of dry DMF. The entire system was kept under nitrogen. By means of cannula, 33 mL of 0.5 M LiCN in DMF (Danger! Extremely toxic solution.) was transferred to the addition funnel. The red brown LiCN solution was added slowly over the course of one hour. The reaction slurry was stirred under nitrogen for 144 hours at room temperature. The purple solid was filtered under nitrogen via Schlenk technique and washed with 8-50 mL aliquots of DMF. The solid was dried first by passing nitrogen over the solid for 5 hours and then under vacuum at 150° C. The final solid was a metallic grey color.

Pore filling addition of cyanide

An alternative method for addition of the cyanide salt to CsCoY was done using a pore filling technique. Also referred to as incipient wetness, this involved

using just enough solvent to dissolve the cyanide salt and wet the solid CsCoY. Pore filling was only possible with water or methanol. A typical run used 5.00 grams of dry CsCoY and the appropriate cyanide salt in 5-8 mL of methanol or water. The solid is then vacuum dries to remove the solvent and worked up as mentioned in the previous section.

Synthesis of CsCo(CN)-Y under Dry, Aprotic Conditions

NaY (20 g) was exchanged in 800 mL of deionized water containing 23.4 grams of NaCl for 24 hours at room temperature. The solid was filtered and washed until it gave a negative chloride test with $AgNO_3$. The white NaY solid was dried at 200° C under vacuum for eight hours. After drying, the NaY was exchanged with 0.1 M CsCl for 24 hours, filtered, washed, and dried again under vacuum at 200°C for eight hours. The exchange with CsCl and drying steps were performed a total of three times.

The CsY material after the final exchange was exhaustively washed with deionized water to ensure that all Cl^- had been removed. 8.00 grams of wet CsY solid was then placed in a tube furnace and dried using the following temperature program under nitrogen: 25°-300° C, 2 hours; 300°- 500° C, 1 hour; 500° C, 24 hours; 500°-200° C, two hours. The white solid was removed from the tube furnace and placed in the dry box. Dried HPLC grade acetonitrile (25 mL) was used to dissolve 0.170 g of anhydrous cobalt(II) acetate in a pressure Parr bottle. The solid was vigorously stirred, with 2.00 grams of the dried CsY being added. The pressure bottle

was placed in a Teflon lined, stainless steel reactor vessel which was then placed in an oil bath at 105° C for 25 hours.

The cooled sample was recovered by vacuum filtration on a frit under N_2. The filtrate is clear with a purple solid CoCsY being recovered. This CoCsY was washed with 4, 25 mL aliquots of dry acetonitrile. This solid was then placed in another pressure bottle containing 60 mL of DMF and 0.24 grams of KCN. The reaction bottle was placed in a Teflon lined, stainless steel reactor vessel, which was then placed in an oil bath at 130° C for 96 hours. The cooled solid was vacuum filtered on a frit and washed with 4, 25 mL aliquots of DMF.

Spectral Measurements

All infrared spectra were recorded as Nujol mulls on a Nicolet 5PC FTIR spectrophotometer and were background corrected. Ultraviolet/visible spectra were recorded using a Perkin Elmer Lambda spectrophotometer and were background corrected. X-band EPR spectra of powder samples were recorded using a Bruker ER200D-SRC spectrophotometer equipped with a variable temperature unit. In order to remove or exclude oxygen from the EPR samples, tubes were equipped with o-ring connectors and attached to high vacuum stopcocks. This allowed for sample evacuation by connection to a vacuum line. EPR spectral simulations were calculated using the "QPOW" EPR simulation program. Elemental analyses of dissolved samples were conducted using a Hewlett Packard atomic adsorption spectrophotometer. Some zeolite samples were submitted for elemental analysis to

Oneida Research Services, Inc. Magnetic susceptibility measurements were performed using a Johnson Matthey magnetic susceptibility balance.

Elemental Analysis

Cobalt and sodium concentrations were determined by atomic adsorption analysis of the dissolved sample. A typical sample was dissolved using the follow procedure: A 0.1 gram sample of the zeolite was dissolved and refluxed for 30 minutes in 5 mL of 6M HCl and 10 mL of water. Next, 10 mL of 6M KOH and 15 mL of 0.2M K_4EDTA were added and the mixture refluxed another 30 minutes. This treatment completely dissolved the solid. Analysis for hydrogen content was carried out by the Microanalysis Laboratory at the University of Florida.

Quantitative EPR measurements

Signal intensities for the oxygen adducts were determined in some cases using double integration of the first derivative spectrum. Spin concentrations were calculated via comparison with the integrated spectrum of $[EtN_4]_3Co(CN)_5O_2$.

Adsorption Measurements

One apparatus used for the uptake of gases by the zeolite materials and determination of adsorption isotherms is shown in Figure 2-1. It consists of various glass chambers and a vacuum pump connected by Teflon screw valves. Pressure measurements were made using a MKS Baritron with a 390A sensor head and a 270B signal conditioning unit. Two sensor heads were attached via a MKS type 274

channel selector to give a readable range of 10^{-5}- 1000 torr (with one sensor having a range of 1-1000 torr and the second sensor having a range of 10^{-5}- 1 torr). The vacuum line system was not thermostated. However, movement in and around the immediate area was restricted during measurements and the fluctuation in temperature was never greater than $\pm$ 1°C.

Using a container of known volume, a reliable method to determine pressure of the system and ideal gas law theory, the solid-gas adsorption isotherms for the zeolite encapsulated cobalt(II)-cyano complexes can be determined. The procedure used is known as a successive addition technique. In a typical analysis run, a CsCo(CN)-Y sample (3-5 grams) was placed in a glass container sealed to the vacuum line apparatus (see Figure 2-8) via Vitcon O-rings and a glass vacuum stopcock. After desorption under vacuum of the sample at a given temperature (25-350°C) for a certain time interval (1- 24 hours), the sample was allowed to return to room temperature.

Prior to exposing the deoxygenated CsCo(CN)-Y sample to oxygen, it is necessary to determine two variables in our system. As you can see in Figure 2-8, the vacuum line apparatus has a total volume consisting of V_k, a glass container of known volume; V_d, the delivery volume of the system; and V_s, the dead volume of the system above the zeolite sample not accounted for in V_d. V_d is determined first using the following procedure.

1. The entire system is evacuated. The vacuum and V_s are then closed off.
2. V_k and V_d are filled with helium. V_k is closed off and the pressure noted (P_1). V_d is then evacuated.

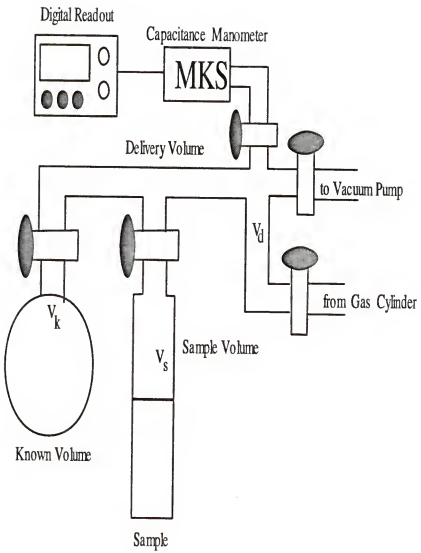

Figure 2-8. Vacuum Line Apparatus.

3. Helium in V_k is now at P_1. Close vacuum and open V_k to V_d. Note pressure (P_2).

4. Steps 1-3 can be repeated with P_2 becoming P_1 for the new set of data.

Initially, moles of helium are given by

$$n = \frac{P_1 V_k}{RT} \tag{2-16}$$

When V_k is opened to V_d, the known number of moles of helium remain constant while pressure changes (P_2) as well as volume ($V_k + V_d$). The ideal gas equation for the system becomes

$$V_k + V_d = \frac{(\frac{P_1 V_k}{RT})RT}{P_2} \tag{2-17}$$

which simplifies to

$$V_d = V_k(\frac{P_1}{P_2} - 1) \tag{2-18}$$

The next experimental variable to be determined is V_s. The procedure used is continued from above:

5. System is at P_2, volume is V_d. Open V_s to V_d and note the pressure (P_3). Close V_s.

6. P_3 now becomes P_1. Open V_k to V_d. Close V_k and note pressure (P_2).

7. Open V_d to V_s. Note pressure (P_3). Close V_s.

8. Repeat 5-6 if necessary.

The ideal gas equation for the system here is

$$V_s + V_k + V_d = \frac{\frac{(P_1 V_k)}{RT} RT}{P_3} \qquad (2\text{-}19)$$

Substituting Equation 2-18 into 2-19 yields Equation 2-20:

$$V_s = \left(\frac{P_1}{P_3} - \frac{P_1}{P_2}\right) V_k \qquad (2\text{-}20)$$

With V_d and V_s now known, gas adsorption experiments now begin. The procedure for performing an analysis using a gas which is either physisorbed and/or chemisorbed by the zeolite material (i.e. argon or oxygen) is similar to the procedure for determination of V_s.

1. Evacuate the entire system (V_k, V_d, and V_s). Note pressure (P_1). Close off V_s and vacuum.
2. Fill V_k with argon or oxygen.
3. Use V_k to fill V_d to specific incremental pressure point. Close V_k and note pressure (P_2).
4. Open V_s to V_d. Allow pressure to equilibrate (change in pressure of no greater than 0.001 torr per minute). Note pressure (P_3). Close V_s.
5. Repeat 2-5. P_3 becomes P_1.

The number of moles of gas adsorbed by the solid is equal to the difference in the number of moles present initially and the number of moles present after physisorption/chemisorption by the zeolite sample, or as seen in Equation 2-21:

$$n_{ads} = n_{init} - n_{final}$$
$$= [\frac{P_2V_d}{RT} + \frac{P_1V_s}{RT} - \frac{P_3(V_s+V_d)}{RT}] \quad (2\text{-}21)$$

This simplifies (in terms of moles of gas adsorbed per gram of zeolite matter) to Equation 2-22:

$$\frac{n_{ads}}{g} = \frac{(P_2-P_3)V_d + (P_1-P_3)V_s}{RTg} \quad (2\text{-}22)$$

Concentration of Active Complex

The concentration of active cobalt complex may be calculated in either of two ways. First, it can be calculated from the difference between the adsorption isotherms of oxygen and argon. The difference in the amount of argon adsorbed from the amount of oxygen at the same pressure above the zeolite gives the amount of cobalt(II)-O_2 adduct. At pressures where the cobalt complex is saturated, this difference is the total concentration of active cobalt complex. This value can also be determined by quantitatively measuring the EPR signal of the cobalt(II)-O_2 adduct.

Equilibrium Constant Determination

The equilibrium constant for oxygen binding, K_{O_2}, to the active complex was experimentally determined by measuring the amount of oxygen adsorbed at different pressures above the CsCoCN-Y material and the amount of argon adsorbed over the same range. The argon adsorption isotherm is linear and the equation for the line

can be determined by linear regression. By this equation, the amount of argon adsorbed by the material can be calculated at any pressure. The difference between the amount of oxygen and argon adsorbed at the same pressure represents the amount of $Co(CN)_5^{3-}$ (CoO_2) present in the zeolite. By calculating this value at different oxygen pressures, a plot of CoO_2 versus CoO_2/p_{O_2} can be constructed. The opposite of the inverse of the slope gives the equilibrium constant for oxygen binding, K_{O_2}, while the intercept gives the total concentration of the active cobalt species present, $[Co]_t$. K_{O_2} is expressed in units of $torr^{-1}$, while $[Co]_t$ is expressed in moles of active complex per gram of material.

Molecular Weight Calculations

The molecular formula for NaY is given by Breck.[6] Calculations here were based on LZY-54 having this formula.

$$\text{NaY} \quad Na_{56}[(AlO_2)_{56}(SiO_2)_{136}] \qquad \text{molecular weight} = 12763$$

$$\text{CsCoNaY} \quad Co_xCs_yNa_{56-2x-y}[(AlO_2)_{56}(SiO_2)_{136}]$$

$$\text{molecular weight} = 59x+133y+23(56-2x-y)+11475 \tag{2-23}$$

From cobalt and cesium analysis, the weight percent of cobalt, $Co_{wt\%}$, and weight percent of cesium, $Cs_{wt\%}$, are determined.

$$Co_{wt\%} = 100*\frac{59x}{\text{mol. wt.}} \tag{2-24}$$

$$Cs_{wt\%} = 100*\frac{133y}{\text{mol. wt.}} \tag{2-25}$$

By solving for x and y in Equations 2-24 and 2-25 then substituting back into

Equation 2-23, the molecular weight of CsCoNaY can be calculated from experimental values using Equation 2-26.

$$MW = \frac{12763}{[1-(0.22*Co_{wt\%}+0.83*Cs_{wt\%})*10^{-2}]} \quad (2\text{-}26)$$

The previous equation is for a dry zeolite sample. The equations must be corrected for the presence of water. As an approximation of the water present, the weight percent hydrogen, $H_{wt\%}$, determined from CHN analysis is assumed to be from water. The weight percent water can be calculated using Equation 2-27 and the molecular weight determined using Equation 2-29.

$$H_2O_{wt\%} = \frac{H_{wt\%}*18}{2} \quad (2\text{-}27)$$

$$H_2O_{wt\%} = \frac{100*18z}{\text{mol. wt.}} \quad (2\text{-}28)$$

$$MW = \frac{12763}{[1-(0.22*Co_{wt\%}+0.83*Cs_{wt\%}+1.0*H_2O_{wt\%})*10^{-2}]} \quad (2\text{-}29)$$

For the cobalt-cyanide containing zeolite samples, CsCo(CN)-Y, the molecular weight calculation is:

$$CsCo(CN)\text{-}Y \quad Co_xCs_y[NaCN]_kNa_{56-2x-y}[(AlO_2)_{56}(SiO_2)_{136}]\cdot zH_2O$$

$$\text{molecular weight} = 59x+133y+18z+49k+23(56-2x-y)+11475 \quad (2\text{-}30)$$

From CHN analysis, the weight percent of nitrogen (Equation 2-31) can be obtained

$$N_{wt\%} = 100*\frac{14k}{\text{mol. wt.}} \quad (2\text{-}31)$$

and used to determine the molecular weight of CsCo(CN)-Y by Equation 2-32.

$$MW = \frac{12763}{[1-(0.22*Co_{wt\%}+0.83*Cs_{wt\%}+H_2Owt\%+3.5N_{wt\%})*10^{-2}]} \quad (2\text{-}32)$$

Results and Discussion

Unlike solution behavior, where exposure to oxygen results in irreversible μ-peroxy dimer formation,[84] $Co(CN)_5^{3-}$ prepared inside the zeolite is a monomer that can be reversibly oxygenated and deoxygenated. This behavior is also in sharp contrast to solid $[NH_4]_3[Co(CN)_5(O_2)]$ where oxygen is only liberated by pyrolysis, resulting in decomposition of the complex.[91] According to Taylor, Drago, and George,[90] the formation of $Co(CN)_4^{2-}$ inside NaY occurs in very low concentrations, roughly 1% of the total cobalt present. The major product formed is $Co(CN)_6^{3-}$. When cesium was added to the cobalt(II)-exchanged zeolite, it was found that the oxidation of the cobalt and formation of $Co(CN)_6^{3-}$ was slightly inhibited (almost 10% of the cobalt present was as the active cobalt complex), and a new complex was identified, $Co(CN)_5^{3-}$.

The first objective of this work has been to develop a synthetic procedure that will optimize the amount of $Co(CN)_5^{3-}$ formed inside zeolite Y. The ultimate goal has been to develop a zeolite material which would chemisorb at least 10 cc of oxygen per gram of material. To be competitive with existing adsorbents and technologies, this objective has to be obtained. The second objective has been to determine the equilibrium constant for oxygen binding, K_{O_2}, for each newly synthesized material. The significance here is that the equilibrium constant will ultimately determine the application of the material.

EPR Characterization of CsCo(CN)-Y

The EPR spectrum of CsCo(CN)-Y at room temperature exhibits a large, broad signal at g=2.03, typical of a cobalt(II)-oxygen adduct (see Figure 2-9a). The $Co\text{-}O_2$ adduct can be deoxygenated with a small signal at g=2.2 attributed to a small amount of deoxygenated cobalt complex. Figure 2-9b shows the EPR spectrum resulting from evacuation of this material for 15 minutes at room temperature. This spectrum shows the presence of both $Co(CN)_5^{3-}$ and $Co(CN)_5O_2^{3-}$.

Complete deoxygenation of this material results after evacuation at 100°C for 10 minutes, yielding a spectrum (Figure 2-10) obtained at 110K, typical of low spin cobalt(II). If the spectral parameters are compared to those of other cobalt non-adducts (see Table 2-2), there is a similarity to the spectrum of $Co(CN)_5^{3-}$ in acetonitrile. These data provide conclusive evidence that the active cobalt complex present in CsCo(CN)-Y is $Co(CN)_5^{3-}$. Dramatic color changes accompany the oxygenation and deoxygenation of this material. The deoxygenated sample is light blue in color. Upon exposure to oxygen, the color changes to a tan yellow. These color changes are reversible.

Hyperfine splitting as a result of ^{59}Co (I=7/2) is small as predicted by the spin pairing model[94] (Figure 2-11) for the $Co\text{-}O_2$ adduct in which the unpaired electron resides mainly on the dioxygen molecule. The spin pairing model of binding dioxygen to a low spin cobalt complex can be viewed as a free radical reaction. The lone

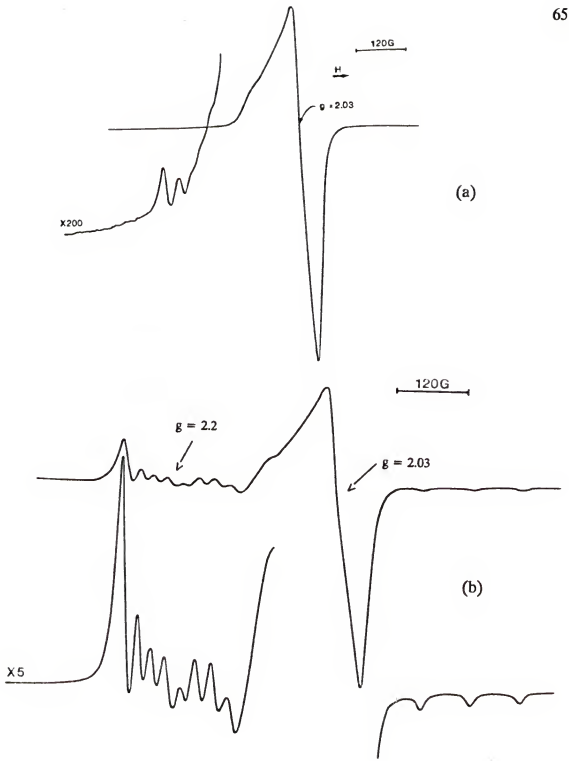

Figure 2-9. EPR Spectra of CsCo(CN)-Y (a) Spectrum of $Co(CN)_5O_2^{3-}$ in Zeolite Y at Room Temperature; (b) Spectrum at 110 K after Evacuation Ten Minutes at Room Temperature.

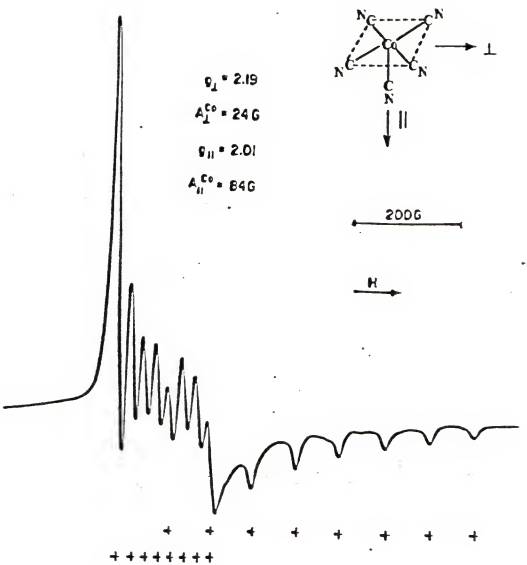

Figure 2-10. EPR Spectrum of $Co(CN)_5^{3-}$ in CsCo(CN)-Y.

Table 2-2. EPR Parameters for Low-spin Cobalt(II) Complexes.

Non-Adducts	$g_{\parallel}$	$g_{\perp}$	$a_{\parallel}$ (G)	$a_{\perp}$ (G)
CsCo(CN)-Y	2.01	2.19	87	28
$Co(CN)_5^{3-}$[a]	1.992	2.157	95	15
$Co(CN)_5^{3-}$[b]	2.00	2.20	87	28
$Co(CN)_5^{3-}$[c]	2.00	2.18	87	29
$Co(CN)_3(NCCH_3)^{-}$[c]	2.00	2.28	112	14
$Co(CNCH_3)_6$-Y[d]	2.000	2.087	68	72
$Co(CNCH_3)_5$-Y[d]	2.003	2.163	89	32
Co(bpy)(terpy)-Y[e]	2.012	2.250	101	15

a: Reference 92

b: Reference 86

c: Reference 91

d: Reference 77

e: Reference 93

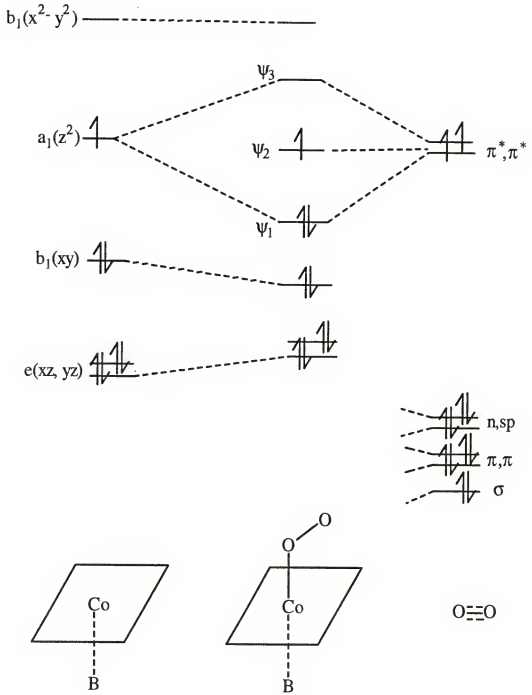

Figure 2-11. Spin Pairing Model.

unpaired electron on cobalt(II) combines with one π^* electron on the dioxygen molecule forming a σ bond, while the remaining π^* electron remains unpaired and resides mainly on the oxygen. Cobalt hyperfine arises from spin polarization of the cobalt-oxygen bond.[94]

Cobalt has a spin of 7/2 and by the 2nI+1 rule, this gives an eight line splitting pattern in the EPR spectrum. The low-spin $Co(CN)_5^{3-}$ cobalt complex has a single unpaired electron mainly in the d_z2 orbital which is involved in σ bonding to the axial ligand. This bonding leads to direct delocalization of the unpaired electron onto the axial ligand.[95] As has been shown in the literature,[96] if the axial cyanide is labelled with ^{13}C, ligand nuclear hyperfine coupling is expected. Indeed, the EPR results in the literature[97] show each eight line cobalt component is split into two lines by coupling with the axial $^{13}CN^-$. Of the five coordinated, labelled cyanides, only the axial cyanide splitting is resolved. The unresolved equatorial cyanide splitting increases the line width.[96]

Quantitative Gas Uptake Measurements

The presence of an entrapped complex which reversibly binds oxygen in a zeolite has a significant influence on the gas uptake characteristics of the material. The gas adsorption properties of CsCo(CN)-Y were studied by volumetric gas uptake measurements. NaY has an enhanced affinity for nitrogen over argon and oxygen. This is due to the quadrupole interaction of the N_2 molecule with the ions present inside the zeolite framework.[6] Gases for which these interactions are minimal, such

as O_2 and argon, show very similar adsorption isotherms. Consequently, argon is used as a blank when trying to determine any increase in oxygen uptake resulting from the oxygen binding complex.

The equilibrium constant expression for the binding of oxygen to the active cobalt complex, $Co(CN)_5^{3-}$, can be expressed as follows:

$$K_{O_2} = \frac{[CoO_2]}{[Co]pO_2} \tag{2-33}$$

where $[CoO_2]$ is the concentration of oxygenated active complex, [Co] is the concentration of active complex which remains uncomplexed at equilibrium, and p_{O_2} is the pressure of O_2 above the zeolite at equilibrium. Since the total concentration of active cobalt complex, $[Co]_t$, is the sum of [Co] and $[CoO_2]$, we can write

$$K_{O_2} = \frac{[CoO_2]}{([Co]_t - [CoO_2])pO_2} \tag{2-34}$$

which through algebraic manipulation translates to

$$[CoO_2] = [Co]_t - \frac{[CoO_2]}{pO_2} * \frac{1}{K_{O_2}} \tag{2-35}$$

The difference between the oxygen and argon adsorption isotherms at the same pressure above the zeolite corresponds to the amount of $Co(CN)_5O_2^{3-}$ ($Co\text{-}O_2$) formed at that pressure. The concentration of $Co\text{-}O_2$ adduct plotted versus the

concentration of Co-O_2 adduct over the equilibrium pressure of O_2 above the zeolite yields a straight line. A linear regression performed on a series of measurements yields the equation of the line. The inverse of the slope will give the equilibrium constant K_{O_2}, and the y-intercept the amount of total active cobalt complex, $[Co]_t$, present.

The $P_{1/2}$ value for the active cobalt complex is the pressure of oxygen necessary to oxygenate half the active complexes. The value can be related to the equilibrium constant for oxygen binding as shown in Equation 2-36:

$$K_{O_2} = \frac{1/2[Co]}{1/2[Co]\ P_{O_2}} = \frac{1}{P_{O_2}} \qquad (2\text{-}36)$$

The $P_{1/2}$ value (units of torr) of the complex is useful in determining the application of the material. A high pressure value would mean the material is saturated at high pressures and would find utility in a pressure swing cycle. A low $P_{1/2}$ value indicates the material is saturated at lower pressures. This type of material would find utility as an oxygen scrubber or as an oxygen scavenger because of its high affinity for oxygen.

Cyanide Addition in Protic Solvents

Cyanide addition in methanol

The first solvent used to synthesize $Co(CN)_5^{3-}$ inside the zeolite was methanol. Gas uptake measurements were used to gauge what effect variations in the synthetic procedure had on the amount of active complex formed. In this phase of the work,

the cyanide to cobalt ratio used was 10:1. The cyanide salt used was NaCN. The starting CsCoY material had a unit cell composition of $Cs_{33.0}Co_{4.2}Na_{14.6}Y$ and was dried under vacuum 24 hours at 150°C prior to the cyanide addition step. The CsCo(CN)-Y materials were deoxygenated under vacuum at 100°C for 24 hours prior to gas adsorption experiments. Reactions were carried out both under inert atmosphere (argon) and with oxygen actually being bubbled into the reaction mixture. A series of reactions was also carried out to test the effect of pre-treatment of the NaY zeolite with various agents prior to the exchange of cobalt and cesium cations.

Cesium is crucial to the formation of $Co(CN)_5^{3-}$ inside the zeolite. When CsCoY is reacted with NaCN, in order to balance charges as cyanide enters the zeolite cages, it is necessary for a cation to enter also, in this case sodium. NaCN enters the zeolite as an ion pair. It is possible during the cyanide addition step that sodium can be exchanged into the zeolite with cesium being exchanged into solution, defeating the purpose of exchanging it into the zeolite in the first place. The answer to this problem was to use cesium cyanide.

Attempts to synthesize CsCN via ion exchange failed. A salt believed to be CsCN was reacted with CsCoY. The resulting material was a purple-blue solid that did not have an EPR signal characteristic of the cobalt-oxygen adduct and did not chemisorb oxygen. Commercial availability of this salt is limited and its cost is high. To get around these problems, it was decided that a mixture of NaCN and CsCl would be used (1:1 CN^-/Cs^+ ratio in solution). Having cesium in solution during the cyanide reaction would increase the chances that the cesium ion concentration inside

the zeolite would remain constant or at least the potential would be greater using the NaCN/CsCl mixture over NaCN.

Table 2-3 shows results from a series of synthesis runs in methanol under various conditions. All of these samples were determined to be $Co(CN)_5^{3-}$ by EPR. The first interesting result from these experiments deals with the variation of using NaCN versus NaCN and CsCl. Samples A and D were run under identical conditions (same starting material, solvent, and reaction time), except A used NaCN and D used NaCN and CsCl. Both of these materials had essentially the same equilibrium constant for oxygen binding (4.34 $torr^{-1}$). Sample A, however, had $3.8x10^{-2}$ mmol/g of active complex present, while D had only $2.0x10^{-2}$ mmol/g of active complex.

Samples G and H were also prepared under the same conditions except for the variation of NaCN and NaCN/CsCl. Again, the sample prepared using NaCN (sample G) had more active complex present ($2.9x10^{-2}$ mmol/g) than with NaCN and CsCl. These data set suggest that the Cs^+ in the zeolite does not exchange with Na^+ in solution and cause a decrease in the amount of active complex formed due to a lack of cesium present. Instead, the lower yields using the NaCN and CsCl combination suggest that having Cs^+ in solution decreases the chance of CN^- entering the zeolite because of the 50% probability that the ion pair is CsCN. The steric constraints of the cage cannot accommodate more cesium, resulting in less $Co(CN)_5^{3-}$ being formed.

The role of oxygen in the formation of $Co(CN)_6^{3-}$ was also studied. Experiments were performed where (1) no precautions were taken to exclude

Table 2-3. Cyanide Addition in Methanol.

Sample	$[Co]_t$ (mmol/g, $x10^{-2}$)	K_{O_2} ($torr^{-1}$)	O_2 Chemi (cc O_2/g)
A[a]	3.8	4.34 ± 0.32	0.85 ± 0.07
B[a]	1.9	3.66 ± 0.33	0.42 ± 0.03
C[a,g]	2.3	4.41 ± 0.28	0.52 ± 0.05
D[b]	2.0	4.35 ± 0.46	0.45 ± 0.03
E[c,h]	5.4	17.8 ± 2.5	1.21 ± 0.05
F[c,i]	3.0	4.72 ± 0.52	0.67 ± 0.05
G[d]	2.9	4.26 ± 0.36	0.64 ± 0.06
H[e]	1.9	4.41 ± 0.22	0.42 ± 0.04
J[f]	1.0	4.76 ± 0.62	0.22 ± 0.03

All samples (except B) starting CsCoY composition: $Cs_{33.0}Co_{4.2}Na_{14.6}Y$.
All samples (except B) were cesium exchanged using CsCl. Sample B cesium exchanged using CsOH.
All samples used NaCN as cyanide salt (10:1 CN^-/Co^{2+} ratio).
All samples deoxygenated 24 hours at 100°C.
a: 24 hours reaction time

b: CsCl in solution (with NaCN), 24 hours reaction time

c: CsCl in solution (with NaCN), 1 hour reaction time

d: 48 hours reaction time

e: CsCl in solution (with NaCN), 1 hour reaction time

f: 96 hours reaction time

g: synthesis in Schlenk, under argon

h: oxygen bubbled into solution during synthesis

i: synthesis in Schlenk, under argon, argon bubbled into solution during synthesis

atmospheric oxygen (A); (2) the sample was prepared under argon using Schlenk procedures (C); and (3) oxygen (or argon) was bubbled into the reaction solution. (E and F). Samples A and C were prepared using NaCN while E and F were prepared using NaCN and CsCl. Sample A was prepared in the air while sample C was prepared in an inert atmosphere. Sample A had an active complex concentration of $3.8x10^{-2}$ mmol/g versus $2.3x10^{-2}$ mmol/g for sample C. Sample E was prepared with oxygen bubbled into solution and had an active complex concentration of 5.4×10^{-2} mmol/g, while sample F, prepared in a Schlenk setup with argon being bubbled into solution, had an active complex concentration of only $3.0x10^{-2}$ mmol/g.

In both sets of experiments, it becomes quite evident that the presence of oxygen actually increases the amount of active complex present. The data suggests that oxygen stabilizes $Co(CN)_5^{3-}$ in the zeolite during the complex's formation. This most likely occurs because oxygen can occupy the sixth coordination site and prevent coordination of either water or a sixth cyanide. Also significant is the K_{O_2} obtained for this sample. Shown in Figure 2-12 are the gas adsorption isotherm curves for Sample E and in Figure 2-13 the plot of $[CoO_2]$ versus $[CoO_2]/p_{O_2}$ used to determine K_{O_2} and $[Co]_t$.This sample was deoxygenated (at 100°C) and oxygenated consistently showing the same isotherm and K_{O_2} over five cycles. The affinity of the $Co(CN)_5^{3-}$ complex for oxygen is enhanced (as is evident in the increased K_{O_2}) by having high concentrations of O_2 present during its formation. This preparation

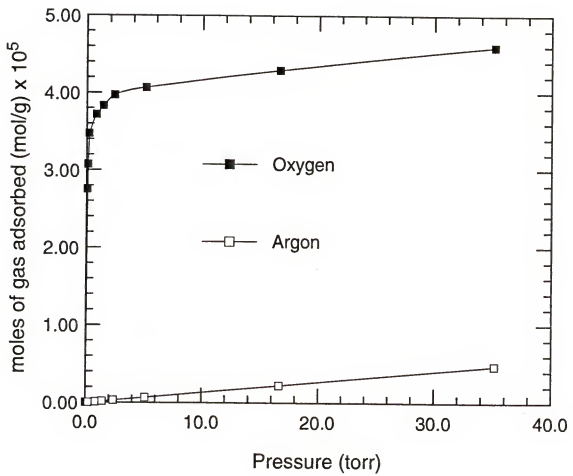

Figure 2-12. Gas Adsorption Isotherms for CsCo(CN)-Y (Sample E).

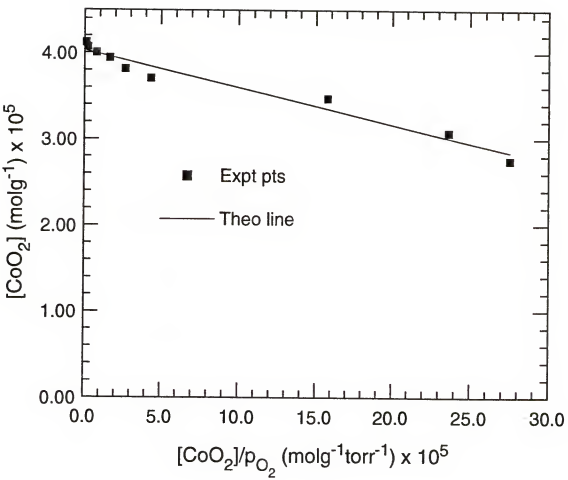

Figure 2-13. Determination of $[Co]_t$ and K_{O_2} of CsCo(CN)-Y (Sample E).

represented a significant achievement because it, at the time, represented the highest concentration of active complex ever achieved in our laboratory.

Two sources of cesium were used to prepare the starting CsCoY material in these experiments, CsOH and CsCl. Sample A was prepared using CsClCoY while sample B was prepared using CsOHCoY, with sample A having an active cobalt complex concentration of $3.8x10^{-2}$ mmol/g and sample B, $1.9x10^{-2}$ mmol/g. Elemental analysis showed that very little of the cobalt is removed during CsOH exchange, in comparison to 40-50% of the cobalt being removed during CsCl exchange. The EPR of CsOHCo(CN)-Y (sample B) was identical to that prepared from CsClCoY (refer to Figure 2-10).

When CsOH was exchanged with CoY, the zeolite material became a black-brown color, indicative of $Co(OH)_2$ formation. When cyanide is added, there is either no interaction between $Co(OH)_2$ and cyanide or ligand competition between the hydroxide and cyanide ligands. This is why the amount of $Co(CN)_5^{3-}$ in sample A is double that of sample B. For this reason, CsCl was the source of cesium in all further preparations of the CsCoY starting material.

The final synthetic variable studied in these experiments was cyanide reaction time. Reaction time ranged from 1 to 96 hours. By allowing the reaction to continue, there is more time for the methanolic solution of cyanide to diffuse into the zeolitic pores. It also means that any $Co(CN)_5^{3-}$ complexes that form have a longer period of time in which to be mobile in the presence of excess cyanide. As can be seen in comparing samples A, G, and J (all prepared using NaCN) the trend

established is as reaction time increases, the concentration of active complex formed decreases, from $3.8x10^{-2}$ mmol/g after 24 hours to $2.9x10^{-2}$ mmol/g after 48 hours, and $1.0x10^{-2}$ mmol/g after 96 hours. It is also worth noting that the highest active complex concentration (sample E) was achieved (using NaCN/CsCl) after a reaction time of only one hour.

Pretreated CsCoY reactions with cyanide in methanol

NaY and NaUSY (or Na-Ultrastable Y) were pretreated with Lewis bases, Bronsted-Lowry bases, and a known aluminum chelator prior to the exchange of cobalt and cesium to see whether the acidity of the zeolite may be involved in oxidation of $Co(CN)_5^{3-}$ to $Co(CN)_6^{3-}$. The acidity of zeolites has been the subject of much study.[98] Each aluminum atom contained within the framework structure induces a potential active acid site. Both Bronsted and Lewis acid models have been used to classify the active sites in zeolites. Bronsted acidity is proton-donor acidity and occurs when the cations balancing the zeolite framework are protons. Lewis acidity is electron acceptor acidity; a trigonally coordinated aluminum atom is electron-deficient and can accept an electron pair, thus behaving as a Lewis acid.

Besides looking at chemical agents to decrease the potential acidity of aluminum atoms in the zeolite framework, a series of experiments were run where the number of aluminum atoms in the zeolite Y framework was decreased. This was accomplished by using a zeolite known as ultrastable Y, which has the same pore structure and dimensionality as NaY. Ultrastable Y is simply a modified zeolite (rare earth and/or ammonium exchanged form) with an SiO_2/Al_2O_3 ratio of 4 or greater.[2]

If indeed the aluminum atoms were functioning as Lewis acids and promoting oxidation of Co(II) to Co(III), then this higher silica zeolite could solve the problem and lead to a higher concentration of active $Co(CN)_5^{3-}$ complex.

Gas uptake measurements again were used to gauge what effect variations in the synthetic procedure had on the amount of active complex formed. The cyanide salt used was NaCN, with the cyanide to cobalt ratio of 10:1. The starting CsCoY materials had a unit cell composition of: $Cs_{30.2}Co_{5.0}Na_{15.8}Y$ (Lewis acid study); $Cs_{27.5}Co_{4.7}Na_{19.1}$ (DMGH study); and $Cs_{25.0}Co_{4.4}Na_{22.2}$ Y (NaOH study); while the starting CsCoUSY material (NaOH study) had a unit cell composition of $Cs_{14.8}Co_{5.5}Na_{7.6}USY$ (USY= $[(AlO_2)_{33.4}(SiO_2)_{158.6}]$). All starting materials were dried under vacuum 24 hours at 150°C prior to the cyanide addition step. The CsCo(CN)-Y (and USY) materials were deoxygenated under vacuum at 100°C for 24 hours prior to gas adsorption experiments.

The results obtained for the first series of experiments using pretreated CsCoY for the synthesis of $Co(CN)_5^{3-}$ are shown in Table 2-4. As a point of comparison, sample A is included even though there was no special pretreatment involved in its preparation. NaY was pretreated with two Lewis bases: triethylphosphate (neat) and 0.1M aqueous sodium fluoride. Regardless of which Lewis base was used, the equilibrium constant for oxygen binding was determined through gas adsorption experiments to be 4.21-4.60 ($\pm$0.40) $torr^{-1}$. Liquid nitrogen EPR (for the deoxygenated samples) on these materials (samples K-N) exhibited spectra characteristic of the five coordinate $Co(CN)_5^{3-}$ complex (see Figure 2-10).

Table 2-4. NaY Pretreated Reactions.

Sample	Pretreatment Agent	$[Co]_t$ (mmol/g) ($x10^{-2}$)	K_{O_2} ($torr^{-1}$)	O_2 Chemi (cc O_2/g)
A[a]	none	3.8	4.34 ± 0.32	0.85 ± 0.07
K[a]	$(EtO)_3PO$	2.2	4.60 ± 0.34	0.49 ± 0.04
L[b]	$(EtO)_3PO$	2.5	4.33 ± 0.42	0.56 ± 0.05
M[a]	0.1 M $NaF_{(aq)}$	2.4	4.40 ± 0.36	0.53 ± 0.04
N[b]	0.1 M $NaF_{(aq)}$	2.6	4.26 ± 0.47	0.63 ± 0.06
O[a]	0.1 M $N_2H_{4(aq)}$	1.1	4.21 ± 0.28	0.27 ± 0.04
P[b]	0.1 M $N_2H_{4(aq)}$	1.2	4.40 ± 0.30	0.28 ± 0.04

All samples used NaCN as cyanide salt (10:1 CN/Co ratio).

All pre-treated samples starting CsCoY composition: $Co_{30.2}Co_{5.0}Na_{15.8}Y$

All samples deoxygenated 24 hours at 100°C.

a: 24 hours reaction time

b: 1 hour reaction time

Samples which were prepared from NaY pretreated with either triethylphosphate or sodium fluoride showed no increase in the amount of active complex. Reaction time of CsCoY and NaCN in methanol was also varied (one or 24 hours), but there was no appreciable increase in the amount of active cobalt complex. The results suggest that the pre-treatment step actually decreased the amount of active cobalt complex present. Comparing samples A, K, and M, we see that pretreatment with triethylphosphate results in a decrease in the amount of active cobalt complex from $3.8x10^{-2}$ mmol/g in sample A, to $2.2x10^{-2}$ mmol/g in sample K, a decrease of 42%. Pretreatment with aqueous sodium fluoride causes a decrease in the amount of active cobalt complex from $3.8x10^{-2}$ mmol/g to $2.6x10^{-2}$ mmol/g in sample M, a decrease of 36%.

In order to rule out cyanide reaction time as a variable (with the potential prolonged exposure and mobility of $Co(CN)_5^{3-}$ to excess cyanide) the reaction time was decreased from 24 hours to one hour. As seen in Table 2-4, pretreated samples L and N show no appreciable increase in the amount of active cobalt complex formed. Sample L, pretreated in triethylphosphate and reacted with NaCN for one hour, had an active cobalt complex concentration of $2.5x10^{-2}$ mmol/g, an increase of 12% over sample K (reacted 24 hours). Sample N, pretreated in aqueous NaF and reacted with NaCN for one hour had an active cobalt complex concentration of $2.6x10^{-2}$ mmol/g, an increase of 7% over sample M. The data suggest that the pretreatment of the zeolite with Lewis bases is in fact having the effect of decreasing the amount of complex. If Lewis acidity of Al^{3+} is playing a role in the oxidation of

Co(II) to Co(III), and the formation of $Co(CN)_6^{3-}$, this effect is only enhanced by pre-treating NaY with Lewis bases.

NaY samples were also pretreated with hydrazine, then used to form CsCo(CN)-Y. Hydrazine, a reducing agent, was used to see if any potential oxidizing centers in NaY could be reduced prior to the formation of the $Co(CN)_5^{3-}$ complex. The five-coordinate complex was identified by EPR at liquid nitrogen temperatures (for the deoxygenated samples). The equilibrium constant for oxygen binding was found by gas adsorption experiments to be 4.30 ± 0.30 $torr^{-1}$. The hydrazine pre-treated samples O and P showed a significant decrease in the amount of active cobalt complex formed relative to a nontreated sample (A). Samples A and O were both reacted with NaCN in methanol for 24 hours. Hydrazine treatment caused a decrease in the amount of active cobalt complex from 3.8×10^{-2} mmol/g in sample A to 1.1×10^{-2} mmol/g in sample O, a decrease of 71%.

There was no significant change in the amount of active cobalt complex concentration when reaction time was decreased from 24 hours to one hour. The decrease in the amount of active complex formed from treatment of the zeolite with aqueous hydrazine is nearly double that observed for either of the two Lewis bases used.

Having no success approaching the problem of neutralizing acid centers with Lewis bases or by using a reducing agent, the next approach was to attempt to decrease the acidity of the zeolite by using a known aluminum chelator. The most important complexes of Group IIIA elements are those containing chelate rings,

especially those of ß-diketones, pyrocatechol, dicarboxylic acids, and 8-quinolinol.[99] Dimethylglyoxime (DMGH) is a known chelator of aluminum. The second series of experiments centered around pretreatment of NaY with DMGH. Samples of pentacyanocobaltate prepared in NaY pretreated with DMGH are shown in Table 2-5.

The results show that DMGH treatment did not cause an increase in the amount of active $Co(CN)_5^{3-}$ complex formed. However, there is a significant change in the equilibrium constant for oxygen binding. This decrease in the K_{O_2} is dependent on the concentration of DMGH used to pretreat the NaY. For example, four samples (R-U) were prepared with an active cobalt complex concentration of 3.0-3.6x10^{-2} mmol/g. The K_{O_2} for these samples was 0.24-0.30 ($\pm$ 0.04) $torr^{-1}$ as determined by gas adsorption measurements, a decrease by a factor of 18. The concentration of DMGH used to pretreat the NaY was 0.1M. When the concentration of DMGH used to pretreat the NaY was decreased to 0.01M (samples V and W), the K_{O_2} value was found by gas adsorption measurements to be 1.52-1.65 ($\pm$0.17) $torr^{-1}$, a decrease by a factor of 3, with a total active cobalt complex concentration of 2.0-2.4x10^{-2} mmol/g. Shown in Figure 2-14 are the plots of $[CoO_2]$ versus $[CoO_2]/p_{O_2}$ used to determine both K_{O_2} values. Liquid nitrogen EPR (for the deoxygenated samples R-W) exhibited spectra characteristic of the five coordinate pentacyanocobaltate(II) complex.

The goal to increase the amount of $Co(CN)_5^{3-}$ formed in the zeolite is not achieved by pretreatment of NaY with DMGH and then reacting the CsCoY with NaCN in methanol for one hour or 24 hours. The data suggests that DMGH is

Table 2-5. Dimethylglyoxime Pretreated CsCoY.

Sample	Concentration DMGH (M)[a]	$[Co]_t$ (mmol/g) ($x10^{-2}$)	K_{O_2} ($torr^{-1}$)	O_2 Chemi (cc O_2/g)
A[b]	--	3.8	4.34 ± 0.32	0.85
R[b]	0.10	3.6	0.24 ± 0.02	0.80
S[c]	0.10	3.4	0.29 ± 0.07	0.76
T[b]	0.10	3.0	0.27 ± 0.02	0.67
U[c]	0.10	3.3	0.30 ± 0.06	0.74
V[b]	0.01	2.4	1.52 ± 0.15	0.54
W[c]	0.01	2.0	1.65 ± 0.20	0.45

a: 20 g of NaY exchanged in 200 mL ethanolic solution of specified concentration of DMGH

All samples prepared from starting CsCoY with composition: $Cs_{27.5}Co_{4.7}Na_{19.1}Y$.

All samples deoxygenated 24 hours at 100°C.

All samples used NaCN as cyanide salt (10:1 CN/Co ratio).

b: 24 hours reaction time

c: 1 hour reaction time

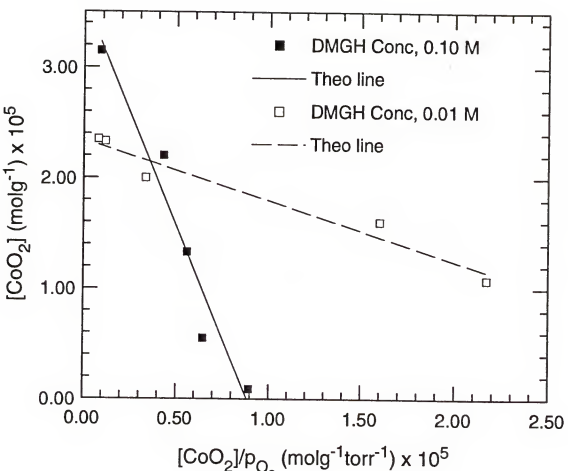

Figure 2-14. K_{O_2} and $[Co]_t$ Determination for DMGH Samples.

coordinating to the Al^{3+} of the zeolite framework because the five coordinate complex is forming. However, the K_{O_2} is significantly lower. It appears that DMGH is coordinating to aluminum in the framework and decreasing the acidity of any Al-OH groups. This decreases the hydrogen-bonding to the pentacyanocobaltate bound O_2 by surface hydroxyl groups. It is also possible that DMGH on the walls of the cavity may prevent interaction of the bound O_2 with OH groups or Lewis sites on the walls causing a decrease in K_{O_2}. Both of these explanations would account for the fact that when the concentration of DMGH used is decreased, the equilibrium constant increases but is still much less than the K_{O_2} value obtained from the complex in non-treated NaY (sample A).

This type of hydrogen-bonding interaction with metal bound dioxygen and the effects on the equilibrium constant for binding oxygen has been reported in the literature by Drago and coworkers.[100] They studied the equilibrium constant for formation of the dioxygen adduct of bis(salicylideniminato-3-propyl)methylamino cobalt(II), or CoSMDPT (see Figure 2-15), in various solvents. The observed value of the dioxygen equilibrium binding constant near -26°C in CH_2Cl_2 solvent increases over that observed in toluene ($K_{O_2}(CH_2Cl_2)$= 2.56, K_{O_2}(toluene)= 1.16). When a small amount of the strong hydrogen-bonding trifluoroethanol (TFE) was added to the CH_2Cl_2 solution, the equilibrium constant was found to be 12.06. This stabilization was interpreted as resulting from a specific interaction of the alcohol with the dioxygen adduct.

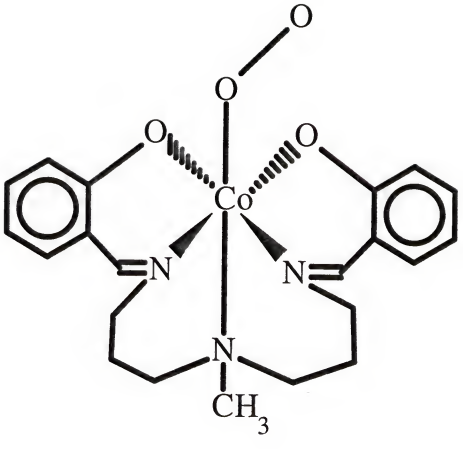

Figure 2-15. Structure of CoSMDPT.

In the zeolite case, the nontreated sample (A) has an equilibrium constant of 4.34 $torr^{-1}$. There is hydrogen bonding through Al-OH which stabilizes the cobalt(II) complex-dioxygen adduct. As DMGH is added to the zeolite, the interaction of these Al-OH groups with the adduct decreases, either through steric hindrance due to DMGH or a decrease in the acidity of the Al-OH and a decrease in the hydrogen bonding interaction. The greater the amount of DMGH used the greater the effect and the lower the K_{O_2} value becomes.

The third series of experiments dealt with pretreatment of the zeolite with sodium hydroxide. In this case, both NaY and NaUSY zeolites were used. The comparison between NaY (with a silicon to aluminum ratio of 2.5) and NaUSY (with a silicon to aluminum ratio of 4.4) was to see what affect having less aluminum in the framework would have on the amount of pentacyanocobaltate(II) complex formed. Pre-treatment with base was done to neutralize any potential zeolitic acid sites, this time using a Bronsted base. The results of these experiments are seen in Table 2-6.

Samples X-Z (the deoxygenated form) were identified by EPR at liquid nitrogen temperatures to be the five coordinate complex. Sample X, prepared in base treated NaY had an equilibrium constant for oxygen binding of 4.21 ± 0.20 $torr^{-1}$ and an active cobalt complex concentration of 2.9×10^{-2} mmol/g. There is a 23% decrease in the amount of cobalt complex formed when sample X is compared to sample A which was not base treated. Sample Y (reacted with NaCN in methanol for 24 hours) and sample Z (reacted with NaCN for one hour) were prepared using base treated NaUSY. Sample Y had an equilibrium constant for oxygen binding of

Table 2-6. Sodium Hydroxide Pretreated CsCoY/CsCoUSY.

Sample	Zeolite	$[Co]_t$ (mmol/g) ($x10^{-2}$)	K_{O_2} ($torr^{-1}$)	O_2 Chemi (cc O_2/g)
A[a]	NaY	3.8	4.34 ± 0.32	0.85 ± 0.07
X[b]	NaY	2.9	4.21 ± 0.20	0.65 ± 0.05
Y[b]	NaUSY	3.8	1.44 ± 0.15	0.85 ± 0.07
Z[c]	NaUSY	2.6	1.15 ± 0.20	0.58 ± 0.05

All reactions use NaCN (CN/Co ratio 10:1).

Starting CsCoY material: $Cs_{25.0}Co_{4.4}Na_{22.2}Y$

Starting CsCoUSY material: $Cs_{14.8}Co_{5.5}Na_{7.6}Y$

All samples deoxygenated 24 hours at 100°C.

a: 24 hours reaction time, NOT treated with NaOH

b: 24 hours reaction time

c: 1 hour reaction time

1.44 $\pm$ 0.15 $torr^{-1}$ and an active cobalt complex concentration of $3.8x10^{-2}$ mmol/g. Sample Z had a K_{O_2} of 1.15 $\pm$ 0.20 $torr^{-1}$ and an active cobalt complex concentration of $2.6x10^{-2}$ mmol/g.

The data suggest that under identical synthesis conditions it is possible to prepare the same amount of active $Co(CN)_5^{3-}$ complex in NaY or NaUSY. The only difference between the two complexes is the equilibrium constant for oxygen binding. Again the decrease in the K_{O_2} for the samples prepared in USY was attributed to a decrease in the ability of the Al-OH groups to hydrogen-bond to the oxygen adduct, due either to their neutralization by hydroxide or because there are fewer aluminum atoms in the framework.

The final series of pretreatment experiments again involved both NaY and NaUSY. The pretreatment was with $CaCl_2$ and NaOH. The attempt was to load the zeolite with a cation that would selectively fill the ß-cages and then could be treated with base to form an insoluble hydroxide. With the ß-cages inaccessible, any cobalt exchanged in the zeolite would only be present in the α-cages to form active cyanocomplexes.

Calcium preferentially fills cation positions within the ß-cages[6]. The concern with filling the ß-cages arises from the fact that any cobalt exchanged into the ß-cages will not be accessible to form cyanocomplexes due to the size. This concern of cobalt in inaccessible sites grows as one considers that as the CsCoY material is dried under vacuum at 150°C for 24 hours, the chances of driving dehydrated Co^{2+} into the ß-cages increases.

The calcium is exchanged into the zeolite, then filtered and washed until the filtrate gives a negative chloride test. The calcium exchanged zeolite is then placed in a tube furnace at 500°C for 24 hours under nitrogen to drive the calcium into the ß-cages. The zeolite is then exchanged with aqueous base, filtered and dried. The synthetic procedure then proceeds as normal for CsCoY preparation. Elemental analysis through atomic adsorption spectroscopy on the starting materials showed the CsCoY material had a unit cell composition of $Cs_{16.0}Co_{4.8}(Na,Ca/2)_{30.4}Y$, and the CsCoUSY material had a unit cell composition of $Cs_{6.2}Co_{4.0}(Na,Ca/2)_{19.2}USY$.

The results of the cyanide addition to these pretreated samples are shown in Table 2-7. Samples AA-CC were determined through EPR of the deoxygenated samples (at liquid nitrogen temperatures) to contain as the active complex $Co(CN)_5^{3-}$. Again, there was a decrease in the equilibrium constant for oxygen binding observed in the samples prepared using USY (BB: 1.55 ± 0.25 $torr^{-1}$; CC: 1.30 ± 0.20 $torr^{-1}$). None of these samples, however, showed an increase in the amount of active cobalt complex formed after pretreatment of the zeolite with $CaCl_2$ and NaOH. In fact, all of the samples showed a decrease in the amount of active cobalt complex formed relative to sample A which was not pretreated. This could be attributed to crowding in the α-cages from Ca^{2+} or $Ca(OH)_2$.

Pore filling with protic solvents

Another synthetic variation involved attempts at forming the $Co(CN)_5^{3-}$ complexes using water as the solvent. NaCN is very soluble in water and the zeolite has a high affinity for adsorbing water. However, when water was the solvent in the

Table 2-7. Calcium Hydroxide Pre-treated CsCoY/CsCoUSY.

Sample	Zeolite	$[Co]_t$ (mmol/g) ($x10^{-2}$)	K_{O_2} (torr-1)	O_2 Chemi (cc O_2/g)
A[a]	NaY	3.8	4.34 ± 0.32	0.85 ± 0.07
AA[b]	NaY	2.8	4.60 ± 0.30	0.62 ± 0.05
BB[c]	NaUSY	2.9	1.55 ± 0.25	0.65 ± 0.06
CC[b]	NaUSY	2.6	1.30 ± 0.20	0.58 ± 0.05

All used NaCN (CN/Co ratio of 10:1).

Starting CsCoCaY composition: $Cs_{16.0}Co_{4.8}(Na,Ca/2)_{30.4}Y$

Starting CsCoCaUSY composition: $Cs_{6.2}Co_{4.0}(Na,Ca/2)_{19.2}USY$

All samples deoxygenated 24 hours at 100°C.

a: 24 hours reaction time, NaY NOT pre-treated

b: 1 hour reaction time

c: 24 hours reaction time

reaction of CoY with NaCN, more than 80% of the cobalt is removed from the zeolite and the cobalt cyanide complexes formed in solution.[90] The effectiveness of the solvent depends on the ability to solvate the cyanide ion and the ability to carry cyanide into the zeolite to coordinate with Co^{2+} without extracting the cyanocomplexes into solution. One way to get around the extraction problem with water is to use a pore filling technique. Pore filling, also referred to as incipient wetness, involves using only enough solvent to dissolve the cyanide salt and wet the solid CsCoY material. By using minimal solvent, there is no excess solution for the cobalt to be extracted into and thereby lost. The solid is then dried under vacuum and washed with methanol.

The samples seen in Table 2-8 were prepared from a starting material that had a unit cell composition of $Cs_{29.0}Co_{4.0}Na_{19.0}Y$. The CsCoY starting material was dried under vacuum at 150°C for 24 hours. The CsCo(CN)-Y materials were deoxygenated under vacuum at 100°C for 24 hours prior to gas adsorption experiments. Cyanide addition was performed using the mixture of CsCl and NaCN based on the results obtained in MeOH. All the samples in Table 2-8 were identified by EPR to contain $Co(CN)_5^{3-}$ as the active cobalt complex.

Samples DD-FF were prepared using identical conditions. The only variable was the temperature at which the solvent was removed under vacuum: sample DD, 100°C for one hour; sample EE, 80°C for one hour; and sample FF, 25°C for one hour. As the evacuation temperature for the removal of solvent decreases from DD to FF, the amount of active cobalt complex present increases: DD, $0.4x10^{-2}$mmol/g,;

Table 2-8. Cyanide Pore Filling Reactions using Protic Solvents.

Sample	$[Co]_t$ (mmol/g) ($x10^{-2}$)	K_{O_2} ($torr^{-1}$)	O_2 Chemi (cc O_2/g)
DD[a,c]	0.4	3.71 ± 0.40	0.10 ± 0.02
EE[a,d]	1.4	4.90 ± 0.50	0.30 ± 0.03
FF[a,e]	1.6	5.10 ± 0.44	0.37 ± 0.04
GG[b,e]	2.2	4.12 ± 0.35	0.48 ± 0.04

All samples used NaCN/CsCl (CN/Co ratio- 5:1; CN/Cs(in solution) ratio- 1:1).

Starting CsCoY material composition: $Cs_{29.0}Co_{4.0}Na_{19.0}Y$.

All samples deoxygenated 24 hours at 100°C.

a: pore filled with water

b: pore filled with methanol

c: solvent removed under vacuum at 100°C

d: solvent removed under vacuum at 80°C

e: solvent removed under vacuum at 25°C

EE, $1.4x10^{-2}$ mmol/g; and FF, $1.6x10^{-2}$ mmol/g. Another trend is that the equilibrium constant for oxygen binding also increases from DD-FF as the solvent removal temperature decreases. DD has a K_{O_2} value of 3.71 $\pm$ 0.40 $torr^{-1}$; EE, 4.90 $\pm$ 0.50 $torr^{-1}$; and FF, 5.10 $\pm$ 0.44 $torr^{-1}$. The data suggests that the $Co(CN)_5^{3-}$ complexes are unstable towards oxidation in the presence of water when heated to temperatures between 80-100°C in the presence of excess cyanide. The complexes that are formed from synthesis using water as solvent show a slightly increased affinity for oxygen binding oxygen when the water is removed without heating the sample.

One sample, GG, was prepared using the pore filling technique with methanol as the solvent. Although it is unnecessary to use this technique with methanol as the solvent, it was performed to see if an increase in the amount of active cobalt complex would result. Sample GG had an active cobalt complex concentration of $2.2x10^{-2}$ mmol/g, and an equilibrium constant for oxygen binding of 4.12 $\pm$ 0.35 $torr^{-1}$, an increase over samples DD-FF, but comparable to other preparations using the standard slurry technique, pore filling using H_2O or methanol will not result in a significant increase in the amount of $Co(CN)_5^{3-}$ complex inside the zeolite.

The overall conclusion reached from this phase of the research is that the concentration of active cobalt complex cannot be significantly increase using protic solvents, regardless of whether the zeolite is pretreated, or a higher silica zeolite is used or the pore filling technique is used for cyanide addition. This research has pointed out that significant modification of the equilibrium constant for oxygen binding can be made by forming the $Co(CN)_5^{3-}$ complex in USY or in DMGH pre-

treated in NaY. The $Co(CN)_5^{3-}$ complexes in DMGH pre-treated CsCoY have an extremely low equilibrium constant, comparable to that seen for $Co(CN)_4^{2-}$ in NaY. If the $Co(CN)_5^{3-}$ concentration could be increased with an equilibrium constant for oxygen binding around 0.27 $torr^{-1}$, this material would have high potential for use in a pressure swing cycle.

The low yields of active complex with water as the solvent may be attributed to the decomposition of $Co(CN)_5^{3-}$, which has been shown to occur in solution[101] as described in Equation 2-33.

$$2Co(CN)_5^{3-} + H\text{-}OH \longrightarrow Co(CN)_5H^{3-} + Co(CN)_5OH^{3-} \quad (2\text{-}33)$$

In air, the hydride species would not be expected because it quickly reacts with O_2 to form $Co(CN)_5OOH^{3-}$, which decomposes to the hydroxide.[102] In the presence of free cyanide, the next step in the reaction is the irreversible formation of the very stable hexacyano species,[103] as shown in Equation 2-34.

$$Co(CN)_5OH^{3-} + CN^- \longrightarrow Co(CN)_6^{3-} + OH^- \quad (2\text{-}34)$$

This chemistry is very applicable in methanol also. Furthermore, it is possible that the chemistry illustrated in Equations 2-33 and 2-34 could occur with the waters of hydration found in the zeolite pores and channels.

It becomes quite evident that the goal of synthesizing high concentrations of $Co(CN)_5^{3-}$ in zeolite Y will not be accomplished using a protic solvent or a hydrated zeolite. Ultimately, what is needed is dry zeolite Y containing cesium and cobalt in

accessible cation positions in α-cages with cyanide addition from an aprotic solvent that can not only solubilize the metal cyanide salt but will also carry the cyanide into the zeolite micropores where it can coordinate with the cobalt. Previously, CsCoY samples were simply dried at elevated temperatures under vacuum to remove water. This, unfortunately, can also drive the cobalt into inaccessible cation positions in the ß-cages. A novel drying procedure was developed to remove water from the zeolite, introduce aprotic solvents into the CsCoY starting material and do so without using elevated temperatures under vacuum.

A Novel Drying Procedure for CsCoY

In this novel drying procedure, the CsCoY is prepared using the normal experimental procedure: aqueous exchange with a solution of $CoCl_2$ followed by aqueous exchange with CsCl. However, after the final cesium exchange, collection and washing of the solid, instead of evacuating the sample at elevated temperatures, the solid is placed in a dry, aprotic solvent, either N,N-dimethylformamide (DMF) or acetonitrile. The solid is stirred in the aprotic solvent for 12 hours, filtered, collected, then placed in a fresh solution of the appropriate aprotic solvent. This is carried out a total of three times. After the third stirring, the filtered solid is placed in dry benzene. The solid is refluxed for 12 hours and the benzene is distilled off with a new solution of benzene being added to the CsCoY solid. This reflux and distillation process in benzene is carried out three times also. On the final distillation, the solid is heated until it is a powdery blue solid.

Through the process of this drying procedure, the CsCoY goes through many color changes. The solid starts out a pink color, indicative of hydrated Co^{2+} ($Co(H_2O)_6^{2+}$). During the aprotic slurrying steps, the solid goes from pink to red violet to a violet purple. During the benzene step, the solid becomes a violet purple color, indicative of dehydrated Co^{2+}.

During the aprotic solvent slurry steps, the purpose is to force the Co^{2+} to remain in the α-cages by forming cobalt(II) complexes with the solvent, such as $Co(DMF)_4^{2+}$ or $Co(CH_3CN)_6^{2+}$, for example. These complexes can only fit in the α-cages. The benzene reflux/distillation steps are then used in order to remove water as an azeotrope of benzene and water.

Observations during the azeotroping steps on a sample which had been slurried in acetonitrile indicate this indeed is what is occurring. On distilling off the first benzene solution three fractions were observed: 66-67°C, indicative of a $C_6H_6/CH_3CN/H_2O$ azeotrope; 69°C, a C_6H_6/H_2O azeotrope; and 72°C, an CH_3CN/H_2O azeotrope. On the second distillation, two fractions were observed at 69° and 72°C. By the third distillation, only one fraction came off at 80.1°C, the boiling point of pure benzene.

Synthetic Variations in Aprotic Solvents

In the synthesis of the cobalt(II)-cyanide complexes in aprotic solvents, such as DMF or acetonitrile, there were many new ideas to increase the amount of active cobalt complex. Besides the novel drying procedure, these included:

1. KCN and LiCN as the cyanide salts (in comparison to NaCN).
2. Increased reaction time of CsCoY with the cyanide salt (48-192 hours).
3. Variation of deoxygenation time and temperature.
4. Increased concentrations of $Co(CN)_4^{3-}$ in NaY using the novel drying procedure and aprotic solvents for cyanide addition.
5. Formation of $Li_3Co(CN)_5$ in DMF inside LiY.
6. Formation of $Co(CN)_5^{3-}$ under dry, aprotic conditions.
7. Hydrogenation of samples at various temperatures prior to deoxygenation.

In these experiments, LiCN (0.5 M, in DMF), as well as KCN were used besides using NaCN to see what effect the size of the countercation would have on the amount of active cobalt(II) complex formed. From previously discussed work, CsCN was desired as the cyanide salt, but was unavailable. KCN, on the other hand is readily available, while K^+ cation is larger than Na^+ and similar in size to Cs^+ (Na^+: 0.95 Å; K^+: 1.33 Å; Cs^+: 1.69 Å). This made KCN appear as the next best choice to CsCN. LiCN was used in some experiments to synthesize $Li_3Co(CN)_5$. More on this subject will be discussed later. With the solubility of these cyanide salts being low in these solvents, large volumes were required. Therefore, reaction time was increased, varying anywhere between 48 hours and eight days to ensure maximum adsorption of the solutions and coordination of the cyanide. Using DMF and acetonitrile as the cyanide addition solvent, attempts were made to form the $Co(CN)_4^{2-}$ complex using CoY which had been dried using the aprotic solvent and benzene refluxing procedure.

Attempts were also made to study what affects the deoxygenation temperature and the length of time a sample was deoxygenated at this temperature had on the amount of oxygen chemisorbed by the active cobalt complexes as well as the equilibrium constant for oxygen binding. This study was extended to samples prepared in methanol as well. Finally, it was discovered that in certain cases (using CH_3CN as cyanide solvent) samples pre-treated under hydrogen at elevated temperature prior to deoxygenation chemisorbed greater amounts than the same samples without the pre-treatment. In other cases, (DMF as cyanide solvent) hydrogenation prior to deoxygenation did not increase the amount of chemisorbed oxygen.

Formation of Cobalt Cyanide Complexes in Aprotic Solvents

As early as 1972, work had already begun using aprotic solvents as the synthesis media for $Co(CN)_5^{3-}$. White and co-workers[91] did a study of the preparation, properties, and reactivity of tetraalkylammonium pentacyanocobaltates prepared in acetonitrile. Then, in 1984, what started out as an attempt to isolate and characterize $Co(CN)_4^{2-}$ became an extensive study of the formation of cobalt(II) cyanide complexes in aprotic solvents by Stuhl and co-workers.[104] Their goal was to synthesize monomeric $Co(CN)_4^{2-}$ as the salt $(PNP)_2Co(CN)_4$ (PNP^+ = bis(triphenylphosphine)iminium cation). This was accomplished, but only when the reaction solvent was DMF. X-ray structure determination on the single green crystals from

DMF revealed that DMF solvate was contained in the crystal. The resultant formula they proposed from the data was $(PNP)_2Co(CN)_4 \cdot 4DMF$.

Extending this study, they found evidence for the existence of cobalt(II)-cyanide species containing one to five cyanide ligands per cobalt in aprotic solvents (acetonitrile and DMF).[105] Perhaps the greatest achievement from this work was the isolation and spectral characterization of what was reported as $Li_3[Co(CN)_5] \cdot 3DMF$. The $Co(CN)_5^{3-}$ complex was also prepared and characterized using PNP^+ and K^+ as countercations. They were, however, unable to purify their material produced in the case of $Co(CN)_5^{3-}$ ($Co(CN)_4^{2-}$ and $Co(CN)_3(solvent)^-$ were impurities). Furthermore, they did not mention the suitability of any of their complexes for reversibly binding oxygen.

Recently, Air products reported in the patent literature[106] the formation of solid state cyanocobaltate(II) complexes having the formula

$$[(A)_a(R_4N)_b]^z{}_{x/z}[Co(CN)_n]^{x-} \cdot pS$$

where A is an alkali, alkaline earth metal atom, Zn, Cd, or Hg atom, a= 0-2.5, R is an alkyl, or aryl hydrocarbon (C_1- C_{10}); z= 1-3; n= 3-5; x= n-2; p= 0.5-6; and S is a ligand capable of coordinating to the countercation, Co, or both. Synthesis of these complexes is accomplished using aprotic solvents including (but not limited to) DMF, N,N-dimethylacetamide (DMAC), acetonitrile, acetone, and pyridine. The solids they identify in this patent reversibly bind oxygen, are reversible over numerous cycles, and can be regenerated either by purging the solid with nitrogen or evacuating the solid

to subambient pressures as low as 0.05 atmospheres. The adsorbents they report on may take up as much as 2.3 mmoles of O_2 per gram.

Based on Air Products disclosure, formation of stable, monomeric four and five coordinate cobalt(II)-cyanide complexes is very possible from aprotic solvents. Some of their solid materials, such as $(Et_4N)_{1.5}Mg_{0.75}Co(CN)_5 \cdot 0.5DMF$ and $[(Bu_4N)_2[Co(CN)_4]_2 \cdot DMF$ were shown to be stable toward repeated oxygen and nitrogen recycling over 100 cycles. Regeneration was accomplished by purging under nitrogen 25 minutes. These complexes show great promise for application in gas separation processes. Based on the encouraging results shown with all the work done in aprotic solvents, DMF and acetonitrile seem like the best choice for the cyanide addition solvent to attain our goal of increased active cobalt complex formation inside zeolite Y.

Cyanide Addition in Methanol to Aprotic Dried CsCoY

Before the work using strictly aprotic dried CsCoY and cyanide addition in aprotic solvents was started, a series of experiments were run to see if it was possible to use methanol as the cyanide addition solvent in connection with KCN and aprotic dried CsCoY to obtain higher concentrations of active cobalt complex. Table 2-9 shows the results of a sample prepared from reacting CsCoY ($Cs_{22.7}Co_{4.8}Na_{22.7}Y \cdot 119H_2O$, dried by slurrying in DMF followed by benzene azeotroping) with KCN (5:1 CN/Co ratio) in methanol. Also given in the table are the deoxygenation conditions for the sample prior to each gas uptake experiment.

Table 2-9. Synthesis using Aprotic Dried CsCoY and KCN in Methanol.

Evacuation Procedure	$[Co]_t$ (mmol/g)	K_{O_2} ($torr^{-1}$)	O_2 Chemi (cc O_2/g)
24 hrs, 100° C[a]	0.098 ± 0.001	6.56 ± 0.15	2.20 ± 0.02
24 hrs, 150° C[a]	0.082 ± 0.002	8.81 ± 0.39	1.80 ± 0.04
7 hrs, 300° C	0.074 ± 0.002	29.4 ± 1.6	1.66 ± 0.06
24 hrs, 300° C[a]	0.080 ± 0.004	35.7 ± 3.2	1.78 ± 0.12

CsCoY ($Cs_{22.7}Co_{4.8}Na_{22.7}Y \cdot 119H_20$, azeotrope dried) + KCN (5:1 CN/Co ratio), 48 hrs.

a: consecutive runs made on same sample

The first run on this sample was done after deoxygenation at 100°C for 24 hours which was, up to this time, standard procedure. This material chemisorbed 2.20 ± 0.02 cc of O_2 per gram of material which represents 0.098 ± 0.001 mmol of active cobalt(II) complex per gram of material. This represented a two fold increase in the amount of active cobalt complex compared with the previous best sample prepared in methanol. The deoxygenation temperature was increased from 100 to 150 and eventually 300°C, but no increase in the amount of oxygen chemisorbed was observed. In fact, the amount of oxygen chemisorbed decreased by 18% as the temperature increased. Even when the deoxygenation time was decreased from 24 to seven hours at 300°C, there was still a decrease in the amount of O_2 chemisorbed relative to that seen after desorption at 100°C.

Liquid nitrogen EPR of the deoxygenated sample indicated that the sample was indeed $Co(CN)_5^{3-}$. After deoxygenation at 100°C, the EPR spectra showed no O_2 adduct present, only the five coordinate complex. Furthermore, cycling of this material (via desorption at 100°C) was reproducible through five cycles. No loss of complex chemisorption ability or change in K_{O_2} was observed.

Whereas the data suggests that desorbing the methanol prepared sample at temperatures greater than 100°C partially deactivates a portion of the active cobalt complexes toward reversibly binding oxygen, the elevated desorption temperature causes an increase in the K_{O_2}. After deoxygenation for 24 hours at 100°C, the sample had a K_{O_2} of 6.56 ± 0.15 $torr^{-1}$. This increased to 8.81 ± 0.39 $torr^{-1}$ after deoxygenation at 150°C and 35.7 ± 3.2 $torr^{-1}$ after deoxygenation at 300°C. When

the deoxygenation time at 300°C was decreased from 24 to seven hours, the K_{O_2} value decreased from 35.7 $\pm$ 3.2 $torr^{-1}$ to 29.4 $\pm$ 1.6 $torr^{-1}$. The temperature used to remove oxygen under vacuum has an effect on the affinity the $Co(CN)_5^{3-}$ complex has for binding oxygen. A possible explanation for this behavior will be given in the next section. The next step was to use aprotic dried CsCoY with KCN addition in aprotic solvents. The first solvent used was DMF.

Cyanide Addition in DMF to Aprotic Dried CsCoY

Characterization of CsCo(CN)-Y

Complete deoxygenation of samples prepared in DMF after evacuation at 150°C for 10 minutes, yields an EPR spectrum obtained at 110K characteristic of $Co(CN)_5^{3-}$ (Figure 2-10). No Co-O_2 adduct was observed in the sample's spectrum after it was deoxygenated at 150°C.

Infrared (IR) and ultraviolet/visible spectroscopy were also used to identify the CsCo(CN)-Y samples and further confirm that the active cobalt(II) complex was indeed $Co(CN)_5^{3-}$. CsCo(CN)-Y samples prepared in DMF consistently showed a major sharp band (see Table 2-10) at 2121-2122 cm^{-1}. This band was attributed to the C-N stretching frequency for $Co(CN)_5O_2^{3-}$ as compared to the value attained in the literature for $(Et_4N)_3Co(CN)_5O_2$[91] of 2120 cm^{-1}. A sharp, minor peak was also consistently observed at 2162-2170 cm^{-1}. This band was attributed to $Co(CN)_2$, which has a $\nu_{cm^{-1}}$ reported[115] at 2165 cm^{-1}. The shift in the value may be attributed to the

Table 2-10. Infrared Frequencies for Cobalt Cyanide Compounds.

Compound	C-N Stretching (cm^{-1})
$Cs_{20.4}Co_{4.0}Na_{27.6}(KCN)_{16.0}$-Y (from DMF)	2121-2122
CsCo(CN)-Y (see above, deoxygenated)	2080
$(Et_4N)_3Co(CN)_5$[a]	2080
$(Et_4N)_3Co(CN)_5O_2$[a]	2120
$(PNP)_2Co(CN)_4$[b]	2095
$K_3Co(CN)_6$[c]	2129
$Cs_2Li[Co(CN)_6]$[d]	2142
$Cs_2Na[Co(CN)_5H]$[e]	2113
$Co_3[Co(CN)_6]_2$[f]	2176
$K_6[(CN)_5Co\text{-}Co(CN)_5]$[g]	2130 (m), 2100 (s),2073 (vs)
$K_6[(CN)_5Co\text{-}O_2\text{-}Co(CN)_5]$[h]	2146, 2132, 2125, 2120
$Co(CN)_2 \cdot 2H_2O$[i]	2165
$K_2Co(CN)_4$[j]	2170, 2122, 2100, 2080
$K_3[Co(CN)_5H_2O]$[k]	2095
$K_2[Co(CN)_5H_2O]$[k]	2140
$K_3[Co_2(CN)_8]$[k]	2120, 2062

a: Reference 91; b: Reference 104; c: Reference 107; d: Reference 108; e: Reference 109; f: Reference 110; g: Reference 111; h: Reference 112; i: Reference 113; j: Reference 114; k: Reference 115.

degree of zeolite solvation by DMF, H_2O, or both. Another critical observation is that no band is observed at 2131 cm^{-1} which would indicate the presence of $Co(CN)_6^{3-}$.

To further confirm by IR that the active species was indeed $Co(CN)_5^{3-}$, a CsCo(CN)-Y sample prepared in DMF was deoxygenated under vacuum at 300°C in a sealed tube, then transferred to a dry box where a nujol mull was prepared under an oxygen free environment. A sharp band was observed at 2080 cm^{-1}. Upon exposing this blue-grey deoxygenated sample to air, the solid became a tan-orange solid with the band at 2080 cm^{-1} disappearing and the band at 2121 cm^{-1} reappearing. The band at 2080 cm^{-1} was attributed to ν_{CN} for $Co(CN)_5^{3-}$ as has been reported in the literature.[91,106]

CsCo(CN)-Y prepared in DMF was also characterized by ultraviolet/visible spectroscopy. A nujol mull of the solid was prepared and placed on a piece of filter paper which had been cut to fit in the spectrophotometer's sample beam. A piece of filter paper with only nujol was placed in the reference beam. Seen in Figure 2-16 is the resultant spectrum. Based on a standard check, the band at 214 nm was attributed to DMF. The major band has a λ_{max} at 318 nm, while there is a shoulder at 391 nm. These values agree with those observed for $Co(CN)_5O_2^{3-}$ in DMF solution in a study done by Gubelmann and co-workers.[116] They report seeing three bands in DMF: 530 nm (metal-to-ligand charge transfer), 400 nm (d-d transition), and 320 nm (ligand-to-metal charge transfer). The agreement with our observed values once again confirm that the active cobalt(II) complex is $Co(CN)_5^{3-}$.

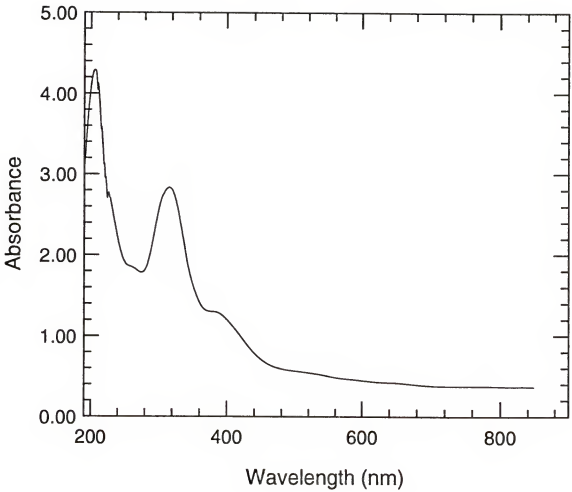

Figure 2-16. Ultraviolet/Visible Spectrum for CsCo(CN)-Y Prepared in DMF.

Deoxygenation time and temperature variation

The first sample prepared using aprotic solvents showed very promising results. This sample was prepared by reacting CsCoY ($Cs_{30.3}Co_{4.3}Na_{17.1}Y \cdot 135H_2O$) and KCN (10:1 CN/Co ratio) for 96 hours in DMF. The color changes during its preparation and analysis were very interesting. When CsCoY was added to the DMF/KCN solution, the slurry's initial color was blue. After the 96 hours of reaction time had elapsed, the slurry was a red-purple color. After filtration, the solid was a purple color. Air drying the solid on the frit caused the solid to become a tan brown color.

In this study, the sample was first deoxygenated under vacuum 24 hours at 50°C. Results (see Table 2-11) after gas adsorption measurements on this sample showed the material had chemisorbed 0.22 cc of O_2 per gram of material, with a K_{O_2} of 4.33 $\pm$ 0.25 $torr^{-1}$. Again, the temperature was increased, starting at the customary 100°C, and progressing up at 100° intervals, until reaching a point at which thermal deactivation of the complexes occurs. Up to 100°C, the oxygenated solid was a tan brown color. At deoxygenation temperatures greater than 100°C, the oxygenated solid was a grey color. These color changes many be attributed to loss of DMF solvent. The grey color change is most likely due to fragmentation of DMF and possible carbonization of the zeolite.

Preliminary results obtained after deoxygenating the sample at 50°C were not encouraging. The low concentration of active cobalt(II) complex contradicted what had been observed after taking the EPR spectrum of the sample. EPR (at room

Table 2-11. Temperature Studies on Sample Prepared in DMF.

Deoxy Temp (24 hrs, °C)	$[Co]_t$ (mmol/g)	K_{O_2} ($torr^{-1}$)	O_2 Chemi (cc O_2/g)
50	0.010 ± 0.001	4.33 ± 0.25	0.22 ± 0.02
100	0.030 ± 0.003	4.20 ± 0.11	0.59 ± 0.02
200	0.056 ± 0.004	10.1 ± 1.9	1.25 ± 0.09
300	0.131 ± 0.001	16.7 ± 0.7	2.94 ± 0.02
400	0.067 ± 0.008	1.41 ± 0.17	1.51 ± 0.18

Sample Preparation:
CsCoY ($Cs_{30.3}Co_{4.3}Na_{17.1}Y \cdot 135H_2O$, azeotrope dried) + KCN (10:1 CN/Co ratio) for 96 hours.

temperature) showed a very intense signal distinctive for the Co-O_2 adduct. By increasing the deoxygenation temperature by 50 degrees to 100°C, results indicated that the amount of oxygen chemisorbed by the zeolite increased by a factor of two, 1.25 $\pm$ 0.09 cc O_2 per gram, while K_{O_2} remained constant at a value of 4.20 $\pm$ 0.11 $torr^{-1}$. When the deoxygenation temperature was increased to 200°C, the amount of oxygen chemisorbed was found to be 1.25 $\pm$ 0.09 cc of O_2 per gram and a K_{O_2} of 10.1 $\pm$ 1.9 $torr^{-1}$. With the deoxygenation temperature at 300°C for 24 hours, the sample chemisorbed 2.94 $\pm$ 0.02 $torr^{-1}$ or 0.131 $\pm$ 0.001 mmol of active cobalt(II) complex per gram of material and had a K_{O_2} of 16.7 $\pm$ 0.7 $torr^{-1}$. This sample had 60% of the cobalt in the zeolite present as active cobalt(II) complex.

When the deoxygenation temperature was increased to 400°C, there was a marked decrease in the amount of active cobalt(II) complex. The final 100 degree increment decreased the oxygen chemisorption capacity by a factor of 50% from 2.94 to 1.51 $\pm$ 0.18 cc O_2 per gram. This material does apparently have a thermal stability limit at which some of the cobalt(II) complexes are partially deactivated toward reversibly binding oxygen. The deactivation temperature based on this study was somewhere between 300 and 400°C.

In order to find this thermal limit, another sample was prepared in DMF and tested using gas uptake measurements. This sample was prepared by reacting CsCoY ($Cs_{20.4}Co_{4.0}Na_{27.6}Y \cdot 123H_2O$) with KCN (5:1 CN/Co ratio) in DMF for 96 hours. In this study (Table 2-12), the maximum deoxygenation time was seven hours. After this sample was deoxygenated seven hours at 300°C, the material chemisorbed 3.39$\pm$

Table 2-12. Temperature Studies on Sample Prepared in DMF.

Temp (°C)	Deoxy Time (hrs)	$[Co]_t$ (mmol/g)	K_{O_2} ($torr^{-1}$)	O_2 Chemi (cc O_2/g)
300[a]	7.0	0.151 ± 0.004	59.6 ± 1.8	3.39 ± 0.09
325[a]	7.0	0.145 ± 0.003	71.2 ± 1.8	3.24 ± 0.07
350[a]	7.0	0.110 ± 0.007	71.9 ± 4.4	2.45 ± 0.15
350	2.0	0.165 ± 0.023	4.52 ± 0.36	3.68 ± 0.18
350[b]	2.0	0.146 ± 0.001	4.54 ± 0.30	3.29 ± 0.01

Sample Preparation:

CsCoY ($Cs_{20.4}Co_{4.0}Na_{27.6}Y \cdot 123H_2O$, azeotrope dried) + KCN (5:1 CN/Co ratio), 96 hrs

a: consecutive runs made on same sample

b: pre-treated CsCo(CN)-Y with H_2 1.5 hrs. @ 350° C

0.09 cc of O_2 per gram and had a K_{O_2} of 59.6 $\pm$ 1.8 $torr^{-1}$. When the same sample was deoxygenated for seven hours at 325°C, 3.24 $\pm$ 0.07 cc of O_2 per gram were chemisorbed with a K_{O_2} of 71.2 $\pm$ 1.8 $torr^{-1}$. Continuing on with the same sample, after deoxygenation for seven hours at 350°C, the material showed a decrease in chemisorption capacity, with a decrease to 2.45 $\pm$ 0.15 cc O_2 per gram, while K_{O_2} was found to be 71.9 $\pm$ 4.4 $torr^{-1}$. The curves used to determine the K_{O_2} and $[Co]_t$ for the runs made after deoxygenation at 300 and 325°C are seen in Figures 2-16 and 2-17. The data suggested that the thermal deactivation point for this sample is 350°C.

To test this, starting with virgin material, the sample was deoxygenated at 350°C but only for two hours. The material chemisorbed 3.69 $\pm$ 0.18 cc of O_2 per gram (0.165 $\pm$ 0.023 mmoles of active cobalt(II) complex), with a K_{O_2} of 4.52 $\pm$ 0.36 $torr^{-1}$. At this point, this was the highest amount of oxygen chemisorbed by our material. It became evident from all the experiments in DMF that the deoxygenation temperature not only had an affect on how much oxygen the sample would chemisorb, but also the affinity for oxygen reflected in the equilibrium constant for oxygen binding. Both of these behaviors are readily explained if this work is considered in comparison to the work disclosed in the previously mentioned Air Products patent.[106]

Ramprasad and co-workers claim that their solid state cyanocobaltate complexes could be activated toward binding oxygen reversibly by either heating at elevated temperatures or by drawing a vacuum on the solid to remove a portion of

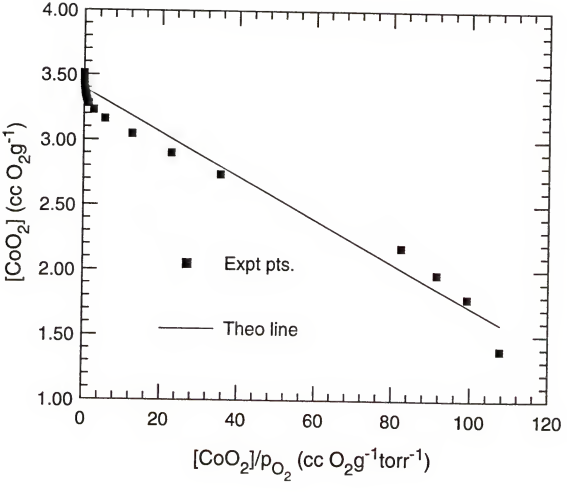

Figure 2-17. K_{O_2} and $[Co]_t$ for CsCo(CN)-Y Dexoygenated Seven Hours at 300°C.

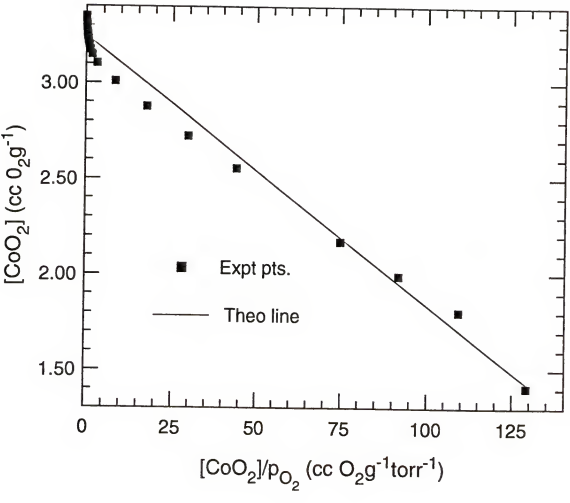

Figure 2-18. K_{O_2} and $[Co]_t$ Plot for CsCo(CN)-Y Deoxygenated Seven Hours at 325°C.

the ligand S (refer back to formula located on page 102). For example, three samples were prepared:[106] $Li_3[Co(CN)_5]\cdot 3.5DMF$ (Sample I), $Li_3[Co(CN)_5]\cdot 2DMF$ (Sample II), and $Li_3[Co(CN)_5]$ (Sample III). Sample I chemisorbed 0.15 mmoles O_2/gram; sample II, 1.5 mmoles O_2/g; and sample III, did not chemisorb O_2 at all. The same trend is occurring in the zeolite case. As the deoxygenation temperature is increased, the number of DMF molecules within the zeolite cages or on the surface decrease. Oxygen is not impeded by blocked pores and has easy accessibility to all the active complexes. Up to a certain point (300°C, 24 hours in the first study, 350°C for 2 hours in the second), increased chemisorption capacity is observed. By recycling under vacuum at elevated temperatures (above 350°C, the complexes start to decompose, resulting in a decrease in the amount of oxygen chemisorbed.

Ramprasad and co-workers[106] also believed that the ability of their complexes to reversibly bind oxygen was made possible because the countercations', $[(A)_a(R_4N)_b]^{z+}$, interactions with the nitrogen of the cyanide ligand to form Co-CN-A^{z+} linkages, with the coordinating ligand S (DMF, for example) moderating the interaction. This entire interaction affects the electron density on the cobalt and therefore has an effect on the complexes affinity for oxygen. This is ultimately reflected in the equilibrium constant for oxygen binding.

The explanation for the observed increase in K_{O_2} with increased deoxygenation temperatures over prolonged periods of time is as follows. As the deoxygenation temperature increases, more DMF is removed. As the DMF is removed, the interaction between DMF and the countercations present (Na^+, Cs^+,

and possibly H^+ or Co^{2+}) decreases as the interaction between the countercations and $Co(CN)_5^{3-}$ increases. In the zeolite's anionic framework, the way to stabilize the anionic $Co(CN)_5^{3-}$ is through greater interaction with the countercations.

This stabilization is reflected in the greater affinity of the complexes to bind oxygen, or in other words, K_{O_2} increases. Deoxygenation at 325°C for seven hours removes more DMF molecules than deoxygenation at 350°C for two hours. Hence, the first example has a K_{O_2} of 71.2 $\pm$ 1.8 $torr^{-1}$, while the second is only 4.52 $\pm$ 0.36 $torr^{-1}$. Because in the first example interaction between DMF and countercations is less, $Co(CN)_5^{3-}$ has greater stabilization in the anionic framework. This is reflected in the larger K_{O_2} value.

Synthesis in DMF with NaCN versus KCN

Attempts were made in DMF to use NaCN as the cyanide salt to form quantities of active cobalt(II) complex comparable to what was observed using KCN. Aprotic dried CsCoY was reacted with NaCN (CN/Co ratio was either 5:1 or 10:1) with a cyanide reaction time from 96 to 192 hours. The resulting CsCo(CN)-Y materials, deoxygenated two hours at 350°C, however, did not chemisorb as much oxygen as some of the early samples prepared with methanol or water as the solvent. For example, one synthesis which had a cyanide reaction time of 168 hours only chemisorbed 0.26 $\pm$ 0.05 cc of O_2 per gram, while another which had a cyanide reaction time of 192 hours only chemisorbed 0.43 $\pm$ 0.05 cc of O_2 per gram. These represent the best results obtained using NaCN in DMF.

The infrared spectra for these materials show two bands, a sharp peak at 2121 cm^{-1}, which was assigned to $Co(CN)_5O_2^{3-}$ and a sharp peak at 2170 cm^{-1}. The major band is in fact at 2170 cm^{-1}, with the 2121 cm^{-1} being the minor peak. The oxygen adsorption data coupled with this IR data suggests that with NaCN as the cyanide source in DMF, the major product formed is $Co(CN)_2$. No band was observed at 2131 cm^{-1}, ruling out the possibility of formation of $Co(CN)_6^{3-}$

The color of the CsCo(CN)-Y product material also points to the formation of $Co(CN)_2$ being the major product. The CsCo(CN)-Y was not the characteristic tan brown color as has been observed in the past, but instead was blue. $Co(CN)_2$ is also blue. The overall conclusion is that in DMF as the reaction solvent, the choice of cyanide salt is critical for formation of the active $Co(CN)_5^{3-}$. KCN leads to significant amounts of $Co(CN)_5^{3-}$, while NaCN leads to the formation of $Co(CN)_2$.

Cyanide Addition in Acetonitrile to Aprotic Dried CsCoY

Samples were prepared in acetonitrile using KCN and NaCN as was done in the DMF experiments, with a cyanide to cobalt ratio of five to one. Reaction time of CsCoY and the cyanide salt varied between 24 and 168 hours. Deoxygenation of the samples was done at temperatures of 300-350^{0}C for between one and two hours. In the work done using acetonitrile as solvent, new variations were tested in the preparation of the CsCoY starting material, including cesium exchange before cobalt (instead of the customary cobalt then cesium exchange) and simultaneous exchange of cobalt and cesium. A new pre-treatment of CsCo(CN)-Y with hydrogen at

elevated temperatures which increases the chemisorption capacity of the materials was discovered. Finally, experiments with calcium loading of the zeolite to selectively fill the ß-cages and increase the amount of cobalt residing in the α-cages was attempted using the novel drying procedure and cyanide addition in CH_3CN.

Characterization of CsCo(CN)-Y

Complete deoxygenation of samples prepared in acetonitrile was accomplished by evacuation at 150°C for 10 minutes in which the tan-orange CsCo(CN)-Y solid becomes a blue-grey color with the removal of oxygen. Deoxygenated samples yielded an EPR spectra (obtained at 110K characteristic of $Co(CN)_5^{3-}$ (see Figure 2-10)). The samples were also deoxygenated repeatedly through many cycles at temperatures between 150- 350°C with no loss of signal integrity or intensity.

CsCo(CN)-Y samples prepared in acetonitrile consistently showed two bands in the infrared spectra. The first peak was observed at 2120-2125 cm^{-1} and was attributed to ν_{cm}-1 for $Co(CN)_5O_2^{3-}$. This sharp band represents the major peak in the spectra. The variance in the location of the band was attributed to the degree of solvation of the zeolite sample by water, CH_3CN or both. The second band, sharp but minor relative in intensity to the first appeared at 2167-2170 cm^{-1}. This band was attributed to $Co(CN)_2$, which has a ν_{cm}-1 reported[115] at 2165 cm^{-1}. As was the case with DMF as the solvent, no band was observed at 2131 cm^{-1}, indicative of the formation of $Co(CN)_6^{3-}$.

The acetonitrile prepared samples were also characterized using UV/visible spectroscopy. Nujol mull prepared solids yielded spectra characteristic of what is

seen in Figure 2-19. Based on a standard check, any bands appearing at wavelengths less than 250 nm may be attributed to acetonitrile. Similar to what was observed for CsCo(CN)-Y prepared in DMF, the spectra have two bands. The first major band has a k_{max} at 320 nm, while there is a shoulder at around 390 nm. These values agree with those observed for $Co(CN)_5O_2^{3-}$ in acetonitrile solution in work by Gubelmann and co-workers.[116] They reported seeing three bands in CH_3CN: 530 nm (metal-to-ligand charge transfer), 400 nm (d-d transition), and 320 nm (ligand-to-metal charge transfer). These data again suggest that the assignment of $Co(CN)_5^{3-}$ as the active cobalt(II) complex is indeed a valid one.

Another Synthetic Variation in Acetonitrile: Preparation of CsCoY

Up to this point, the preparation of the CsCoY was done by exchanging Co^{2+} into NaY as the chloride salt at 70°C, with a loading of eight cobalts per unit cell. This is readily accomplished and has been verified by atomic adsorption spectroscopy. The second step has been to exchange with 0.1 M aqueous CsCl three times to ensure that the maximum amount of Cs^+ is exchanged into the zeolite. However, typically the cesium exchange step leads to loss of up to nearly 60% of the cobalt. This was observed by Taylor[97] using ion coupled plasma spectroscopy (ICP) and verified in this work by atomic adsorption. An alternate synthetic route to increase the loading of Co^{2+} in the zeolite was to exchange the cesium first followed by exchange with cobalt.

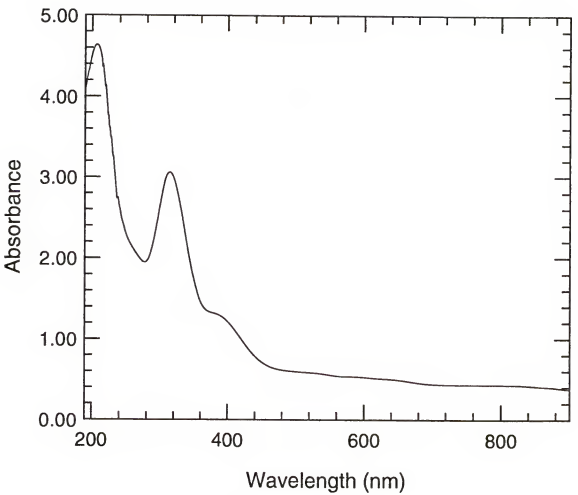

Figure 2-19. Ultraviolet/Visible Spectrum for CsCo(CN)-Y Prepared in CH_3CN.

Another important factor considered was the amount of time to prepare the starting CsCoY material. Sodium, cobalt, and cesium exchanges ultimately add up to five days of work, coupled with at least three days of stirring in the appropriate aprotic solvent, and three days of reflux/distillation with benzene. Coupled with the potential of four days of reaction time with the cyanide salt in aprotic solvents, the total reaction time for a sample is easily over two weeks. Perhaps the synthesis could shortened by three days if the metal exchange steps were shortened by doing sodium exchange followed by simultaneous exchange of cobalt and cesium.

Using the exact same solution volumes, equivalents of exchanged metal cations, and slurrying times, CsCoY samples were prepared by three different methods. In the first method (I), cobalt was exchanged at 70°C, followed by three exchanges with 0.1 M aqueous CsCl at room temperature. In the second method(II), the order was reversed: three 0.1 M aqueous exchanges followed by aqueous cobalt exchange at 70°C. The third method (III) exchanged the cobalt and cesium simultaneously at room temperature. All samples were then dried using the aprotic/benzene drying method. All samples were then analyzed using atomic adsorption spectroscopy on the dissolved zeolite sample (see Experimental).
As a comparison a sample was prepared where only cobalt was exchanged at 70°C.

When only cobalt was exchanged, the unit cell formula was found to be $Co_{8.0}Na_{40.0}Y$. By the three methods, the unit cell composition was found to be as follows: method I, $Cs_{30.3}Co_{4.2}Na_{17.3}Y$; method II, $Cs_{23.9}Co_{8.0}Na_{16.1}Y$; method III, $Cs_{22.2}Co_{6.4}Na_{21.0}Y$. It is no surprise that in method II, there are eight cobalts per

unit cell because what happens in method I happens most likely in method II, except the case of method II the cobalt exchanges out some of the cesium. What was impressive and somewhat surprising was that using method III (simultaneous exchange), the cobalt composition is halfway between that of method I and II (6.4 (III) versus 4.2 (I) and 8.0 (II)), yet the synthesis time was decreased by three days.

Simultaneous exchange of cobalt and cesium at room temperature for longer periods of time (greater than 24 hours) or at 70°C resulted in no significant increases in the amount of cobalt or cesium exchanged into the zeolite, but in fact resulted in decreases of the amounts of cesium and cobalt present in the zeolite. For example, a sample prepared identically as above, yet where the simultaneous exchange at room temperature was allowed to stir for 48 hours resulted in a unit cell composition of $Cs_{12.7}Co_{3.4}Na_{36.5}Y$. If the simultaneous cobalt and cesium exchange was performed at 70°C instead of room temperature for 24 hours, the unit cell composition was found to be $Cs_{11.4}Co_{4.9}Na_{34.8}Y$.

Deoxygenation time and temperature variation

As was the case for CsCo(CN)-Y prepared in DMF, the solid was deoxygenated at elevated temperatures to see whether by removing the solvent the oxygen chemisorption capacity could be increased. The thermal stability limit for desorption of these CsCo(CN)-Y materials could also be determined. Based on the results accumulated with DMF as solvent and the desire to draw conclusions using identical conditions, the deoxygenation starting point was 300°C.

Table 2-13 shows results of a temperature study performed in acetonitrile. CsCoY ($Cs_{24.4}Co_{5.8}Na_{20.0}Y$) was reacted with KCN (CN/Co ratio- 5:1) for 96 hours. The sample was started by deoxygenating seven hours at 300°C. Through gas uptake experiments, the material was found to chemisorb 1.75 $\pm$ 0.10 cc O_2/g with a K_{O_2} of 3.34 $\pm$ 0.17 $torr^{-1}$. The same sample was then subjected to runs after being deoxygenated for seven hours at 350°C and then 24 hours at 350°C. There was a slight increase in the amount of oxygen chemisorbed in both runs to 2.46 cc O_2/g, but the encouraging result was that there was no loss of activity by deoxygenation at 350°C, even after a desorption time of 24 hours. This had been the case in DMF.

Also encouraging was the behavior of K_{O_2}. The K_{O_2} remained relatively unchanged at 3.66 $\pm$ 0.17 $torr^{-1}$ (within experimental limits) after being deoxygenation at 350°C for seven hours, while there was a 23% increase in the K_{O_2} value to (4.49 $\pm$ 0.14 $torr^{-1}$) after the sample was deoxygenated at 350°C for 24 hours. Still, this is small compared to the enormous change displayed by the sample prepared in DMF. The K_{O_2} value is much like that exhibited in samples prepared in methanol.

As a final point of comparison, a fresh amount of the sample was deoxygenated two hours at 350°C. Again, the sample chemisorbed 2.42 cc O_2/g, and had a K_{O_2} value of 4.32 $\pm$ 0.20 $torr^{-1}$. Unlike the sample prepared in DMF, deoxygenation of this sample does not affect the chemisorption capacity. There is some change in the K_{O_2} value, but this change is relatively minor. The key point

Table 2-13. Temperature Studies on Sample Prepared in Acetonitrile.

Evacuation Procedure	K_{O_2} ($torr^{-1}$)	O_2 Chemi (cc O_2/g)
7 hrs @ 300°C[a]	3.34 ± 0.17	1.75 ± 0.10
7 hrs @ 350°C[a]	3.66 ± 0.17	2.46 ± 0.15
24 hrs @ 350°C[a]	4.49 ± 0.14	2.45 ± 0.20
2 hrs @ 350°C	4.32 ± 0.20	2.42 ± 0.13

Sample Preparation:
CsCoY ($Cs_{24.4}Co_{5.8}Na_{20.0}Y \cdot 109H_2O$, azeotrope dried) + KCN (5:1 CN/Co ratio) for 96 hours

a: consecutive runs made on same sample

here is the reproducibility after repeated cycling regardless of the deoxygenation conditions the sample encounters. The $Co(CN)_5^{3-}$ complex prepared in acetonitrile appears not to be thermally deactivated towards reversibly binding oxygen, at least under conditions where the DMF prepared $Co(CN)_5^{3-}$ was partially deactivated.

One other sample was prepared using acetonitrile which had a high affinity for oxygen. This sample was prepared using azeotrope dried (CH_3CN/C_6H_6) CsCoY ($Cs_{35.7}Co_{5.6}Na_{9.1}Y$) added to KCN (CN/Co ratio 5:1) in CH_3CN for 96 hours. The resulting CsCo(CN)-Y material was found to chemisorb 3.40 $\pm$ 0.10 cc O_2/g and had a K_{O_2} value of 3.38 $\pm$ 0.21 $torr^{-1}$. The room temperature gas adsorption isotherm curves for this sample, as well as the plot used to determine the K_{O_2} value, are shown in Figures 2-20 and 2-21. This sample had an oxygen capacity similar to that observed for DMF, and like that sample, the amount of $Co(CN)_5^{3-}$ complex (0.152 $\pm$ 0.005 mmol/g) was significantly increased over that seen using protic solvents. This sample was oxygenated and deoxygenated (one hour at 350°C) and showed reproducibility in the amount of active $Co(CN)_5^{3-}$ and the K_{O_2} value through three cycles.

There is one final point worth noting here. Nearly a full cc of oxygen is gained in the second sample over the first. If you look at the starting CsCoY material composition, they both contain essentially the same amount of cobalt cations per unit cell (5.8 and 5.6). The difference is in the cesium present in the zeolite. The one cc of oxygen chemisorption capacity is gained by having more cesium (11.3

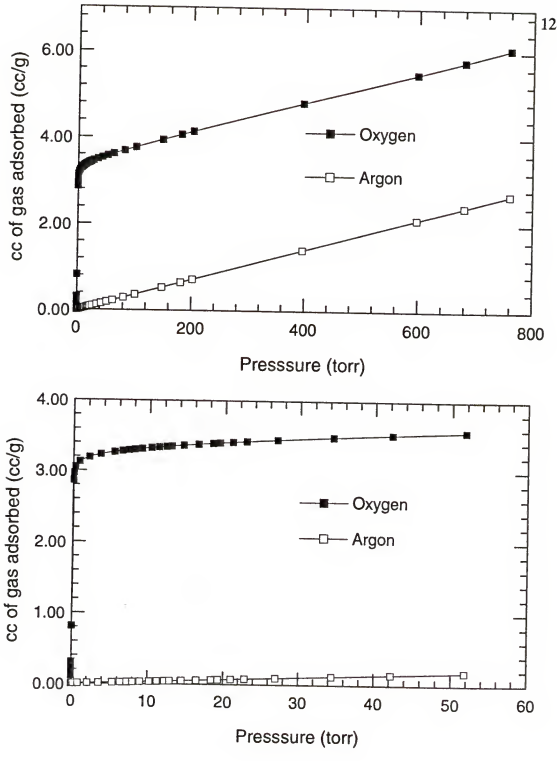

Figure 2-20. Gas Adsorption Isotherms for CsCo(CN)-Y Prepared in CH_3CN.

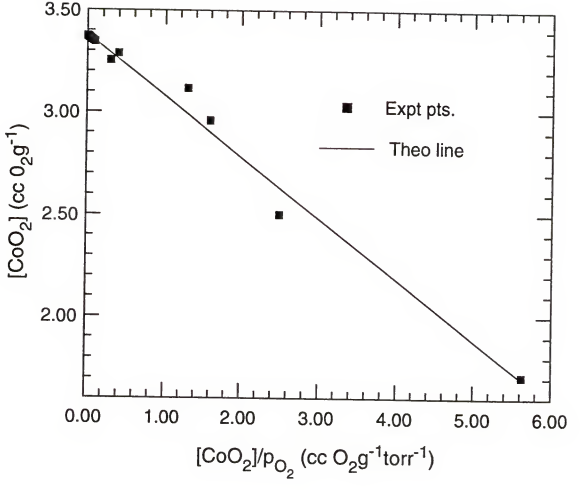

Figure 2-21. K_{O_2} and $[Co]_t$ Plot for CsCo(CN)-Y Prepared in CH_3CN.

more cesium cations) per unit cell. This further verifies that cesium plays a vital role in formation and stabilization of $Co(CN)_5^{3-}$. The trend of oxygen chemisorption capacity based on the amount of cesium present in the zeolite will be discussed in greater detail.

Synthesis in Acetonitrile with NaCN versus KCN

Attempts were made in acetonitrile to use NaCN as the cyanide salt to form quantities of active cobalt(II) complex comparable to what was observed using KCN. The best synthetic preparation with NaCN involved reacting aprotic dried $CoCsY$ ($Cs_{21.4}Co_{6.1}Na_{22.4}Y$) and NaCN (5:1 CN/Co ratio) in CH_3CN for 48 hours. The sample was deoxygenated for one hour at 350°C under vacuum, chemisorbed 1.86 $\pm$ 0.02 cc O_2/g and had a K_{O_2} of 4.39 $\pm$ 0.36 $torr^{-1}$.

The NaCN results were encouraging especially when compared to the results in DMF. However, with NaCN, the amount of active $Co(CN)_5^{3-}$ complex per gram of material is 45% less than the best synthetic preparation using KCN. Again, the data suggests that the potassium cation is favoring increased stabilization of the $Co(CN)_5^{3-}$ complex over sodium, either through size effects (immobilization of the complex in the zeolite cage) or through stabilization of the complex by interaction with the solvent. Regardless of exactly what is the cause of the stabilization, the fact is clear that when using aprotic solvents for the cyanide addition step, KCN leads to formation of greater concentrations of active cobalt(II) complex.

This previous statement holds true if there is no consideration of pre-treatment of the zeolite prior to gas adsorption. Quite by chance, it was discovered

that if a CsCo(CN)-Y sample (prepared in CH_3CN using NaCN) that had a low concentration of $Co(CN)_5^{3-}$ present (i.e., low chemisorption of O_2) was heated to 350°C under flowing hydrogen for 1.5 hours and then deoxygenated at 350°C under vacuum for one hour showed an enormous increase in the amount of oxygen chemisorbed by the sample. Some of the hydrogenated CsCo(CN)-Y materials showed increases in their oxygen chemisorption capacity of over 500%. The focus of this research project became to study the hydrogenation process, determine what exactly was occurring to account for the increased activity, and whether the process was reversible.

Hydrogenation Pretreatment of CsCo(CN)-Y

Characterization of hydrogenated CsCo(CN)-Y

The first experiment that was performed after the discovery of this hydrogenation phenomenon was hydrogenation of the starting CsCoY material. This was done in order to see if any cobalt hydrido species were forming in the zeolite then binding with oxygen to form a Co-O-O-H peroxy species. As you can see from Figure 2-22, the oxygen adsorption isotherm for a sample of hydrogen treated CsCoY showed a Type I isotherm characteristic of physisorption. No chemisorption can therefore be attributed to simply a cobalt or cobalt hydrido species in the zeolite.

The next step was to see if the hydrogenation step was acting as a cleansing step orienting the cobalt complexes within the cages, decreasing the interaction with

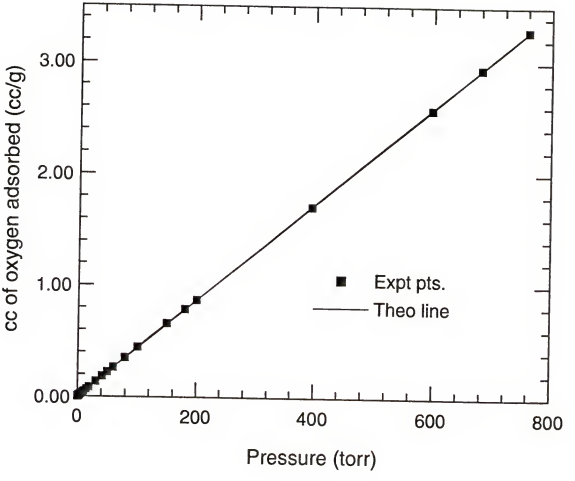

Figure 2-22. Gas Adsorption Isotherm for Hydrogenated CsCoY.

any solvent molecules (or H_2O) present and increasing the interaction with cations, thereby stabilizing the anionic complex. Perhaps this hydrogenation step was acting much in the manner that heating under vacuum samples prepared in DMF did (removing solvent increased the amount of chemisorbed oxygen). To test this, the series of pre-treatments and gas adsorption runs seen in Table 2-14 were performed. Please note that all these experiments were performed on the same sample in sequential order, and in each case the same was deoxygenated for one hour at 350°C.

The first adsorption run (no treatment) showed the sample chemisorbed only 0.89 ± 0.09 cc of O_2/g and had a K_{O_2} of 9.67 ± 0.59 torr^{-1}. In order to test whether the increase in activity of the CsCo(CN)-Y was due to perhaps having a flowing gas over the zeolite at an elevated temperature, nitrogen was purged over the sample at 350°C for 1.5 hours. This resulted in a slight increase in the amount of oxygen chemisorbed to 1.28 ± 0.11 cc O_2/g, while K_{O_2} was measured to be 8.12 ± 0.37 torr^{-1}. When the sample was hydrogenated at 350°C then evacuated, the sample chemisorbed 5.19 ± 0.24 cc O_2/g with a K_{O_2} measured to be 7.25 ± 0.31 torr^{-1}. The gas isotherms and the plot used to determine K_{O_2} are shown in Figure 2-23 (a) and (b).

The hydrogenation procedure increased the amount of active cobalt complex by nearly 500%. This represented the highest amount of active cobalt complex ever prepared in a sample (0.232 ± 0.010 mmol/g). After the run in which the sample chemisorbed over five cc of oxygen, the sample was simply deoxygenated at 350°C for one hour and re-run. However, this time the sample only chemisorbed 2.50

Table 2-14. Hydrogenation Study on Sample Prepared in Acetonitrile.

Pre-Treatment Conditions	K_{O_2} ($torr^{-1}$)	O_2 Chemi (cc O_2/g)
none	9.67 ± 0.59	0.89 ± 0.09
1.5 hrs flowing N_2 @ 350°C	8.12 ± 0.37	1.28 ± 0.11
1.5 hrs flowing H_2 @ 350°C	7.25 ± 0.31	5.19 ± 0.24
none	8.65 ± 0.43	2.50 ± 0.19
1.5 hrs flowing H_2 @ 350°C	10.3 ± 0.4	5.68 ± 0.15
stirred in CH_3CN	7.44 ± 0.34	3.52 ± 0.17
1.5 hrs flowing H_2 @ 350°C	11.3 ± 1.5	5.60 ± 0.24
1.5 hrs flowing H_2 @ 350°C	9.48 ± 0.66	5.20 ± 0.22
1.5 hrs flowing H_2 @ 350°C	4.47 ± 0.33	4.20 ± 0.26

Sample Preparation:

CsCoY ($Cs_{33.4}Co_{6.3}Na_{10.0}Y \cdot 142H_2O$, azeotrope dried) + NaCN (5:1 CN/Co ratio for 48 hours).

Runs performed on same sample in sequential order. In each run, the sample was deoxygenated under 10^{-6} torr vacuum @ 350°C for one hour.

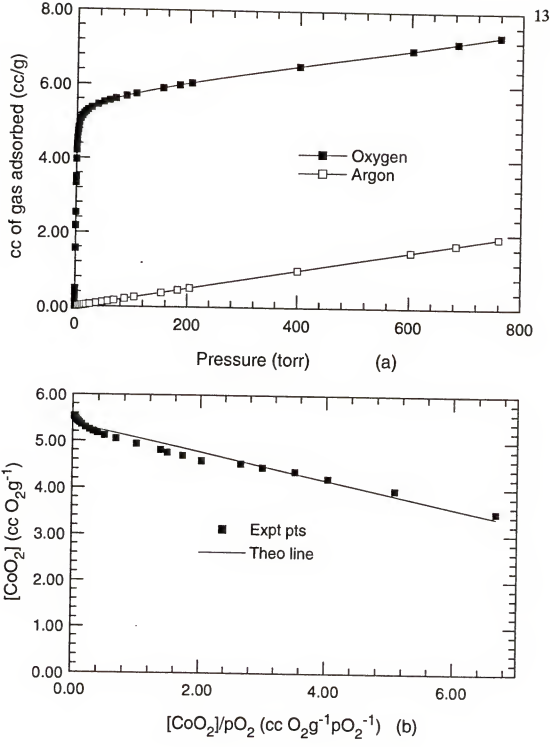

Figure 2-23. Experimental Curves after Hydrogenation of CsCo(CN)-Y (a) Gas Adsorption Isotherms; (b) K_{O_2} and $[Co]_t$ Curve.

$\pm$ 0.19 cc O_2/g, a decrease of 50% with a K_{O_2} measured to be 8.65 $\pm$ 0.43 $torr^{-1}$. However, upon hydrogenation and deoxygenation on the next run, the sample was found to have chemisorbed 5.68 $\pm$ 0.15 $torr^{-1}$ cc O_2/g with a K_{O_2} measured to be 10.3 $\pm$ 0.4 $torr^{-1}$. The data suggest that this high capacity for oxygen is only completely reversible if the sample is rehydrogenated after each oxygenation step and prior to the deoxygenation step.

Prior to the sixth cycling run with this sample, the solid was stirred in acetonitrile, then evacuated at 350°C. This was done in order to see if perhaps re-solvating the sample after the hydrogenation step would help us to achieve the high capacity reversibility without the need to rehydrogenate the material again. However, this was not the case. The sample was found to have chemisorbed only 3.52 $\pm$ 0.17 cc of O_2/g, a decrease of over 40%, with a K_{O_2} measured to be 11.3 $\pm$ 1.5 $torr^{-1}$. Yet, on the next two cycles in which the sample was hydrogenated the sample again chemisorbed over 5.00 cc of O_2/g.

After the eighth run, the amount of oxygen chemisorbed was found to be 5.20 $\pm$ 0.22 cc O_2/g, a slight decrease over the seventh run value which was determined to be 5.60 $\pm$ 0.24 cc O_2/g, but well within experimental limits. After hydrogenation and deoxygenation for the ninth run, the sample was found to have chemisorbed 4.20 $\pm$ 0.26 cc of O_2/g with a K_{O_2} measured to be 4.47 $\pm$ 0.33 $torr^{-1}$. This decrease in the amount of active cobalt complex by nearly 25%, coupled with the decrease in the equilibrium constant value suggested that the sample was finally being partially deactivated. The K_{O_2} value's decrease to 4.47 $torr^{-1}$, which had in the previous eight

runs ranged in value between 7.25- 11.3 $torr^{-1}$, was a definite sign of deactivation of the complex towards oxygen binding. This is much like what was seen with the DMF experiments where upon partial deactivation by elevated desorption temperatures caused a decrease in the K_{O_2} value. The reason why the hydrogenation step was eventually causing loss of activity for oxygen binding was discovered using observation and infrared spectroscopy.

The sample was taken and placed in a glass tube with a frit at one end which was then placed in an oven and heated to 350°C with hydrogen passing through the tube. As the off-gas was bubbled into a solution of aqueous Fe^{2+}/Fe^{3+}, a blue precipitate formed, indicating the presence of Prussian blue. This indicates that using the hydrogenation treatment at elevated temperatures causes HCN ejection from the zeolite. This behavior was shown to occur in any acetonitrile prepared sample that was subjected to hydrogenation at 350°C.

The previously mentioned sample which had been hydrogenated and gone through ten adsorption/desorption cycles was also analyzed at various points by infrared. Shown in Figure 2-24 (a-c) are three infrared spectra taken of the sample during the oxygenation/deoxygenation cycles. The first spectrum (a) is the sample prior to any heating under vacuum or hydrogenation. There are two sharp bands: the first major peak at 2125 cm^{-1} attributed to the active cobalt(II) complex and the second minor peak at 2170 cm^{-1} attributed to $Co(CN)_2$. After being hydrogenated, deoxygenated, then oxygenated through two cycles, spectrum (b) is obtained. In this case, the peaks are nearly equal in intensity with the band in this case at 2172 cm^{-1}

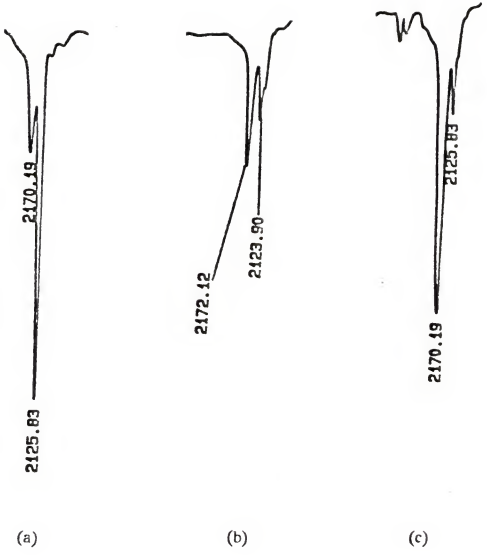

Figure 2-24. Infrared Spectra of a Hydrogenated Sample (a) Prior to H_2 Treatment; (b) After H_2 Treatment #2; (c) After H_2 Treatment #5.

being the major peak, while the band at 2125 cm^{-1} being the minor peak. Finally, after being hydrogenated, deoxygenated, then oxygenated through five cycles, spectrum (b) is obtained. Now, clearly the band at 2170 cm^{-1} is the major peak, while the band at 2125 cm^{-1} is the minor peak.

The data suggest that as the sample is continuously hydrogenated, HCN is ejected from the zeolite. In the initial stages, apparently this is leading to activation of cobalt that is either uncoordinated to cyanide or is present as $Co(CN)_2$ or $Co(CN)_3^-$ which both would not coordinate with oxygen. Another explanation could be that HCN removal leads to formation of $Co(CN)_5^{3-}$ from $Co(CN)_6^{3-}$, with hydrogen being oxidized and cobalt being reduced from the +3 to the +2 oxidation state. This is a viable hypothesis, but there is no indication of any $Co(CN)_6^{3-}$ present initially. Perhaps, the response to this is that in this system, the $Co(CN)_6^{3-}$ and $Co(CN)_5O_2^{3-}$ infrared bands overlap one another. Hence $Co(CN)_5O_2^{3-}$ and $Co(CN)_6^{3-}$ are both decreased by hydrogenation and thus the marked decrease of the band at 2125 cm^{-1}.

Another interesting phenomenon is occurring during the hydrogenation which was uncovered by analyzing the CsCo(CN)-Y samples before and after hydrogenation and determining their magnetic susceptibilities. Shown in Table 2-15 are the sample compositions, O_2 chemisorption data and μ_{eff} values for various. NaY has a negative χ_g value due to the fact it is diamagnetic and also contains water. CsCoY samples (A-E in Table 2-15) are paramagnetic because they contain Co^{2+}, with a d^7

Table 2-15. Magnetic Susceptibility Results for CoY, CsCoY and CsCo(CN)-Y.

Sample	Type	O_2 Chemi (cc O_2/g)	χ_g (c.g.s.)	μ_{eff} (B.M.)
NaY	NaY	-	-4.48×10^{-7}	-
A	CoY	-	$+2.04 \times 10^{-6}$	4.4
B	CsCoY	-	$+5.58 \times 10^{-6}$	3.4
C	CsCoY	-	$+3.34 \times 10^{-6}$	3.6
D	CsCoY	-	$+3.90 \times 10^{-6}$	4.5
E	CsCoY	-	$+5.36 \times 10^{-6}$	4.7
F	CsCo(CN)-Y		$+4.89 \times 10^{-7}$	1.2
F, H_2 treated		3.40	$+1.81 \times 10^{-4}$	24.9
G	CsCo(CN)-Y		$+1.10 \times 10^{-6}$	2.5
G, H_2 treated		5.68	$+9.17 \times 10^{-6}$	5.1
H	CsCo(CN)-Y		$+1.43 \times 10^{-6}$	3.1
H, H_2 treated		3.95	$+2.30 \times 10^{-4}$	41.2
I	CsCo(CN)-Y		$+1.00 \times 10^{-6}$	2.5
I, H_2 treated		3.57	$+2.44 \times 10^{-4}$	41.4
J	CsCo(CN)-Y		$+1.80 \times 10^{-6}$	3.4
J, H_2 treated		3.52	$+1.72 \times 10^{-5}$	10.8
K	CsCo(CN)-Y		$+3.90 \times 10^{-7}$	1.4
K, H_2 treated		4.90	$+1.07 \times 10^{-4}$	40.8

Table 2-15 (cont)

Sample	Type	O_2 Chemi (cc O_2/g)	χ_g (c.g.s.)	μ_{eff} (B.M.)
L	CsCo(CN)-Y	3.24	$+4.80 \times 10^{-7}$	1.7
L, H_2 treated			$+2.12 \times 10^{-4}$	37.7
M	CsCo(CN)-Y		$+8.68 \times 10^{-7}$	2.8
M, H_2 treated		5.31	$+1.02 \times 10^{-4}$	37.8
N	CsCo(CN)-Y		$+5.68 \times 10^{-7}$	1.8
N, H_2 treated		3.52	$+2.56 \times 10^{-4}$	41.3

A: $Co_{8.0}Na_{40.0}Y·186H_2O$

B: $Cs_{15.2}Co_{3.0}Na_{34.8}Y·116H_2O$

C: $Cs_{25.8}Co_{8.0}Na_{14.2}Y·184H_2O$

D: $Cs_{23.9}Co_{8.0}Na_{16.1}Y·150H_2O$

E: $Cs_{14.1}Co_{5.1}Na_{30.9}Y·131H_2O$

F: $Cs_{35.7}Co_{5.6}Na_{9.1}(KCN)_{15.4}Y$

G: $Cs_{33.4}Co_{6.3}Na_{10.0}(NaCN)_{32.5}Y$

H: $Cs_{31.5}Co_{7.1}Na_{10.3}(NaCN)_{18.8}Y$

I: $Cs_{19.4}Co_{5.5}Na_{25.6}(NaCN)_{14.3}Y$

J: $Cs_{21.4}Co_{6.1}Na_{22.3}(NaCN)_{15.5}Y$

K: $Cs_{15.4}Co_{6.5}Na_{27.6}(NaCN)_{19.0}Y$

L: $Cs_{16.7}Co_{5.4}Na_{28.5}(NaCN)_{7.6}Y$

M: $Cs_{38.0}Co_{6.1}Na_{5.8}(NaCN)_{26.5}Y$

N: $Cs_{11.7}Co_{3.5}Na_{37.3}(NaCN)_{10.0}Y$

high spin electronic configuration, containing three unpaired electrons. The μ_{eff} values range from 3.6- 4.7 Bohr magnetons which corresponds rather well with the μ_{eff} values of 4.3- 5.2 B.M. for Co^{2+} found in the literature[117] (three unpaired electrons).

Samples F-N are CsCo(CN)-Y samples prepared in acetonitrile. The magnetic susceptibility of these samples was determined before and after the hydrogenation treatment. CsCo(CN)-Y samples prior to hydrogenation have μ_{eff} values in the range of 1.2- 3.4 B.M. The value for Co^{2+}, d^7, low-spin with one unpaired electron is reported in the literature to be 1.7- 2.7 B.M. which agrees fairly well with our experimentally determined numbers (which are not corrected for the diamagnetic effects of water in the zeolite). The result of greatest interest is the μ_{eff} values obtained after hydrogenation. The values range from 5.1- 41.2, with most of the measured values hovering around 10, 20 and 30 B.M. The only possible explanation is that a small amount of the free cobalt that is not bound to cyanide in the zeolite is being reduced to cobalt metal. Cobalt metal, being ferromagnetic, would account for these enormous values. Both Ni^{2+} and Pd^{2+} have been exchanged into NaX zeolites and then reduced by hydrogen at 400° C to give the metal dispersed Pd^0 and Ni^0X.[118]

To summarize thus far, hydrogenation of CH_3CN prepared samples at 350°C leads to large increases in the amount of O_2 pickup. However, for the complexes to give repeated, high levels of O_2 adsorption, it is necessary to hydrogenate and evacuate at 350°C before adsorption. Eventually, the complexes are deactivated

because repeated hydrogenation at elevated temperature leads to expulsion of HCN from the zeolite and eventual formation of the inactive $Co(CN)_2$. The hydrogenation step also appears to reduce any uncomplexed Co^{2+} to cobalt metal. It should also be pointed out here that the hydrogenation pretreatment did not have any affect on either the K_{O_2} or the amount of O_2 pickup for a sample prepared in DMF (refer to Table 2-12).

Synthetic variation and the effects of hydrogenation

Continuing the studies of the hydrogenation treatment, the next logical step seemed to be to combine synthetic variation with the hydrogenation treatment to see if indeed the goal of 10 cc of O_2 chemisorption per gram was attainable even though reversibility over hundreds of cycles was questionable. The results for this synthetic variation study are given in Table 2-16. Two starting materials were used CsCoY (with a unit cell content of $Cs_{30.3}Co_{4.2}Na_{17.3}Y$) and CoCsY (with a unit cell content of $Cs_{23.9}Co_{8.0}Na_{16.1}Y$). Obviously, the more cobalt present in the zeolite, the higher the potential to form the active cobalt(II) complex.

Another variable studied was introduction of hydrogen into the solution during the cyanide addition step in CH_3CN. It was speculated that perhaps the hydrogen treatment was forming the pentacyanocobaltate(III) hydrido species, $Co(CN)_5H^{3-}$. This would readily react with O_2 to irreversibly form the $Co(CN)_5OOH$,[102] which readily decomposes to $Co(CN)_5OH^{3-}$.[103] It would then readily form $Co(CN)_6^{3-}$ in the presence of cyanide. This would be one explanation for the nonreversibility of

Table 2-16. Synthetic Variation in Acetonitrile and Effects of Hydrogen Pre-Treatment.

Starting Material	H_2 in synth	H_2 pre-treat	K_{O_2} ($torr^{-1}$)	O_2 Chemi (cc O_2/g)	%Co Active
CsCoY[a]	no[c]	yes	3.86 ± 0.07	5.00 ± 0.05	85
	no[d]	no	3.55 ± 0.24	0.64 ± 0.03	11
	no[d]	yes	3.35 ± 0.15	5.37 ± 0.22	92
	no[e]	yes	4.34 ± 0.20	4.54 ± 0.27	78
CoCsY[b]	no[c]	yes	7.98 ± 0.29	3.57 ± 0.08	31
	yes[d]	no	4.39 ± 0.36	1.86 ± 0.02	16
	yes[d]	yes	6.86 ± 0.59	3.52 ± 0.53	30
	no[e]	yes	3.28 ± 0.26	3.95 ± 0.02	34

a: CsCoY- $Cs_{30.3}Co_{4.2}Na_{17.3}Y$

b: CoCsY- $Cs_{23.9}Co_{8.0}Na_{16.1}Y$

c: 24 hours cyanide reaction time

d: 48 hours cyanide reaction time

e: 96 hours cyanide reaction time

CN/Co ratio- 5:1

the sample. It goes from the hydrido to hexacyanocobaltate(III) and only hydrogen can take hexacyanocobaltate(III) back to $Co(CN)_5^{3-}$.

The first sample prepared from CsCoY ($Cs_{30.3}Co_{4.2}Na_{17.3}Y$) and NaCN reacted for 24 hours. The sample was found to chemisorb 0.64 $\pm$ 0.03 cc O_2/g with a K_{O_2} value of 3.55 $\pm$ 0.24 $torr^{-1}$. After the hydrogenation treatment, the same sample chemisorbed 5.00 cc O_2/g with a K_{O_2} value of 3.86 $\pm$ 0.07 $torr^{-1}$. Based on the amount of cobalt present in the starting material and the amount of oxygen chemisorption, only 11% of the cobalt is active initially. This increases to 85%, however, after hydrogenation. When the reaction time of CsCoY and NaCN was increased to 48 hours, this sample chemisorbed 5.37 $\pm$ 0.22 cc O_2/g with a K_{O_2} value of 3.35 $\pm$ 0.15 $torr^{-1}$ after undergoing hydrogenation. This represented an astonishing 92% of the cobalt present as the active $Co(CN)_5^{3-}$ complex.

The final sample prepared using CsCoY and NaCN reacted for 96 hours. This sample chemisorbed 4.54 $\pm$ 0.27 cc O_2/g with a K_{O_2} value of 4.34 $\pm$ 0.20 $torr^{-1}$ after undergoing hydrogenation. This translates to 78% of the cobalt present as the active $Co(CN)_5^{3-}$ complex. The data suggests that the optimal amount of active complex is formed (with the hydrogenation treatment included) when the reaction time of CsCoY and NaCN in acetonitrile is 48 hours instead of 96 hours as was the case for non-hydrogenated samples. Furthermore, it is encouraging that up to 92% of the cobalt exchanged into the zeolite could be made active. However, the amount of O_2 pickup using CsCoY ($Cs_{30.3}Co_{4.2}Na_{17.3}Y$) was only half of what was desired. That was remedied by using a CoCsY sample that had eight Co^{2+} per unit cell.

The first sample prepared reacted CoCsY ($Cs_{23.9}Co_{8.0}Na_{16.1}Y$) and NaCN in CH_3CN for 24 hours. This sample chemisorbed 3.57 $\pm$ 0.08 cc O_2/g with a K_{O_2} value of 7.98 $\pm$ 0.29 $torr^{-1}$ after undergoing hydrogenation. This corresponds to 31% of the cobalt present chemisorbing O_2. The next sample prepared with a reaction time of 48 hours also had hydrogen bubbled into the reaction mixture during the synthesis. If indeed the hydrido species was the reactive complex, this would facilitate it's formation. The sample was found to chemisorb 1.86 $\pm$ 0.02 cc O_2/g with a K_{O_2} value of 4.39 $\pm$ 0.36 $torr^{-1}$. After the hydrogenation treatment at elevated temperatures, the same sample chemisorbed 3.52 $\pm$ 0.53 cc O_2/g with a K_{O_2} value of 6.86 $\pm$ 0.59 $torr^{-1}$. This equates to 16% of the cobalt present as the active complex with no hydrogenation treatment and 30% of the cobalt active after the hydrogenation treatment. The data suggest that the hydrido species is not the active complex which is binding with oxygen, or at least its formation is not facilitated or increased by having hydrogen present during the formation of $Co(CN)_5^{3-}$.

The final sample prepared using CoCsY ($Cs_{23.9}Co_{8.0}Na_{16.1}Y$) was reacted with NaCN for 96 hours. The sample was found to chemisorb 3.57 $\pm$ 0.08 cc O_2/g with a K_{O_2} value of 7.98 $\pm$ 0.29 $torr^{-1}$ after hydrogenation. This equates to 31% of the cobalt present as the active $Co(CN)_5^{3-}$ complex. An interesting conclusion can be reached here with the data obtained from the preparation and hydrogenation of these samples.

The data suggest that when there are four Co^{2+} per unit cell, over 90% of the cobalt can be converted into the active cobalt complex. Whenever there are eight

Co^{2+} per unit cell, the amount of active cobalt decreases by a factor of three to just over 30%. Either acetonitrile is not transporting the cyanide salt into the zeolite for coordination to cobalt or there is a tendency towards the hexacyano species. Another possible explanation for the observed data is that the cobalt is forming agglomerates of two or more in an α-cage. When the cobalt coordinates with cyanide, $Co(CN)_x^{y-}$ species start to form, but due to the sizes of the cage, $Co(CN)_5^{3-}$ cannot form. There is a definite trend based on zeolite composition as relates to oxygen capacity. This topic will be discussed in a later section.

Hydrogenation reversibility

Prior to the hydrogenation treatment experiment, $Co(CN)_5^{3-}$ in zeolite Y was regenerable and recyclable to repeated adsorption and desorption of oxygen regardless of which solvent it was prepared in or what cyanide salt was used. However, as has already been shown, the hydrogenation step is only recyclable if hydrogenation treatment precedes each desorption step. Furthermore, the hydrogenation treatment at 350°C is a dead end because of the expulsion of HCN leading to formation of inactive $Co(CN)_2$.

The large amounts of active cobalt(II) complex gained by the hydrogenation treatment step were very encouraging. A method was needed to make the process reversible over many cycles. One possibility was to perform the hydrogenation and subsequent evacuation at lower temperatures. The results of a study in which this was attempted are shown in Table 2-17.

Table 2-17. Hydrogen Pretreatment at Various Temperatures.

Temp (°C)	K_{O_2} ($torr^{-1}$)	O_2 Chemi (cc O_2/g)	curve diff @ 760 torr (cc O_2/g)
25	5.01 ± 0.44	2.07 ± 0.25	0.30
100	4.24 ± 0.33	2.07 ± 0.22	0.31
200	4.69 ± 0.25	1.94 ± 0.10	0.29
250	4.37 ± 0.26	2.92 ± 0.18	0.28
300	5.82 ± 0.41	5.71 ± 0.54	1.98
350	13.5 ± 1.5	5.31 ± 0.12	4.21

H_2 pretreatment: 1.5 hours H_2 treatment at specified temperature followed by evacuation at same temperature for 1.0 hour.

Sample Preparation:
$CsCoY$ ($Cs_{37.9}Co_{6.1}Na_{5.9}Y_{\ddot{a}}184H_2O$, azeotrope dried) + NaCN (5:1 CN/Co ratio) for 48 hours.

A CsCo(CN)-Y sample was prepared by reacting CsCoY ($Cs_{37.9}Co_{6.1}Na_{5.9}Y$) with NaCN (5:1 CN/Co ratio) for 48 hours in acetonitrile . In these experiments, the sample was hydrogenated at a set temperature, evacuated at that temperature and then oxygenated. Following oxygenation of the sample, it was evacuated again at room temperature for 15 minutes, then reoxygenated. This was done to see if after the initial hydrogenation at a lower temperature whether the sample could be regenerated by evacuation at room temperature. All runs were performed sequentially on the same sample.

After hydrogenating and evacuating the sample at 25, 100, and 200°C, the sample chemisorbed approximately 2.00 cc O_2/g with an equilibrium constant around 4.69 $torr^{-1}$. In each of these runs after the chemisorption of oxygen, the sample was desorbed under vacuum at room temperature for 15 minutes. In these three cases, nearly all the chemisorbed oxygen was removed.

Shown in Figure 2-25 are the isotherm curves for the run where the sample was hydrogenated at room temperature. The first and second adsorption isotherms are nearly identical, indicating the oxygen can be removed by evacuation at room temperature after hydrogenating the sample between 25 and 200°C. This was very encouraging. However, the higher amount of oxygen chemisorption was not observed after hydrogenating at 25- 200°C. When the sample was hydrogenated at 250°C, the amount of chemisorbed oxygen was found to be 2.92 ± 0.18 cc/g, nearly a 33% increase with a K_{O_2} value of 4.37 ± 0.26 $torr^{-1}$. Again after evacuating the sample

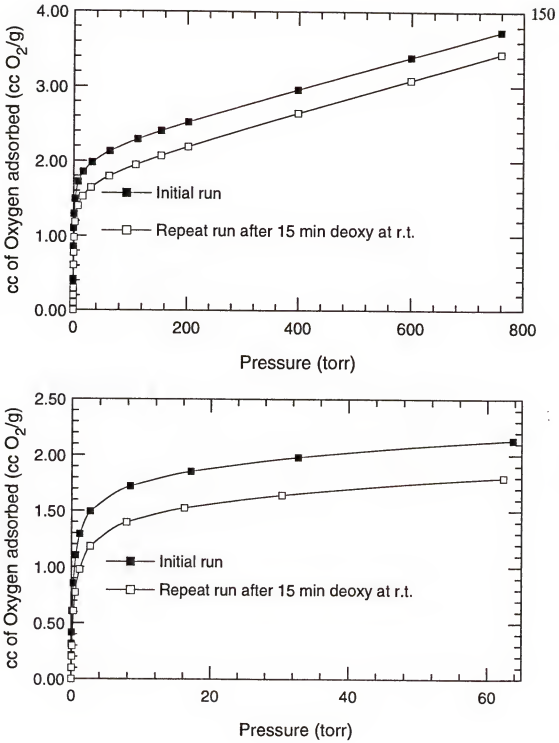

Figure 2-25. Isotherms for Cs(Co)CN-Y after Hydrogenation at Room Temperature.

15 minutes at room temperature, the isotherm is nearly identical (see Figure 2-26) indicating nearly complete removal of chemisorbed oxygen.

The hydrogenation treatment performed at 250°C appeared to be reversible. When the hydrogenation temperature was increased to 300°C, the amount of chemisorbed oxygen was found to be 5.71 $\pm$ 0.54 cc/g with a K_{O_2} value of 5.82 $\pm$ 0.41 $torr^{-1}$. After evacuation at room temperature for 15 minutes, the sample only chemisorbed 3.73 cc O_2/g (see Figure 2-27). Evacuation at room temperature for one, 12, and 24 hours as well as one hour at 300°C could not bring the sample's oxygen chemisorption capacity back up to 5.71 cc/g. The results indicate that of the 5.71 cc of oxygen chemisorbed, only 3.73 cc of it is reversible.

The final hydrogenation was performed at 350°C. On the first adsorption run, the sample chemisorbed 5.31 $\pm$ 0.12 cc O_2/g. After evacuation at room temperature for 15 minutes, the sample only chemisorbed approximately 1.10 cc of O_2/g. Without rehydrogenation, the sample will not exhibit this high chemisorption ability.

The explanation for this behavior was found in the tube furnace experiments discussed earlier. Hydrogenation of the CsCo(CN)-Y at temperatures below 300°C does not cause the evolution of HCN from the zeolite. The effluent gas bubbled into a solution of Fe^{2+}/Fe^{3+} does not show Prussian blue until the oven temperature is 300°C or greater. In the absence of reaction with H_2, approximately 3.00 cc of oxygen chemisorbed is reversible.

Quantitative EPR measurements were also run on the sample after hydrogenation at 25, 250 and 300°C. In the first set of experiments, after the sample

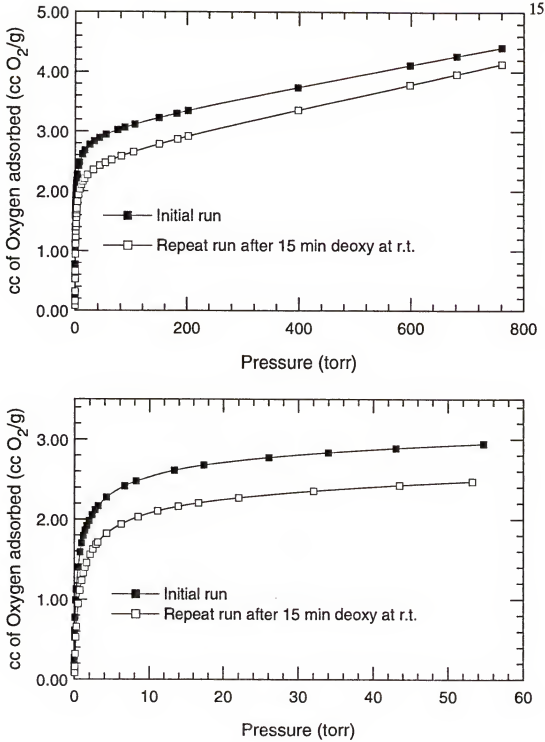

Figure 2-26. Isotherms for CsCo(CN)-Y after Hydrogenation at 250°C.

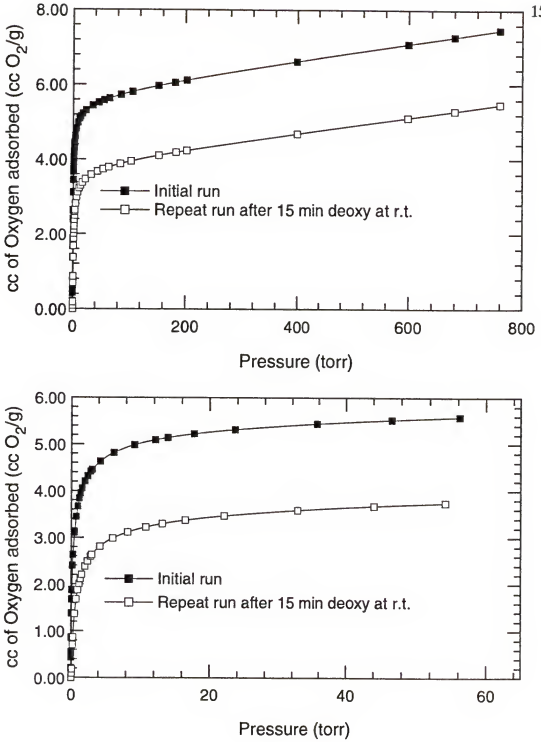

Figure 2-27.Isotherms for CsCo(CN)-Y after Hydrogenation at 300°C.

had been treated and oxygenated, the EPR spectrum of a sample of known weight was taken. The Co-O_2 curve obtained was then double integrated and the area per gram determined. The data (Table 2-18) verify the results from gas uptake experiments. As the sample was hydrogenated at higher temperatures, it had a higher oxygen chemisorption capacity. The area of the EPR Co-O_2 curve also increased. By changing the hydrogenation temperature from 25 to 250^{o}C, the chemisorbed oxygen increased by a factor of 1.5 (from 2.07 to 2.92 cc/g), and the relative intensity of the Co-O_2 signal also increased by a factor of 1.5. The intensity of the Co-O_2 adduct's signal increases by a factor of 2.4 after hydrogenation at 300^{o}C relative to the original signal. The amount of oxygen chemisorbed also increased by a factor of 2.8 from 2.07 to 5.71 cc/g.

A sample of known weight was taken after being hydrogenated and deoxygenated at 300^{o}C. The EPR spectrum was taken at 110K yielding a curve characteristic of the $Co(CN)_5^{3-}$ complex (refer to Figure 2-10). The sample was then exposed to oxygen. Using a known amount of a standard, $(Et_4N)_3Co(CN)_5O_2$, a solid, the Co-O_2 adduct signal from the CsCo(CN)-Y was quantified by EPR. The zeolite sample produced an Co-O_2 EPR signal which was determined by double integration and averaging of nine spectral runs to have an area units/g figure of 2.988×10^6. Double integration and averaging of nine EPR spectra of the standard Co-O_2 curve gave a figure of 1.076×10^6 area units/mol. This means that the CsCo(CN)-Y sample by EPR was found to contain 0.278 mmol/g of $Co(CN)_5^{3-}$. Oxygen adsorption experiments determined that the sample had 0.227 mmol/g of

Table 2-18. Quantitative EPR Results for Hydrogenated CsCo(CN)-Y.

Evacuation/ Hydrogenation Temperature (^{o}C)	curve[a] area/g	relative intensity
25	2.013×10^{6}	1
250	3.019×10^{6}	1.5
300	4.831×10^{6}	2.4

a: determined by double integration

$Co(CN)_5^{3-}$ after hydrogenation at 300°C. There is a 22% discrepancy between the two values. These results are significant because they only further verify that $Co(CN)_5^{3-}$ is the active complex and that indeed the hydrogenation treatment is increasing the amount of $Co(CN)_5^{3-}$ present.

Hydrogenation mechanism

Based on the data accumulated in this study, the mechanism seen in Figure 2-28 has been proposed to explain what is occurring during the hydrogenation at temperatures of 300°C or greater. There are four pathways in this mechanism. In pathway I, we see the cycling of $Co(CN)_5^{3-}$ as it encounters solvent (CH_3CN or H_2O) and/or oxygen. During the hydrogenation step, HCN is evolved (pathway III). This subjects the five coordinate complex to another mobile cyanide which can lead to the formation of $Co(CN)_6^{3-}$. At these elevated temperatures, HCN is either ejected from the zeolite or can interact with the zeolite's hydroxyl groups in an acid-base reaction. Furthermore, the proton can exchange with cations to give NaCN or KCN in the zeolite. This neutral pair can then potentially migrate within the pore structure with the CN^- coordinating to the $Co(CN)_5^{3-}$ complex to yield $Co(CN)_6^{3-}$.

Pathways II and III illustrate why this hydrogenation treatment process is not reversible. Although you can gain $Co(CN)_5^{3-}$, ultimately the driving force is to produce HCN and $Co(CN)_2$ which is not active towards binding oxygen. Pathway IV addresses what was observed when the hydrogenated material was stirred in acetonitrile. If, as shown, there is $Co(CN)_2$ formed in the presence of HCN (or more

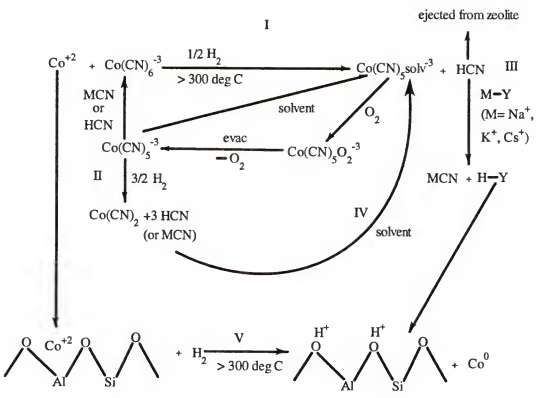

Figure 2-28. Hydrogenation Mechanism.

likely MCN), adding CH_3CN coordinates the two again forming $Co(CN)_5^{3-}$ again. However, this is not a cure-all way to attain regenerability because to regain the high chemisorption capacity you must hydrogenate the sample again, meaning further loss of cyanide as HCN.

The final pathway, V, addresses the formation of cobalt metal. Co^{2+} within the zeolite is reduced to cobalt metal in the presence of hydrogen at elevated temperatures. Meanwhile, hydrogen is oxidized to two protons. These protons can proceed in many different ways. They can interact with the zeolite in acid-base chemistry, coordinate with cyanide and be expelled from the zeolite as HCN, or can act as countercations to maintain electroneutrality within the zeolite.

The problem, however, still remains that the hydrogenation step at temperatures of 300°C or higher is not reversible. Below this temperature, it is reversible, but we can already obtain materials which chemisorb 3.00 cc O_2/g in DMF without hydrogenation. The hydrogenation treatment is very interesting because it is a way of going from $Co(CN)_6^{3-}$ to $Co(CN)_5^{3-}$ that has never been seen before. Furthermore, the reduction of Co^{2+} to cobalt metal could have potential applications. From a practical viewpoint, the final conclusion is hydrogenation will not help to obtain a material which chemisorbs 10 cc of O_2/g.

Zeolite Unit Cell Composition and the Concentration of Active Cobalt(II) Complex

In this section, the discussion will center around the unit cell composition and how this relates to the amount of active $Co(CN)_5^{3-}$ complex which is formed. This

is to establish trends which can help in our goal to achieve the best chemisorption sample possible. In Table 2-19, the unit cell formulas of representative CsCo(CN)-Y samples prepared in methanol, acetonitrile (hydrogenated and non-hydrogenated cases) and DMF are given (as determined by atomic adsorption spectroscopy and CHN analysis). Also given are the amount of chemisorbed oxygen for the sample as determined by gas uptake measurements, as well as the theoretical maximum amount of oxygen the sample could chemisorb (based on the actual amount of cobalt present). Finally, the percent of active cobalt for each sample is given based on the amount of oxygen chemisorbed versus the theoretical maximum amount of oxygen which could be chemisorbed if every cobalt formed one $Co(CN)_5^{3-}$ complex.

As can be seen from the data in this table, significant progress has been made not only in increasing the amount of cobalt complex formed in the zeolite and the amount of oxygen chemisorbed by the zeolite, but also in increasing the amount of cobalt which is active. Prior to this work, Taylor et al.[90] reported that roughly 10% of the cobalt in the zeolite was active as $Co(CN)_5^{3-}$ in CsCo(CN)-Y prepared using methanol as the cyanide addition solvent. After using the aprotic solvent/benzene drying method (sample E1), the amount of cobalt in the zeolite which was present as $Co(CN)_5^{3-}$ was 38.6%, a threefold increase in methanol.

When the solvent is switched to acetonitrile, without hydrogen treatment, the synthesis yields a CsCo(CN)-Y material (sample J1) where over 50% of the cobalt present is there as the active $Co(CN)_5^{3-}$ complex. When the hydrogenation procedure is factored in, we see in Table 2-19 that close to 90% of the cobalt is

Table 2-19. Unit Cell Composition and Percent Active Cobalt.

Preparation Solvent	ID	Unit Cell Formula	O_2 Chemi (cc O_2/g)
CH_3OH	A1	$Cs_{14.8}Co_{5.5}Na_{7.5}(NaCN)_{12.1}Y$	0.30
	B1	$Cs_{33.1}Co_{7.2}Na_{8.5}(NaCN)_{17.5}Y$	0.50
	C1	$Cs_{34.1}Co_{4.9}Na_{12.1}(NaCN)_{17.5}Y$	1.16
	D1	$Cs_{32.1}Co_{3.7}Na_{16.5}(NaCN)_{16.4}Y$	1.54
	E1	$Cs_{22.7}Co_{4.8}Na_{23.7}(KCN)_{25.2}Y$	2.20
CH_3CN	F1	$Cs_{33.4}Co_{6.3}Na_{10.0}(NaCN)_{32.5}Y$	0.89
	G1	$Co_{8.0}Na_{40.0}(NaCN)_{2.3}Y$	0.20
	H1	$Cs_{13.2}Co_{5.1}Na_{32.6}(NaCN)_{6.9}Y$	0.66
	I1	$Cs_{24.4}Co_{5.8}Na_{20.0}(KCN)_{10.4}Y$	2.46
	J1	$Cs_{35.7}Co_{5.6}Na_{9.1}(KCN)_{15.4}Y$	3.40
CH_3CN (H_2)	K1	$Cs_{21.4}Co_{6.1}Na_{22.3}(NaCN)_{15.5}Y$	1.86
	L1	$Co_{8.0}Na_{40.0}(NaCN)_{2.3}Y$	1.00
	M1	$Cs_{15.1}Co_{4.8}Na_{31.3}(NaCN)_{13.2}Y$	2.92
	N1	$Cs_{16.7}Co_{5.4}Na_{28.5}(NaCN)_{7.6}Y$	3.24
	O1	$Cs_{11.7}Co_{3.5}Na_{37.3}(NaCN)_{10.0}Y$	3.52
	P1	$Cs_{21.4}Co_{6.1}Na_{22.4}(NaCN)_{15.5}Y$	3.57
	Q1	$Cs_{19.4}Co_{5.5}Na_{25.6}(NaCN)_{14.3}Y$	3.57
	R1	$Cs_{31.5}Co_{7.1}Na_{10.3}(NaCN)_{16.8}Y$	3.95
	S1	$Cs_{19.4}Co_{7.7}Na_{21.2}(NaCN)_{18.8}Y$	4.80
	T1	$Cs_{16.8}Co_{5.1}Na_{29.0}(NaCN)_{19.2}Y$	4.90
	U1	$Cs_{15.4}Co_{6.5}Na_{27.6}(NaCN)_{19.0}Y$	4.90
	V1	$Cs_{17.8}Co_{4.8}Na_{28.6}(NaCN)_{19.3}Y$	4.93
	W1	$Cs_{38.0}Co_{6.1}Na_{5.8}(NaCN)_{26.5}Y$	5.31
	X	$Cs_{33.4}Co_{6.3}Na_{10.0}(NaCN)_{32.5}Y$	5.68

Table 2-19 (continued)

Preparation Solvent	ID	Unit Cell Formula	O_2 Chemi (cc O_2/g)
DMF	Y1	$Cs_{10.9}Co_{5.6}Na_{33.9}(NaCN)_{3.4}Y$	0.26
	Z1	$Cs_{16.5}Co_{3.8}Na_{31.9}(NaCN)_{8.8}Y$	0.43
	AA1	$Cs_{20.4}Co_{4.0}Na_{27.6}(KCN)_{13.3}Y$	3.69
	BB1	$Cs_{30.3}Co_{4.3}Na_{17.1}(KCN)_{12.3}Y$	2.94

Table 2-19 (continued)

ID	Cs/Co	CN/Co	Theo Max. Chemi O_2 (cc O_2/g)	% Co Active
A1	2.7	2.2	7.98	3.8
B1	4.6	2.4	7.98	6.3
C1	7.0	3.6	5.70	20.4
D1	8.7	4.4	4.18	36.8
E1	4.7	5.2	5.70	38.6
F1	5.3	6.8	6.84	13.0
G1	0	0.3	11.0	1.8
H1	2.6	1.4	6.46	10.2
I1	4.2	1.8	7.2	34.1
J1	6.3	2.7	6.46	52.6
K1	3.5	2.5	7.60	24.5
L1	0	0.3	11.0	9.1
M1	3.2	2.8	6.08	48.0
N1	3.1	1.4	6.84	47.4
O1	3.4	2.9	4.56	77.2
P1	3.5	2.5	7.60	47.0
Q1	3.5	2.6	6.84	52.2
R1	4.4	2.4	8.36	47.3
S1	2.5	2.4	9.88	48.6
T1	3.3	3.8	6.46	78.9
U1	2.4	2.9	8.36	58.6
V1	3.7	4.1	6.08	81.1
W1	6.3	4.4	6.08	87.3
X1	5.3	5.2	6.84	83.0

Table 2-19 (continued)

ID	Cs/Co	CN/Co	Theo Max. Chemi O_2 (cc O_2/g)	% Co Active
Y1	1.9	0.6	7.98	3.26
Z1	4.4	2.3	4.56	9.43
AA1	5.1	3.3	4.94	74.7
BB1	7.1	2.9	4.94	59.5

active as the $Co(CN)_5^{3-}$ complex. Unfortunately, again, this is a dead end due to the fact that the material is not fully reversible.

When the solvent is DMF, CsCo(CN)-Y samples have been prepared that have high affinities for reversible chemisorption of oxygen (samples AA1 and BB1). These samples also have 60-75% of the cobalt present in the zeolite in the form of the active $Co(CN)_5^{3-}$ complex. Ultimately, the work in this dissertation has increased the amount of active complex formed in CsCo(CN)-Y by a factor of 3.5. In the meantime, the efficient use of cobalt present in forming $Co(CN)_5$ has been increased by a factor of at least 5 and 6 depending on the solvent used.

There are definite trends in the concentration of $Co(CN)_5^{3-}$ formed in the zeolite based on the solvent used, the amount of cesium and cobalt present and the amount of cyanide which is present in the zeolite. Seen in Figure 2-29 is a plot of the amount of Co^{2+} per unit cell versus the amount of oxygen chemisorbed. The four curves represent the different solvents used (including the hydrogenated cases for acetonitrile). In DMF, based on the collected data, maximum complex formation appears to occur when there were four cobalt per unit cell. Maximum $Co(CN)_5^{3-}$ complex formation in methanol and acetonitrile occurred when there were five cobalt per unit cell. This also seemed to hold true when the acetonitrile samples were hydrogenated. The trend with respect to cobalt in the zeolite suggests that loading the zeolite with eight cobalt will lead to a decrease in the amount of $Co(CN)_5^{3-}$ formed. Loading should be four to six cobalt per unit cell or approximately less than one cobalt per α-cage (or one cobalt per every two α-cages).

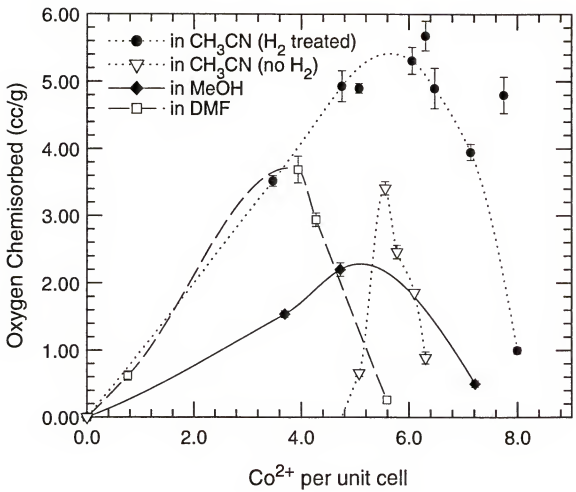

Figure 2-29. Cobalt Content Versus Oxygen Chemisorption.

The plot in Figure 2-30 shows the number of cesium ions per unit cell versus oxygen chemisorption. In methanol and DMF, the data suggests that the maximum amount of $Co(CN)_5^{3-}$ is formed if there are approximately 22-24 cesium per unit cell. In acetonitrile, for maximum $Co(CN)_5^{3-}$ formation, you would like to have at least 30 cesium. Looking at Figure 2-31, the Cs/Co ratio for maximum $Co(CN)_5^{3-}$ formation in DMF and acetonitrile (aprotic solvents) is at approximately 6. For maximum $Co(CN)_5^{3-}$ formation in methanol, the Cs/Co ratio should be 4.

These curves suggest that the maximum amount of $Co(CN)_5^{3-}$ complex is formed with fairly high loadings of cesium (20-30 per unit cell) and low loadings of cobalt (4-6 per unit cell). Cesium is vital to the formation of the active cobalt complex in large concentrations. In fact, when no cesium is present in the zeolite, the highest amount of oxygen chemisorbed was 1.00 cc/g. This sample was prepared in acetonitrile (sample L1) and chemisorbed this much oxygen only after hydrogenation of the sample. Based on what has been observed, cesium appears to be promoting the formation of $Co(CN)_5^{3-}$. It must be acting to shield the complexes in the formation step from adding another cyanide. The cesium also decreases the mobility of the complexes (which is increased by the presence of solvent during the cyanide addition step) thereby decreasing interaction with cyanide and the surface groups on the interior walls of the zeolite which could be promoting oxidation.

The final trend seen in Figure 2-32 compares the cyanide to cobalt ratio in the zeolite and the amount of chemisorbed oxygen. In each of the solvents studied, the greater the amount of cyanide which was present in the zeolite, the more active

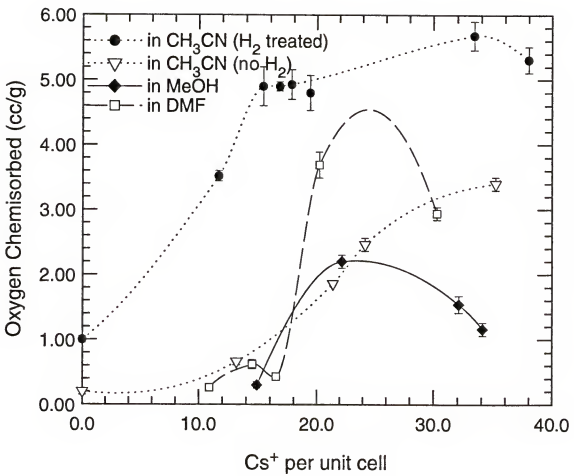

Figure 2-30. Cesium Content Versus Oxygen Chemisorption.

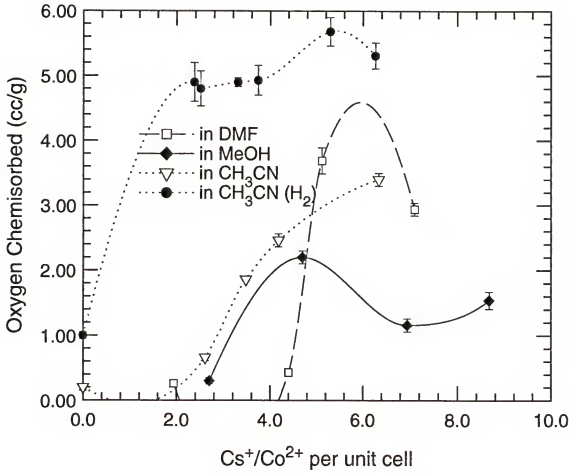

Figure 2-31. Cesium to Cobalt Ratio Versus Oxygen Chemisorption.

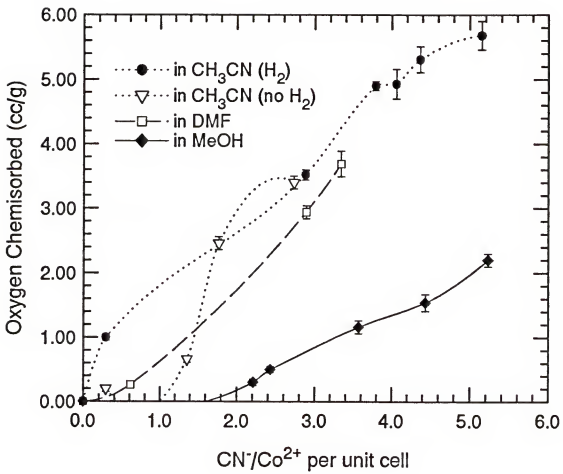

Figure 2-32. Cyanide to Cobalt Ratio Versus Oxygen Chemisorption.

complex was formed. This trend suggests two possible explanations. The first is that the problem with acetonitrile and DMF (if not methanol) is not that $Co(CN)_6^{3-}$ is forming, but that not enough cyanide is entering the zeolite to coordinate with cobalt. Even if $Co(CN)_6^{3-}$ is forming, based on these trends, having increased amounts of cyanide in the zeolite increases the chance of forming $Co(CN)_5^{3-}$. The second is that the aprotic solvents are favoring $Co(CN)_2$ formation in the α-cages. There is spectroscopic evidence for $Co(CN)_2$. This polymeric species would prevent formation of the active complex regardless of how much cyanide was added. In the future, studies should be considered where the cyanide addition step in DMF or acetonitrile is done at elevated temperatures. This will increase the solubility of the cyanide salt and increase the chances of cyanide entering the zeolite pores. One possible problem could be that elevated temperatures could increase the chances of cobalt oxidation and the formation of $Co(CN)_6^{3-}$.

Optimal Synthesis Conditions

The final synthetic procedure utilizing CsCoY to form the active cobalt(II)-cyanide complexes took advantage of conditions known to produce large amounts of $Co(CN)_5^{3-}$. First, NaY was slurried with aqueous cesium chloride (0.1 M) three times with vacuum drying at 200° C in between each exchange step. The goal here was to get as much cesium into the zeolite (at least 30 Cs^+ per unit cell) and drive them into the β-cages. Following the final washing to remove chloride, the CsY solid was

dried in a tube furnace at 500°C for 24 hours. This was done to remove water and to attempt to drive the cesium into the β-cages.

Cobalt was exchanged into the zeolite using dry acetonitrile and anhydrous cobalt(II) acetate. This cobalt exchange into CsY was performed at 110°C in a Parr pressure bottle (8 Co^{2+}/unit cell). After stirring for 25 hours, the CoCsY was washed by vacuum filtration (clear filtrate) on a frit under N_2 with CH_3CN. The resulting purple solid was immediately placed in a pressure bottle containing a DMF solution of KCN. The cyanide to cobalt ratio used was 5:1. The bottle was then fitted with a pressure head, placed in a Teflon lined steel reactor vessel and heated in an oil at 130°C for 96 hours. Afterwards, the solid was filtered and washed with DMF.

The synthetic procedure utilizes a number of things which were found to increase the amount of chemisorbed O_2. The entire procedure is carried out in DMF and CH_3CN. The zeolite was dehydrated to remove water without driving cobalt into the inaccessible β-cages. Eight Co^{2+} per unit cell were exchanged into the zeolite under aprotic conditions. Exchanged cobalt can be directed to the α-cages with $Co(NCCH_3)_6^{2+}$ being accessible only to the α-cages. KCN was used as the cyanide salt because of the favorable results obtained in DMF previously. Finally, the temperature was increased to increase the solubility of KCN in DMF and also increase the chances of DMF transporting KCN into the zeolite. The cyanide reaction time was 96 hours because this was found to be the optimal reaction time in DMF from previous experiments.

The resulting gray CsCo(CN)-Y solid had a single sharp, intense band in the infrared spectrum at 2120 cm^{-1}. This is similar to what had been assigned to $Co(CN)_5O_2^{3-}$. The EPR spectrum of the sample at room temperature gives the characteristic curve seen for Co(II)-O_2 adducts (refer to Figure 2-9(a)).

Gas uptake measurements were performed on the sample after deoxygenation under vacuum at 300°C for one hour. The gas isotherm and equilibrium constant curves are shown in Figure 2-33 ((a) and (b)). This CsCo(CN)-Y sample chemisorbed 5.12 $\pm$ 0.07 cc O_2/g and had a K_{O_2} of 93.5 $\pm$ 1.7 $torr^{-1}$. The high amount of chemisorbed oxygen (without any hydrogen pretreatment) is very encouraging and represents the largest amount prepared for a sample prepared in our laboratory. The high equilibrium constant demonstrates that this material has a high affinity for oxygen. Based on the theory applied to the previous DMF work, the DMF solvent in this case does not impede oxygen gaining access to the active complexes by blocking the zeolite channels and pores. The sample was reversible if it was desorbed by evacuating the sample at 300°C for one hour.

These results show that a high oxygen chemisorption material can be prepared using totally aprotic conditions. Water does not enter the synthetic procedure except in the first step for cesium exchange. This water is accounted for by the tube furnace drying step. It is believed that the combination of rigorous dehydration of the zeolite, addition of cobalt using CH_3CN, and addition of KCN in DMF at 130°C lead to the high amount of active complex and the large O_2 chemisorption.

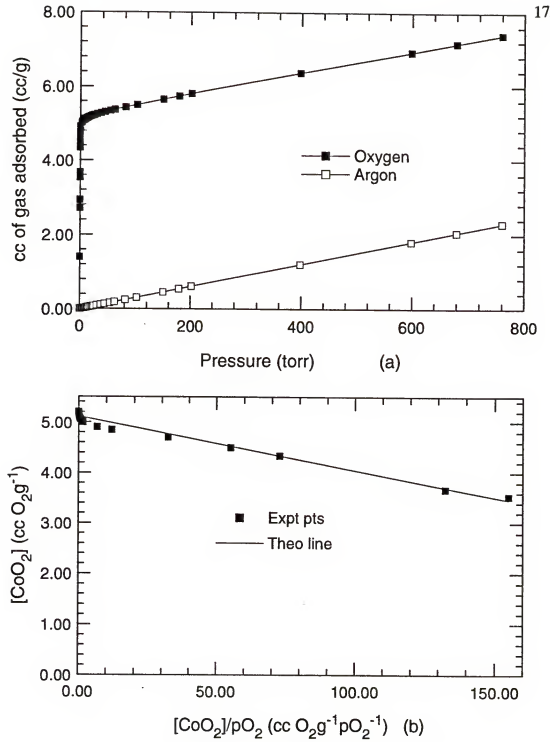

Figure 2-33. Experimental Curves for CsCo(CN)-Y (a) Gas Adsorption Isotherms; (b) K_{O_2} and $[Co]_t$ Curve.

One question which should be answered is whether the material can be deoxygenated and regenerated with desorption under vacuum at temperatures lower than 300°C. At the present it is known that deoxygenating the material by evacuating the sample at room temperature only removes 10% of the oxygen. Based on presently available data, this material will reversibly chemisorb oxygen only if the sample is deoxygenated under vacuum at 300°C for one hour.

Synthesis of $Li_3Co(CN)_5 \cdot nDMF$ in Zeolite Y

Attempts were made to synthesize $Li_3Co(CN)_5 \cdot nDMF$ in the zeolite to isolate the compound patented by Air Products[106] which has a high affinity for chemisorbing oxygen. The zeolite was exhaustively exchanged with lithium chloride to obtain a fully exchanged LiY sample. This is possible because Li^+ will exchange with 100% of Na^+ in zeolite Y according to Breck[6]. Cobalt exchange followed, with the LiCoY material being dried using DMF and benzene. LiCN in DMF was used as the cyanide source. Cyanide reaction time was 96 hours.

The resulting grey material, LiCo(CN)-Y had no Co-O_2 adduct observed in the EPR spectrum. Gas uptake measurements on the LiCo(CN)-Y determined that no oxygen is chemisorbed by the material. The material was evacuated at times ranging from 7-24 hours and temperatures ranging from 300- 350°C. Infrared studies of the material yielded a broad peak at 2137.4 cm^{-1}. Literature values for ν_{CN} in $K_3[Co(CN)_6]$[107] have been reported at 2143 cm^{-1}, with ν_{CN} in $Cs_2Li[Co(CN)_6]$

reported[108] at 2142 cm^{-1}. Cyanide reaction time was varied between 24 and 168 hours, yet analysis (EPR or gas adsorption) showed no active complex formed.

Synthesis of $Co(CN)_4^{2-}$ using Aprotic Dried CoY and Cyanide in Aprotic Solvents

Prior attempts in our laboratory were made to synthesize $Co(CN)_4^{2-}$ in the zeolite. This resulted in 1% of the cobalt present forming active $Co(CN)_4^{2-}$ complex. Since this was done in methanol and such success in forming $Co(CN)_4^{2-}$ had been demonstrated in the patent literature[106] using aprotic solvents, attempts were made to form large concentrations of $Co(CN)_4^{2-}$ complex. CoY was dried using the aprotic solvent/benzene azeotroping method, followed by addition KCN, NaCN, and LiCN in DMF or acetonitrile. Cyanide reaction time ranged from 24 to 96 hours. The Co(CN)-Y materials chemisorbed very small amounts of oxygen (0.30 cc/g maximum) if any at all. Infrared studies of Co(CN)-Y consistently showed one peak at 2131 cm^{-1}, indicative of $Co(CN)_6^{3-}$. One sample of Co(CN)-Y, prepared by reacting NaCN (5:1 CN/Co ratio) with aprotic dried NaCoY for 48 hours. The sample chemisorbed 0.20 $\pm$ 0.05 cc O_2/g which, based on the amount of cobalt present equated to approximately 1.8% of the cobalt being active. The highest capacity Co(CN)-Y material chemisorbed 1.00 $\pm$ 0.05 cc O_2/g, but only after hydrogenation. All other attempted syntheses did not chemisorb oxygen. Although possible, it appears that forming $Co(CN)_4^{2-}$ inside the zeolite will be more difficult than expected. More work in the future is going to be required to understand this system.

Applications of CsCo(CN)-Y

The CsCo(CN)-Y material has a high affinity for binding oxygen. This is reflected in both K_{O_2} and the $P_{1/2}$ value, or the pressure required to oxygenate 50% of the active complexes. In Table 2-20 the $P_{1/2}$ values for CsCo(CN)-Y prepared in various solvents and several cobalt(II) complexes in zeolites and solution are shown. CsCo(CN)-Y has a $P_{1/2}$ value varying from 0.01- 0.24 $torr^{-1}$. Recall that when the material is prepared from DMGH treated NaY, the K_{O_2} is significantly less (0.27 $torr^{-1}$), hence the higher $P_{1/2}$ value.

Consistent with the spin pairing model,[94] the $P_{1/2}$ value for CsCo(CN)-Y is less than that for CoSALENâ€¢py^{2+} prepared in NaY.[74] Cyanide ligands produce a stronger ligand field than SALEN causing the d_z2 orbital containing the unpaired electron to be of higher energy. The higher the energy of the d_z2 orbital, the more energy gained when the Co-O_2 adduct is formed and the unpaired electron forms a σ bond. This results in a lower $P_{1/2}$ value. Comparing the active complex in CsCo(CN)-Y with Co(terpy)(bpy)-Y,[81] the $Co(CN)_5^{3-}$ complex has a smaller $P_{1/2}$ value, indicating a stronger overall ligand field with cyanide than with bipyridine and terpyridine.

Because of the high affinity of the CsCo(CN)-Y material for oxygen, the more practical application for this material would be as an oxygen scavenger. The $P_{1/2}$ values are very low, meaning that any oxygen present in a gas stream would be immediately bound to the complex. This material could be used to assist in the production of ultrapure nitrogen and could possibly find applications in dry box

Table 2-20. $P_{1/2}$ Values for Co-O_2 Adducts.

Complex	$P_{1/2}$ (torr)
CsCo(CN)-Y (from MeOH)	0.24
CsCo(CN)-Y (from DMF)	0.27 (0.01)[d]
CsCo(CN)-Y (from CH^3CN)	0.27 (0.10)[e]
CsCo(CN)-Y (in DMGH treated NaY)	3.70
CoSALENapy^{2+} in NaY[a]	306
CoSALEN^{2+} in pyridine[a]	10.5
CoSALEN^{2+} in DMSO[b]	333
Co(3-FSALEN)$^{2+}$ solid[b]	2
Co(terpy)(bpy)$^{2+}$ in NaY[c]	0.59
Co(terpy)(bpy)$^{2+}$ in LiY[c]	0.34

a: Reference 74

b: Reference 106

c: Reference 81

d: when heated 7 hrs. @ 350°C

e: when hydrogenated 1.5 hrs. @ 350°C

technology. The deoxygenated CsCo(CN)-Y material could be used as an indicator to test the integrity of a dry box for leaks.

CHAPTER 3
HYDROCARBON OXIDATION USING ZEOLITE BASED CATALYSTS

Background

Introduction

Around the turn of the century, it was shown that the oxidation of organic compounds by molecular oxygen involved the formation of organic peroxides.[119] Criegee et al.[120] made an important discovery in 1939 when he showed that the primary product of the autoxidation of cyclohexene is the allylic hydroperoxide. Subsequent mechanistic studies of the interaction of simple hydrocarbons with dioxygen, implemented in the 1940s, provided the basis for the development of the free radical chain theory of autoxidation.[121] Autoxidation, which refers to oxidations with molecular oxygen, can be initiated spontaneously, but is more commonly promoted by metal species, often in trace quantitities. Even though initial studies were concerned with mainly preventing autoxidation, it was soon found that the controlled oxidation of hydrocarbons could be a useful method for preparing a wide range of oxygenated products.

The effects of metal ions on the autoxidation process were studied during the early 1900s by Haber and Weiss who formulated the classical mechanism for the decomposition of peroxides.[122] Shown in Figure 3-1, the autoxidation of

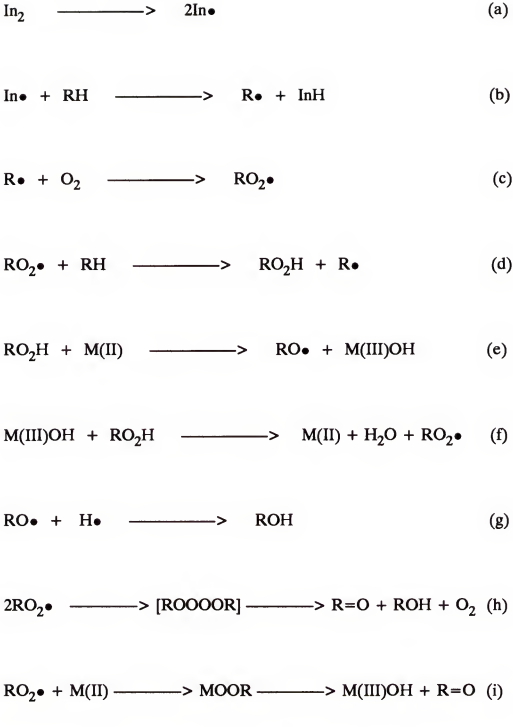

Figure 3-1. Autoxidation and Peroxide Decomposition Pathway.

hydrocarbons is typically accomplished by the deliberate addition of initiators, compounds that yield free radicals on thermal decomposition. The initiator abstracts a hydrogen radical from the substrate yielding an alkyl radical which then reacts rapidly with dioxygen to produce an alkylperoxide radical. The alkylperoxide can then abstract a hydrogen atom to produce the hydroperoxide.

At partial pressures of O_2 above 100 torr, the rate controlling step in autoxidation is hydrogen transfer from the substrate to the alkyl hydroperoxy radical.[119] Oxidations are likely to be rapid if the bond that is formed (ROO-H) is at least as strong as the bond which is broken (R-H). The ROO-H bond strength has been estimated[123] to be about 90 kcal/mol, which is larger than either a benzylic or allylic C-H bond (85 kcal/mol) or an aldehyde C-H bond (86 kcal/mol) but comparable to a tertiary C-H bond (90 kcal/mol) in a saturated hydrocarbon. Alkylperoxy radicals, being relatively stable and persistent, are very selective and preferentially abstract only the most weakly bonded hydrogen.[119]

The hydroperoxide can then decompose in either of two pathways. In the first pathway, the alkylperoxy radicals dimerize to form a tetroxide intermediate which has never been experimentally isolated. This then decomposes to the ketone, alcohol, and dioxygen. Alternately, the metal complex can react with the alkylperoxide radical which decomposes to give the alcohol and ketone. The modes of decomposition are dependent on the alkyl group structure.[124] For example, primary and secondary alkylperoxy radicals undergo disproportionation to an alcohol and a ketone via a

cyclic mechanism.[125] This pathway is unavailable to tetroxides derived from tertiary alkyl peroxides which undergo decomposition to dialkyl peroxides and dioxygen.

Metal complexes react with alkyl peroxides in two ways: first, to decompose the alkyl hydroperoxides, producing intermediates and alcohol or ketone products during autoxidation; and second, during organic synthesis, where the peroxide is the active oxidant for oxidative transformations. Besides hydrogen peroxide, the alkyl hydroperoxides with tert-butyl (TBHP), tert-amyl (TAHP), α-cumyl (CHP), and α-phenethyl groups are readily available.

One of the best known reactions of hydrogen peroxide and a metal catalyst using Fenton's reagent, which consists of ferrous salts and H_2O_2.[126] As shown in Figure 3-2, the iron(II)-catalyzed decomposition of hydrogen peroxide proceeds via a free radical chain process involving hydroxyl radicals as reactive intermediates. Since reaction 3-4 is energetically more favorable than reaction 3-2,[127] the catalytic decomposition proceeds by the sequence 3-1, 3-4, and 3-5. In the presence of organic substrates (reactions 3-6 through 3-8), the hydroxyl radicals produce organic radicals which can undergo either dimerization, oxidation by Fe(III) or reduction by Fe(II). Reaction 3-6 is competitive with reactions that lead to the nonproductive decomposition of H_2O_2, 3-3 and 3-5. These decomposition reactions become more important with increasing iron concentration. The decomposition paths severely limit the utility of Fenton's reagent. Many times, yields are low. Furthermore, the hydroxyl radical is rather indiscriminate in its reactions with organic substrates.[127]

$Fe^{II} + H_2O_2 \longrightarrow Fe^{III}OH + HO\bullet$ (3-1)

$Fe^{III} + H_2O_2 \longrightarrow Fe^{II} + HO_2\bullet + H^+$ (3-2)

$Fe^{II} + HO\bullet \longrightarrow Fe^{III}OH$ (3-3)

$Fe^{III} + HO_2\bullet \longrightarrow Fe^{II} + O_2 + H^+$ (3-4)

$HO\bullet + H_2O_2 \longrightarrow H_2O + HO_2\bullet$ (3-5)

$RH + HO\bullet \longrightarrow R\bullet + H_2O$ (3-6)

$R\bullet + Fe^{III} \longrightarrow [R^+] + Fe^{II} \longrightarrow$ products (3-7)

$R\bullet + Fe^{II} \longrightarrow [R^-] + Fe^{III} (+H_2O) \longrightarrow RH$ (3-8)

Figure 3-2. Fenton Chemistry Mechanism.[126]

With alkyl hydroperoxides, metal catalyzed decomposition is the most common pathway. The rapid decomposition of alkyl hydroperoxides in hydrocarbon solutions in the presence of trace amounts of iron,[128] manganese,[129] cobalt,[130] and copper[131] compounds is well known. The two main reactions of alkyl hydroperoxides with metal complexes are

$$RO_2H + M^{(n-1)+} \longrightarrow RO\bullet + M^{n+} + HO^- \quad (3\text{-}9)$$

$$RO_2H + M^{n+} \longrightarrow RO_2\bullet + M^{(n-1)+} + H^+ \quad (3\text{-}10)$$

Reduction and oxidation in this manner are similar to reactions 3-1 and 3-2 previously described for hydrogen peroxide. In inert solvents, reactions 3-11 and 3-12 can be followed by radical chain decomposition of the hydroperoxide.[132]

$$2RO_2\bullet \longrightarrow 2RO\bullet + O_2 \quad (3\text{-}11)$$

$$RO\bullet + RO_2H \longrightarrow RO_2\bullet + ROH \quad (3\text{-}12)$$

Metal catalyzed decomposition is also possible via reactions (e),(f), and (i) of Figure 3-1. Under these circumstances, the metal ions act as an initiator instead of a catalyst.

The industrial oxidation of hydrocarbons to useful oxygenated compounds is commercially important on a very large scale- on the order of several billion pounds per year. Some of these reactions were discussed in detail in Chapter 2. These reactions are usually carried out at high temperatures ($>150^oC$) and pressures, while lacking high selectivity. The problem often lies in the fact that many times the desired products are easier to oxidize than the starting substrate. Unless conversions are kept to a minimum, the desired products are consumed during the process.

The oxidation of cyclohexane to mixtures of cyclohexanol and cyclohexanone is extremely important industrially[133] because these compounds are intermediates in the manufacture of nylon 6 and nylon 6,6. In the Dutch State Mine (DSM) process,[134] cyclohexanone is oxidized by air in a batch operation at 155°C and 8-10 atmospheres in the presence of a cobalt catalyst. A 1-2:1 ratio of cyclohexanol and cyclohexanone is obtained with roughly 70% selectivity and about 10% cyclohexane conversion. The remainder (30%) of the products are cleavage products such as n-butyric, n-valeric, succinic, glutaric, and adipic acids formed by ring cleavage of cyclohexanone and further oxidation. Figure 3-3 shows a reaction mechanism proposed by Tolman and co-workers for the formation of the cleavage products.[132]

The oxidation of cyclohexane to adipic acid can be achieved in either a two-stage or single stage process. In the two-stage process, cyclohexane is oxidized to a mixture of cyclohexanol and cyclohexanone which is then further oxidized to adipic acid. For example, the DuPont process[135] is performed at 165°C and under 10 atmospheres using a $Co(oct)_2$ (oct= octanoate) catalyst to form the alcohol and ketone. Then, nitric acid is used as the oxidant in the presence of Cu(II) and V(V) salts as catalysts at 75-80°C[136,137] (see Figure 3-4). The reaction sequence is complex,[136] with one possible pathway involving nitrosation of cyclohexanone followed by oxidation of the resulting cyclohexane-1,2-dione or its monoxime with VO_2^+. The resulting VO^+ is reoxidized by nitric acid. The yield of adipic acid is 92% under these conditions.[137]

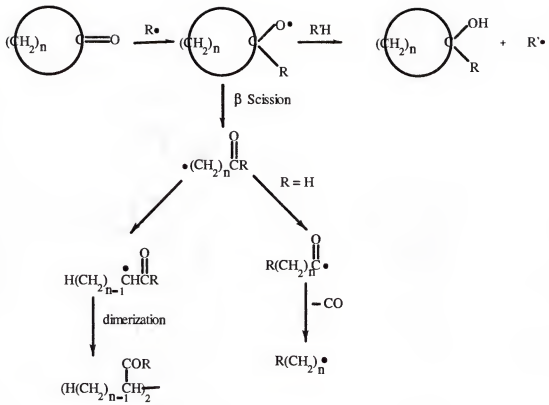

Figure 3-3. Proposed Mechanism for Cleavage Products during Oxidation of Cyclohexane.[132]

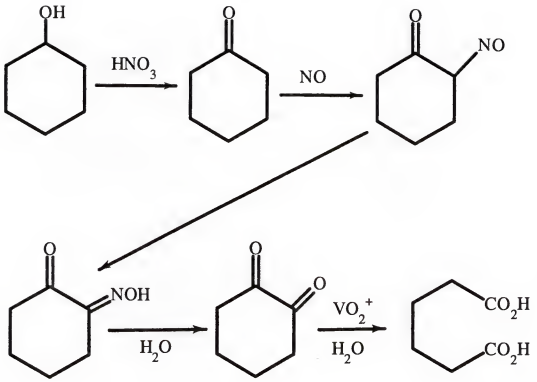

Figure 3-4. DuPont Process[136] for Conversion of Cyclohexanone to Adipic Acid.

An alternative process involves the air oxidation of cyclohexanone,[138] or a mixture of cyclohexanol and cyclohexanone,[139] in acetic acid at 75-85°C in the presence of a manganese(II) acetate catalyst. The selectivity to adipic acid is 90% with conversions of 40-45%.[138] With high concentrations of cobalt(II) acetate are employed as catalyst, the direct oxidation of cyclohexane to adipic acid can be carried out at 90°C in acetic acid.[140-142] Adipic acid is obtained with a selectivity of 70-75% with conversion of cyclohexane at 80-85%. The reaction involves Co(III) (see Figure 3-5) as the chain transfer agent in a direct reaction with the cyclohexane substrate.[140]

Hydrocarbon Oxidation Using Zeolite Catalysts

The catalytic properties of zeolite encapsulated transition metal complexes has become of considerable interest.[143] These materials combine the advantages of homogeneous and heterogenous catalytic systems. The active transition metal site differs from solution species only by the limits placed on it by the zeolite. Because the catalyst is trapped inside the zeolite, products can be easily separated. The zeolite structure can also affect reactant and product selectivity due to size constraints within the cages. Finally, the lifetime of the catalyst is influenced by encapsulation within the zeolite, because degradation pathways from reactions such as dimerization can be prevented.

Past work in the area of zeolite encapsulated metal complexes has included the use of metal carbonyls for the water-gas shift reaction,[144] methanol carbonylation,[145] and hydroformylation.[146] Studies using encapsulated transition

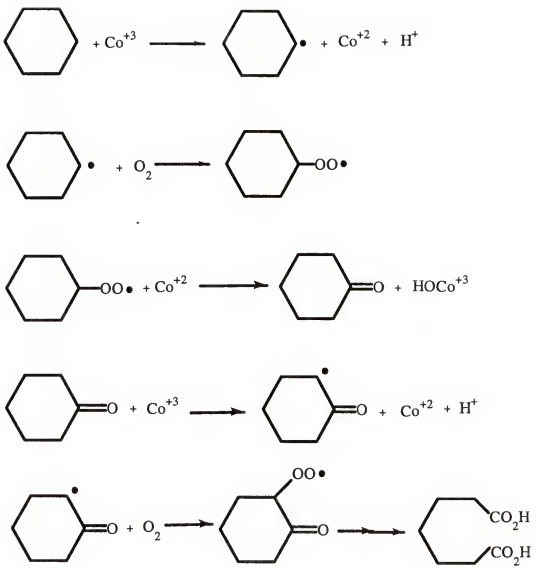

Figure 3-5. Cyclohexane to Adipic Acid Involving Cobalt(III).[140]

metal complexes as oxidation catalysts have been more limited. In the past ten years, the major focus has centered around mimicking natural monooxygenase enzymes. The desire has always been to draw upon the similarities between cavities in a zeolite and those in the protein structure of oxidizing enzymes. For example, cytochrome P-450 displays impressive substrate selectivity,[147] while the ω-hydroxylases regioselectivity hydroxylate the terminal methyl groups of unactivated alkanes.[148]

The predominant amount of work along these lines for the last six years has been done by Tolman and Herron from DuPont. Between 1987 and 1989, their work centered around two zeolite catalysts for hydrocarbon oxidation. The first zeolite oxidation system utilized iron(II) phthalocyanine (FePc) complexes inside the α-cages of zeolites NaX and NaY. Alkane oxidation was accomplished with this "ship-in-the-bottle"[74] FePc catalyst and iodosobenzene in acetonitrile at room temperature.[149] Selectivity of n-alkanes was towards the terminal methyl group. The shift towards oxidation nearer the ends of the molecule was observed for methyl cyclohexane as well as n-octane.[150] The ends of the n-octane molecule sees the iron(II) catalyst first, resulting in oxidation products at the 2-position being greater than at the 4-position.

Stereoselectivity was also observed with this FePc entrapped catalyst. With methyl cyclohexane as substrate, the ratio of trans to cis alcohols produced at the 4-position (relative to the methyl group) was nearly 2 for the zeolite catalyst whereas FePc in solution yielded a ratio of 1:1. With norbornane as substrate, the exo:endo norborneol ratio using the zeolite catalyst was nearly 6, whereas FePc in solution had a ratio of 9.[149] Increased preference for oxidation at one of two diastereotopic

hydrogens again resulted from substrate to catalyst orientation imposed by the zeolite which could have one of two hydrogen atoms closer to active oxidant.

This catalyst system had some problems typically associated with these materials. Low rates for this system were due to the fact that both substrate and oxidant had to diffuse into the active sites and the products had to diffuse out through narrow pores. This problem is aggravated by the partial blockage of the pores by the phthalocyanine complexes themselves. Low turnovers were the result of pore blockage by oxidation products and oxidant disproportionation. Finally, the small changes in selectivity were due to the need for a large pore zeolite where the molecular sieving and orientation properties are not maximized for high selectivities.[150] A smaller pore zeolite would be more desirable for higher selectivities, but less desirable for rates.

The second oxidation catalyst system utilized iron(II) and palladium(0) in zeolite 5A in an oxygen/hydrogen atmosphere to selectively oxidize n-alkanes.[151] This catalyst can easily be prepared with zeolites of any pore size making high selectivities possible. Oxidation with this catalyst involved the generation of hydrogen peroxide at Pd(0) followed by oxidation of the alkane substrate at Fe(II). Substrate selectivity of n-octane versus cyclohexane was greater than 190, while regioselectivity of primary/secondary oxidation was 0.67.[152] This regioselectivity is better than was reported by Cook et al.[153] for (porphyrinato)iron(II) (0.3) and the best manganese systems (0.53) with iodosobenzene oxidant. The main disadvantage of this system was

that the majority of the oxidation products were not recovered until the zeolite had been completely dissolved using concentrated sulfuric acid.

The focus of this work has been to develop zeolite-based catalysts that are capable of oxidizing hydrocarbons using peroxides or oxygen at low temperature (50° C) by varying the hydrophobicity of the zeolite. The reasons for using zeolites here are (1) the possibility of imparting shape selectivity and (2) these inorganic materials are more durable and have longer lifetimes (and can be regenerated) than organometallic catalytic materials. Oxidation studies were performed using both metal exchanged and metal-dmp (dmp= 2,9-dimethyl-1,10-phenanthroline) zeolites. This ligand was chosen because of its resistance to oxidation as well as steric bulk. It can be used like the porphyrin ligand was in Herron's work. The substrate predominantly used in this work is cyclohexane. Selectivity was investigated using n-hexane as the substrate. Three different zeolites were used, each with differing pore structure and size: ZSM5, Y, and large pore mordenite.

Experimental

Reagents and Equipment

All reagents were reagent grade or better. All chloride salts were purchased from Aldrich. Vanadyl sulfate monohydrate and 2,9-dimethyl-1,10-phenanthroline (dmp) were purchased from Aldrich and used as received. Cyclohexane and n-hexane were spectral grade and were purchased from Fischer Scientific. Reagent grade cumene was filtered over an activated alumina column prior to use in order to

remove the inhibitor present. Cyclohexane and n-hexane were distilled prior to use and stored over P_2O_5. Acetonitrile used in this study was distilled over P_2O_5 and stored over 4A activated molecular sieves. Glacial acetic acid and acetic anhydride were purchased from Aldrich and used as received. Hydrogen peroxide (30%) and t-butylhydroperoxide (90%) were purchased from Aldrich and used as received.

Zeolite NaY (Si/Al ratio= 2.4) was obtained from UOP (LZY-54, lot no. 955087001010-S). Zeolite NaY (Si/Al ratio= 80, lot no. 9106691K), large port (10Å) Na-mordenite (Si/Al ratio= 13, lot no. 9106692K), NaZSM-5 (Si/Al ratio= 35, lot no. 9110103K), and NaZSM-5 (Si/Al ratio= 80, lot # 9110103K) were obtained from the PQ Corporation. All were exchanged in a 0.25M aqueous solution of NaCl for 24 hours, followed by washing with deionized water until the filtrate gave a negative chloride test towards $AgNO_3$. The sodium zeolites were then dried under vacuum for 24 hours at 150^{0}C. To differentiate between the two Y zeolites used in this study, one is designated "Y" (Si/Al ratio= 2.4), while the other is designated "HSY" (Si/Al ratio= 80) or "high silica Y".

All oxidation reactions were analyzed using gas chromatography. A Varian 3700 and a Hewlett Packard 2290A integrator were employed equipped with an 8-ft, stainless steel packed column (15% DEGS, diethylene glycol succinate, support on Chromosorb W (80/100 mesh) purchased from Altech) with helium effluent and a flame ionization detector. Substrates and products were identified and quantified using known standards. Calibration curves were used to relate peak areas to moles of products.

Transition Metal Exchanged Zeolites

Samples of M^{n+}-Y (M^{n+}= Fe^{3+}, Co^{2+}, and Mn^{2+}) containing 5.0 x 10^{-4} moles of M^{n+} per gram of material were prepared from the corresponding NaY by ion exchange with the appropriate metal chloride salts. For this ion exchange, 10 grams of the sodium zeolite were stirred in 800 mL of deionized water along with 5.00 x 10^{-3} moles of the metal chloride salt. The exchange was carried out at room temperature for 24 hours. The solid zeolite was separated by vacuum filtration and washed continuously with deionized water until the filtrate gave a negative chloride test with $AgNO_3$. The M^{n+}-Y solid was then dried in vacuo at 150°C for 24 hours.

A sample of $V(O)^{2+}$-Y zeolite containing 5.0 x 10^{-4} moles of metal per gram of material was prepared by the method previously described. The metal salt used here was $V(O)SO_4 \bullet 2H_2O$. A sample of $Ru(NH_3)_6{}^{3+}$-Y containing 5.0 x 10^{-4} moles/g was prepared by the method previously described using $Ru(NH_3)_6Cl_3$.

Samples of M^{n+}-HSY, M^{n+}-ZSM5, and M^{n+}-mordenite zeolites (Fe^{3+}, Co^{2+}, $V(O)^{2+}$, and Mn^{2+}) containing 1.0 x 10^{-5} moles of M^{n+} per gram were prepared from the corresponding NaHSY, NaZSM5, and Na-mordenite by ion exchanging 10 grams of the sodium zeolite with an aqueous solution containing 1.0x10^{-4} moles of the appropriate metal chloride salt.

Metal-2,9-Dimethyl-1,10-Phenanthroline Complexes Inside Zeolite Y

$M^{n+}(dmp)_x$-Y (M^{n+}= Fe^{3+}, Co^{2+}, and Mn^{2+}) were prepared by taking 5.0 g of the appropriate metal exchanged zeolite Y and stirring it in a 400 mL solution

of absolute ethanol containing 2.30 grams of 2,9-dimethyl-1,10-phenanthroline (dmp). The slurry was stirred for 48 hours at room temperature. The solid zeolite was separated by vacuum filtration from the colorless filtrate and washed continuously with absolute ethanol until the filtrate was shown to contain no dmp ligand (tested by using $CoCl_2$). The solid was then dried under vacuum at 150°C for 24 hours.

$Ru(dmp)_x$-Y was prepared by a method similar to the procedure used by Marazewski and co-workers.[154] In a round bottom flask equipped with a vacuum stopcock, 4.0 grams of $Ru(NH_3)_6^{3+}$-Y was stirred in 80 mL of absolute ethanol containing 0.185 grams of dmp. After 24 hours the ethanol was removed by vacuum evaporation. The flask was purged with nitrogen for 30 minutes, then evacuated at 10^{-3} torr for 30 minutes. The evacuated flask was immersed in an oil bath and heated at 180°C for 24 hours. After cooling, the orange solid was collected and washed with 500 mL of absolute ethanol. The solid was first air dried, then dried under vacuum at 70°C for 24 hours.

Hydrocarbon Oxidation Using Peroxide

Unless otherwise stated, oxidation runs were made in the absence of solvent. In a typical oxidation run, 1.00 gram ($5.0x10^{-4}$ moles M^{n+}) of M^{n+}-Y or $M^{n+}(dmp)_x$-Y catalyst was placed in 20.0 mL of cyclohexane (0.185 mol) in a round-bottomed flask. t-Butyl hydroperoxide (TBHP, 90% v/v, 21 mL or 0.189 mol) were added with the resulting mixture being stirred and heated to 50°C. Reaction products were determined by filtering off the zeolite solid and analyzing the filtrate solution by GC.

Peroxide concentrations of the solutions were determined by collecting 1 mL aliquots of the reaction solutions and immediately performing iodometric titrations.[155]

CAUTION! Hydroperoxides are shock and temperature sensitive. They should be treated as potentially explosive.

Hydrocarbon Autoxidation at Elevated Pressures

Autoxidation reactions were carried out in 250 mL Parr pressure bottles equipped with stainless steel Swagelok pressure heads and placed within steel mesh explosion shields. Sampling of each reaction mixture was accomplished by using a gas tight syringe equipped with a Luerlock syringe valve and a 12-inch, 20 gauge needle to withdraw a 1 mL aliquot through a gas tight septum within the pressure head. Reactions were carried out at 75°C in a silicone oil bath monitored by an Omega 6100 temperature controller and thermocouple under an initial oxygen pressure of 50 psig.

CAUTION! Extreme care should be taken when working with a pressurized apparatus at or above room temperature. Appropriate shields must be used and fire extinguishers should be on hand. All reactions at elevated temperatures should be cooled to room temperature before disassembling the pressure apparatus.

For a typical high pressure oxidation, 0.453 moles of substrate (cyclohexane or cumene, NEAT), and 1.00 gram of M^{n+}-Y or $M^{n+}(dmp)_x$-Y (5.00×10^{-4} mol) were added to a 250 mL pressure bottle containing a magnetic stirring bar. The bottle was equipped with a pressure head and purged three times with O_2 (50 psig).

The bottle was then charged up with O_2 to 50 psig and placed in the constant temperature oil bath at 75°C. Reaction products were analyzed by GC. Peroxide concentrations were determined by iodometric titration.

Results and Discussion

Cyclohexane Oxidation at Room Temperature

The first metal exchanged zeolites studied as potential catalysts in the oxidation of cyclohexane were Fe^{3+}-Y and $Fe^{3+}(dmp)_x$-Y. In many of the literature studies involving heterogenous catalysis of alkane oxidation, Fe^{2+} was reported to be preferred over Fe^{3+}. Fe^{3+} was used in this study. Since Fe^{2+} and Fe^{3+} both are involved in Fenton-type oxidation cycles, there should be little difference. Fe^{3+}-exchanged zeolites are also easier to prepare and less air and moisture sensitive.

The first studies (Table 3-1) using the zeolite encapsulated catalysts were conducted at room temperature in the absence of solvent. Two oxidants were used, hydrogen peroxide (30% v/v) and t-butylhydroperoxide (TBHP, 90% v/v). The oxidant to substrate mole ratio used was 2:1 while 0.25 grams of catalyst was used ($1.2x10^{-4}$ moles of Fe^{3+} catalyst). With hydrogen peroxide as the oxidant, a blank was run for 48 hours with no oxidation products detected. Upon addition of the zeolite catalyst, H_2O_2 was preferentially adsorbed to the exclusion of the alkane with decomposition of the peroxide resulting. Iodometric titration indicated that no peroxide remained ten minutes after addition of Fe^{3+}-Y or $Fe^{3+}(dmp)_x$-Y. This is due to the hydrophilic nature of this Y zeolite. No oxidation products were detected.

Table 3-1. Cyclohexane Oxidation using Peroxides at Room Temperature.

Catalyst	Peroxide[a]	Solvent	Products[b] (%)
none	H_2O_2	--	--[c]
none	t-ButOOH	--	--[c]
Fe^{3+}-Y	H_2O_2	--	--
$Fe^{3+}(dmp)_x$-Y	H_2O_2	--	--
Fe^{3+}-Y	H_2O_2	acetic anhydride[d]	--
$Fe^{3+}(dmp)_x$-Y	H_2O_2	acetic anhydride[d]	--
$Fe^{3+}(dmp)_x$-Y	H_2O_2	glacial acetic acid[e]	--
$Fe^{3+}(dmp)_x$-Y	t-ButOOH	--	1.0 -one[c] 1.0 -ol

a: 30% H_2O_2 (v/v); 90% t-ButOOH (v/v)

b: Based on starting moles of substrate.

c: reaction time: 48 hours

d: 45 mL; anhydride:peroxide:substrate mole ratio- 10:2:1

e: 60 mL; glacial acetic acid:peroxide:substrate mole ratio: 10:2:1.

Reaction conditions:

cyclohexane: 9.2×10^{-2} moles

peroxide: 0.20 moles

catalyst: 1.2×10^{-4} moles Fe^{3+} (0.25 g)

Reactions monitored by GC.

Attempts to make the cyclohexane and H_2O_2 reaction system miscible involved using either acetic anhydride or glacial acetic acid as solvent. In both cases the mole ratio of solvent, peroxide and substrate was 10:2:1. With acetic anhydride as the solvent, 24 hours after the addition of the Fe^{3+}-Y or $Fe^{3+}(dmp)_x$-Y catalyst, iodometric titration indicated that no peroxide remained. No oxidation products were detected. When the solvent was switched to glacial acetic acid, with $Fe^{3+}(dmp)_x$-Y as the catalyst, 24 hours after the addition of the zeolite catalyst iodometric titration indicated no peroxide remained in solution. No oxidation products were detected. These results suggest that the aqueous peroxide was preferentially adsorbed by the hydrophilic zeolite to the exclusion of the cyclohexane, with the peroxide being decomposed by the Fe^{3+} sites.

The oxidant was switched to t-butylhydroperoxide, 90% by volume. In this case, the reactants were miscible without solvent. A blank consisting of t-ButOOH and cyclohexane was run for 48 hours at room temperature with no oxidation products detected. On addition of $Fe^{3+}(dmp)_x$-Y, after 48 hours reaction time at room temperature, 1.0% of the cyclohexane had been converted to cyclohexanone, 1.0% to cyclohexanol. Iodometric titration showed that 95% of the initial peroxide remained in solution after 48 hours in the presence of the catalyst. This meant that t-ButOOH could be used for substrate oxidation with minimal decomposition of the peroxide due to the $Fe^{3+}(dmp)_x$-Y catalyst.

Oxidation of Cyclohexane using Various Fe^{3+}-Doped Zeolites

In order to understand what effect hydrophobicity of the zeolite had on the ability of the iron to catalyze the oxidation of cyclohexane with peroxides, studies were conducted using zeolites which were more hydrophobic than the Y zeolite used. As the silicon to aluminum ratio of a zeolite increases (less aluminum in the framework), the zeolite becomes more hydrophobic.[6] Herron addressed this problem by using zeolites that had a Si/Al ratio greater than 16 so that the pores were more hydrophobic, meaning the zeolite preferred to adsorb the starting alkane material rather than oxidized products.[152] He also pointed out that as the number of aluminum atoms in the framework are decreased, the number of cation exchange sites (and hence Fe^{3+} sites) are also decreased. In the work from Table 3-1, the Y zeolite had a Si/Al ratio of 2.5. In the hydrophobic zeolite study, the Y zeolite has a Si/Al ratio of 40. The number of exchangeable cation positions decreases from 56 in the first case to 4.7 in the high silica Y case (hereafter referred to as HSY). That is why the catalyst loading decreases from 5.0×10^{-4} moles of Fe^{3+}/g in Y to 1.0×10^{-5} moles of Fe^{3+}/g in the HSY case.

Results were obtained from a comparison of Fe^{3+}-Y and Fe^{3+}-HSY, using both H_2O_2 and t-ButOOH as the oxidant. CH_3CN was used as solvent to make the reaction system miscible. As can be seen in Table 3-2, with Fe^{3+}-Y as the catalyst, no oxidation products are obtained with H_2O_2 as the oxidant whether CH_3CN was used as the solvent or if the reaction temperature was 25 or 50°C. The only thing accomplished by using CH_3CN as the solvent was that the peroxide decomposition

Table 3-2. Cyclohexane Oxidation Using Fe^{3+}-Doped Y Zeolites.

Catalyst	Oxidant[a]	Temp (°C)	CH_3CN solvent[b]	Products[c] (%)
Fe^{3+}-Y	H_2O_2	25	NO	--
Fe^{3+}-Y	H_2O_2	50	NO	--
Fe^{3+}-Y	H_2O_2	25	YES	--
Fe^{3+}-Y	H_2O_2	50	YES	--
Fe^{3+}-Y	t-ButOOH	50	NO	3.0% -one 3.0% -ol
Fe^{3+}-HSY	H_2O_2	25	NO	--
Fe^{3+}-HSY	H_2O_2	50	NO	--
Fe^{3+}-HSY	H_2O_2	25	YES	--
Fe^{3+}-HSY	H_2O_2	50	YES	--
Fe^{3+}-HSY	t-ButOOH	25	NO	--
Fe^{3+}-HSY	t-ButOOH	50	NO	2.0% -one 1.5% -ol

a: 30% H_2O_2 (v/v); 90% t-ButOOH (v/v)

b: YES: 200 mL CH_3CN; NO: absence of solvent

c: Based on starting moles of substrate.

Reaction conditions:

cyclohexane: 0.185 moles

peroxide: 0.185 moles

catalyst: 1.00 g
5.0×10^{-4} mol Fe^{3+} (Fe^{3+}-Y), 1.0×10^{-5} mol Fe^{3+} (Fe^{3+}-HSY)

reaction time: 48 hours

Reactions monitored by GC.

slowed. With no CH_3CN as solvent, Fe^{3+}-Y totally decomposed H_2O_2 within 10 minutes, while with CH_3CN as solvent the H_2O_2 was totally decomposed after 12 hours.

When t-ButOOH was used as the oxidant, with Fe^{3+}-Y as the catalyst, the oxidation run was made in the absence of solvent at 50°C. There was 3.0% conversion to cyclohexanone and 3.0% conversion to cyclohexanol after 48 hours (based on starting moles of cyclohexane). Iodometric titration indicated that the peroxide concentration after 48 hours was still 3.2 M, 71% of the initial t-ButOOH concentration of 4.5 M. This suggested that oxidation chemistry was possible with these heterogeneous materials because the t-ButOOH appeared stable toward non-productive decomposition in the presence of Fe^{3+}-Y.

The results using Fe^{3+}-HSY as the catalyst were similar to those obtained with Fe^{3+}-Y. No oxidation products were obtained using H_2O_2 as the oxidant regardless of reaction temperature or whether CH_3CN was used as solvent. One significant observation was that Fe^{3+}-HSY did not rapidly decompose the peroxide. After 48 hours at room temperature, iodometric titration of the reaction solution (with H_2O_2, C_6H_{12}, and Fe^{3+}-HSY at room temperature) indicated that the peroxide concentration had decreased by only 10% from the initial H_2O_2 concentration. No oxidation products were observed.

Oxidation products with Fe^{3+}-HSY as the catalyst were observed only when t-ButOOH was the oxidant in the absence of solvent,with a reaction time of 48 hours, and a reaction temperature of 50°C. In this case, there was a 2.0% yield of

cyclohexanone and a 1.5% yield of cyclohexanol. Iodometric titration indicated that the peroxide concentration was 3.9 M, or 88% of the initial t-ButOOH concentration.

The hydrophobicity study was extended to the iron exchanged forms of two other zeolites: ZSM-5 and large pore mordenite. Table 3-3 gives a brief comparison between these two zeolites and zeolite Y. Mordenite and Y are both large pore zeolites (10 Å or greater pore diameter), while ZSM-5 is a medium pore zeolite (6-8 Å). The main repeating unit in ZSM-5 and large pore mordenite is the pentasil unit while the main repeating unit in Y is the sodalite unit. Each is distinctive in their pore structure. Mordenite has a pore structure composed of linear, non-interconnecting channels, while ZSM-5 has a three-dimensional pore structure formed by two interconnected linear systems. As was seen in Chapter 2, Y has a three dimensional pore structure formed by interconnection of the sodalite units through the S6R faces (hexagonal prisms) to form the α-cages.

Shown in Table 3-4 are the results obtained for oxidation of cyclohexane using Fe^{3+}-ZSM-5 or Fe^{3+}-mordenite as the catalyst. All runs were made using 1:1 mole ratios of cyclohexane to t-ButOOH in the absence of solvent. The ZSM-5 zeolite used here had a Si/Al ratio of 35, while the mordenite had a Si/Al ratio of 13. Like the examples with Fe^{3+}-Y and Fe^{3+}-HSY, the Fe^{3+}-ZSM-5 and Fe^{3+}-mordenite catalyzed reactions yielded no oxidation products with H_2O_2 as the oxidant, whether the reaction temperature was 25 or 50°C.

When the oxidant was switched to t-ButOOH , with a reaction temperature of 50°C, after 48 hours the Fe^{3+}-ZSM-5 catalyst gave a 5.5% yield of cyclohexanone

Table 3-3. Comparison of ZSM-5, Mordenite, and Y Zeolites.

Zeolite	ZSM-5	Mordenite	Y
Pore Size	Medium (6-8 Å)	Large (10 Å)	Large (13 Å)
MAX Exchange Capacity	0.75 meq/g	2.6 meq/g	7 meq/g
Building Unit	pentasil unit (5-1)	pentasil unit (5-1)	sodalite unit (S6R, S4R)
Pore Structure	3D linear channels formed by two interconnected linear systems	non-interconnecting linear channels	sodalite units (β-cages) connected by hexagonal prisms, form α-cage pores
General Formula	$Na_nAl_nSi_{96-n}O_{192}$	$Na_nAl_nSi_{56-n}O_{112}$	$Na_nAl_nSi_{192-n}O_{384}$

Table 3-4. Cyclohexane Oxidation Using Fe^{3+} Doped ZSM-5 and Mordenite.

Catalyst (Si/Al)	Oxidant[a]	Temp (^{o}C)	Products[b] (%)
FeZSM-5 (35)	H_2O_2	25	--
FeZSM-5	H_2O_2	50	--
FeZSM-5	t-ButOOH	25	--
FeZSM-5	t-ButOOH	50	5.5% -one 2.5% -ol
Fe-mord (13)	H_2O_2	25	--
Fe-mord	H_2O_2	50	--
Fe-mord	t-ButOOH	25	--
Fe-mord	t-ButOOH	50	9.4% -one 4.1% -ol

a: 30% H_2O_2 (v/v); 90% t-ButOOH (v/v)

b: Based on starting moles of substrate.

Reaction conditions: (absence of solvent)
cyclohexane: 0.185 moles

peroxide: 0.185 moles

catalyst: 1.00 g ($1.0x10^{-5}$ mol Fe^{3+})

reaction time: 48 hours

Reactions monitored by GC.

and a 2.5% yield of cyclohexanol. The peroxide concentration after 48 hours was determined by iodometric titration to be 3.1 M, a decrease of 31% from the original t-ButOOH concentration. Under these same conditions, Fe^{3+}-mordenite as the catalyst gave a 9.4% yield of cyclohexanone and a 4.1% yield of cyclohexanol.

The data up to this point suggest that Fe^{3+} encapsulated zeolites can be used effectively as oxidation catalysts with t-ButOOH at 50°C with stoichiometric ratios of substrate and oxidant in the absence of solvent. The hydrophobic zeolites used, ZSM-5 and large pore mordenite showed very encouraging results after 48 hours. The hydrophilic zeolite Y used also showed some promise. The key appeared to be that the system was miscible and the zeolite was as likely to adsorb the substrate as t-ButOOH. The next step was to use zeolite Y (Si/Al= 2.5) to encapsulate metal-dmp complexes and use these $M^{n+}(dmp)_x$-Y materials as catalysts to oxidize cyclohexane.

Oxidation of Cyclohexane Using $M^{n+}(dmp)_x$-Y and t-ButOOH at 50°C

The studies with Fe^{3+} were extended to include Mn^{2+}. The four catalysts studied here were: Fe^{3+}-Y, $Fe^{3+}(dmp)_x$-Y, Mn^{2+}-Y and $Mn^{2+}(dmp)_x$-Y (5.0×10^{-4} moles M^{n+} catalyst). All reactions were performed in the absence of solvent. In the first series of experiments, the variation was in the number of moles of peroxide used. These results are shown in Table 3-5.

By adding Fe^{3+}-Y or Mn^{2+}-Y catalysts to the reaction, an increase in oxidation products formed was observed after 48 hours (relative to a blank with no

Table 3-5. Variation in Peroxide Concentration for Oxidation of Cyclohexane.

Catalyst	ROOH (mmol)	Products[a] (%) Cyclohexanone	Cyclohexanol
none	189	--	--
NaY	189	--	--
Fe^{3+}-Y	18	0.5	1.0
	45	1.9	2.0
	189	3.0	3.0
$Fe^{3+}(dmp)_x$-Y	18	3.0	2.3
	45	9.1	3.8
	90	10.4	4.2
	189	16.2	5.4
Mn^{2+}-Y	18	1.5	1.8
	45	3.9	3.6
	189	6.1	4.1
$Mn^{2+}(dmp)_x$-Y	45	4.2	3.8
	90	6.0	4.0
	189	18.0	5.0

a: Based on starting moles of substrate.

Reaction conditions: (absence of solvent)
cyclohexane: 0.185 moles

peroxide: 0.185 moles

catalyst: 1.00 g (5.0×10^{-4} mol Fe^{3+} or Mn^{2+})

reaction time: 48 hours

Reaction at 50°C.

Reactions monitored by GC.

zeolite catalyst and a blank with NaY). The results showed that the amount of products increased as the oxidant to substrate ratio went from 1:10 to 1:1. With Fe^{3+}-Y as the catalyst, a ten-fold increase in oxidant increased the amount of ketone produced by a factor of six (0.5% yield to 3.0% yield), while the amount of alcohol increased by a factor of three (1.0% yield to 3.0% yield). With Mn^{2+}-Y as the catalyst, a ten-fold increase in oxidant resulted in an increase in the amount of ketone by a factor of four (from 1.5% to 6.1%) while the amount of alcohol increased by a factor of 2.3 (from 1.8 to 4.1%). These data suggest that the reaction is catalytic with respect to Fe^{3+}-Y or Mn^{2+}-Y, and is dependent on the oxidant concentration.

The zeolite catalyst was switched to $Fe^{3+}(dmp)_x$-Y or $Mn^{2+}(dmp)_x$-Y and the peroxide concentration was again varied. With a ten-fold increase of peroxide in the $Fe^{3+}(dmp)_x$-Y catalyzed system, the amount of ketone produced increased by a factor of five (from 3.0% to 16.2%) while the amount of alcohol increased by a factor of over two (from 2.3% to 5.4%). With $Mn^{2+}(dmp)_x$-Y as the catalyst, a four-fold increase in the amount of peroxide led to an increase in the amount of ketone produced by a factor of over four (from 4.2% to 18.0%) while the amount of alcohol produced increased by a factor of 1.3 (from 3.8% to 5.0%). This data suggests that the $Fe^{3+}(dmp)_x$-Y and $Mn^{2+}(dmp)_x$-Y catalysts in a system containing a 1:1 mole ratio of substrate to oxidant could lead to significant amounts of oxidation products at relatively low temperatures.

The next series of experiments were conducted using a 1:1 substrate to peroxide ratio in the absence of solvent at 50°C with 1.00 g of either $Fe^{3+}(dmp)_x$-Y

or $Mn^{2+}(dmp)_x$-Y as the catalyst. Product yields were based on the number of moles of product formed relative to the starting moles of cyclohexane. The variable in these studies was time in order to determine the amount of products in solution at various intervals between 0 and 96 hours of reaction time. The final peroxide concentration was determined by iodometric titration. The results are given in Table 3-6.

The $Fe^{3+}(dmp)_x$-Y and $Mn^{2+}(dmp)_x$-Y catalyzed reactions each showed the greatest amount of oxidation products formed within the first 24 hour period. Within this time, the $Fe^{3+}(dmp)_x$-Y catalyzed reaction led to a 10.8% and 6.2% yield of the ketone and alcohol, while the $Mn^{2+}(dmp)_x$-Y catalyzed reaction led to a 13.4 and 5.2% yield of the ketone and alcohol. Both zeolite catalysts appeared to reach a point after 72 hours where no further cyclohexanol or cyclohexanone products are formed. At 72 hours, the $Fe^{3+}(dmp)_x$-Y catalyzed reaction led to a 23.0% yield of the ketone and a 5.4% of the alcohol, while $Mn^{2+}(dmp)_x$-Y catalyzed reaction led to a 20.0 and 4.6% yield of the ketone and alcohol.

This may be due to a combination of oxidation products and water by-products of the reaction filling the interior of the zeolite, preventing access of the substrate to the metal complex or blocking egress from the zeolite of the products. Another possibility is that as the ketone and alcohol concentrations increase, they are oxidized preferentially to produce cleavage products and diacids. The cleavage products are not detected by GC. A steady state ketone and alcohol concentration results and

Table 3-6. Reaction Time Variation in Cyclohexane Oxidation at 50°C.

Catalyst	Rxn Time (hrs)	Final [ROOH] (M)	Products[a] (%) Cyclohexanone	Cyclohexanol
$Fe^{3+}(dmp)_x$-Y	0		0	0
	24		10.8	6.2
	48		16.2	5.4
	72		23.0	5.4
	96	1.8	23.0	5.4
$Mn^{2+}(dmp)_x$-Y	0		0	0
	24		13.4	5.2
	48		18.0	5.0
	72		20.0	4.6
	96	0.6	20.0	4.6

a: Based on starting moles of substrate.

Reaction conditions: (absence of solvent)
cyclohexane: 0.185 moles

peroxide: 0.185 moles (initial concentration: 4.5 M)

catalyst: 1.00 g (5.0×10^{-4} mol M^{n+})

reaction time: 48 hours

Reactions monitored by GC.

Reaction at 50°C.

cleavage products are formed. The overall effect is that oxidation continues but there is no net change in the concentration of ketone and alcohol.

Both of these catalyzed reactions begin with an initial t-ButOOH concentration of 4.5 M determined by iodometric titration. After 72 hours of reaction time, the peroxide concentration of the $Fe^{3+}(dmp)_x$-Y catalyzed reaction was found to be 1.8 M, while the peroxide concentration of the $Mn^{2+}(dmp)_x$-Y catalyzed reaction was found to be 0.60 M. A mole of peroxide is required to form a mole of alcohol, while two moles of peroxide are required to form a mole of ketone. Based on this and the peroxide concentrations, the $Fe^{3+}(dmp)_x$-Y catalyst appears to have a higher efficiency based on hydroperoxide utilization than $Mn^{2+}(dmp)_x$-Y. $Fe^{3+}(dmp)_x$-Y had an 89% peroxide efficiency, while $Mn^{2+}(dmp)_x$-Y had a 57% peroxide efficiency.

$Fe^{3+}(dmp)_x$-Y and $Mn^{2+}(dmp)_x$-Y zeolite catalysts were also used with n-hexane as the substrate. In this case, the goal was to selectively oxidize the terminal carbon. This reaction had a 1:1 mole ratio of substrate to oxidant in the absence of solvent at 50°C with 1.00 gram of the zeolite catalyst ($5.0x10^{-4}$ moles M^{n+}). Product yields were based on starting moles of product relative to starting moles of substrate.

The results in Table 3-7 show that with both the $Fe^{3+}(dmp)_x$-Y and $Mn^{2+}(dmp)_x$-Y zeolite catalysts, over 25% of the n-hexane substrate was oxidized after 72 hours, the predominant products being 2- and 3-hexanone. Both catalysts yielded only trace amounts of 1-hexanol and no hexanal was observed.

The $Fe^{3+}(dmp)_x$-Y catalyst is more efficient than the $Mn^{2+}(dmp)_x$-Y catalyst based on hydroperoxide utilization. In this case, $Fe^{3+}(dmp)_x$-Y had a 95% peroxide

Table 3-7. n-Hexane Oxidation Using t-ButOOH at 50°C.

Catalyst	Products[a] (%)
$Fe^{3+}(dmp)_x$-Y	1-hexanol (<1)
	2-hexanol (1.9)
	3-hexanol (2.6)
	2-hexanone (11.3)
	3-hexanone (10.5)
$Mn^{2+}(dmp)_x$-Y	1-hexanol (<1)
	2-hexanol (1.5)
	3-hexanol (2.0)
	2-hexanone (11.3)
	3-hexanone (11.0)

a: Based on starting moles of substrate.

Reaction conditions: (absence of solvent)

n-hexane: 0.185 moles

peroxide: 0.185 moles

catalyst: 1.00 g (5.0×10^{-4} mol M^{n+})

reaction time: 48 hours

Reactions monitored by GC.

Reaction at 50°C.

efficiency, while $Mn^{2+}(dmp)_x$-Y had a 63% peroxide efficiency. In the $Fe^{3+}(dmp)_x$-Y catalyzed reaction, nearly six times as much 2-one is produced as 2-ol (11.3% 2-one, 1.9% 2-ol), while four times as much 3-one is produced in comparison to the 3-ol (10.5% yield for the 3-one, 2.6% yield for the 3-ol). In the $Mn^{2+}(dmp)_x$-Y catalyzed reaction, nearly eight times as much 2-one is produced compared to 2-ol (11.3% 2-one, 1.5% 2-ol), while nearly six times as much 3-one is produced in comparison to the 3-ol (11.0% yield for the 3-one, 2.0% yield for the 3-ol).

The results for $Fe^{3+}(dmp)_x$-Y and $Mn^{2+}(dmp)_x$-Y do not demonstrate the oxidative regioselectivity exhibited by Fe(II)Pc in zeolite Y from Herron and co-worker's work.[149] In those studies, Herron reported regioselective oxidation of n-octane at the 2-position. In these studies, the majority of the zeolite α-cage was occupied by the FePc complex, with the substrate having limited accessibility to the active site. In the case of the encapsulated metal-dmp complexes, the results suggest that there is enough free space to allow rotation of the alkane in the pore (7 Å pore openings, 13 Å pore diameter). The active site is then accessible to all the carbon positions. This would allow for the reaction to proceed through the lowest energy intermediate and would account for the highest amount of oxidation products occurring at the 3-position.

With the success demonstrated using $Fe^{3+}(dmp)_x$-Y and $Mn^{2+}(dmp)_x$-Y as catalysts, the study was extended to include cobalt, ruthenium, and vanadium. All of these metals are known to be very effective catalysts for the decomposition of alkyl hydroperoxides. Extensive work has been done by Mimoun and co-workers in the

area of hydrocarbon hydroxylation by first row transition metal alkyl-peroxides.[156-157] Two of the systems studied by Mimoun involved cobalt(III) alkylperoxy complexes, vanadium(V) peroxo and vanadium(V) alkylperoxy complexes. The oxidation of saturated hydrocarbons utilizing t-ButOOH has been reported to be catalyzed by several cis-$[Ru^{II}(L)_2(OH_2)_2]^{2+}$ complexes,[158] (L= substituted 2,2'-bipyridine or 1,10-phenanthroline).

The results for the studies performed with cobalt, vanadium and ruthenium catalysts are seen in Table 3-8. Reactions were run at 50°C for 48 hours using a 1:1 mole ratio of cyclohexane to t-ButOOH in the absence of solvent. In each case, 1.00 g of zeolite catalyst was used (5.00×10^{-4} moles of M^{n+}). With Co^{2+}-Y as the catalyst, there was a 6.5% yield of the ketone and a 7.0% yield of alcohol. This represented the first time that the alcohol yield was greater than the ketone yield. When the catalyst was changed to $Co^{2+}(dmp)_x$-Y, there was an 11.1% yield of the ketone and 7.0% yield of the alcohol.

The next system studied utilized the vanadyl cation as the catalyst. With $V(O)^{2+}$-Y as the catalyst, there was a 15.5% yield of the ketone, and a 4.8% yield of the alcohol. When $V(O)^{2+}(dmp)_x$-Y was used as the catalyst, there was a 21.8% yield of the ketone and a 2.6% yield of the alcohol. Again, introduction of the dmp ligand caused an increase in the amount of ketone. With $V(O)^{2+}$-Y as the catalyst, the ketone to alcohol ratio was 3.2, while with $V(O)^{2+}(dmp)_x$-Y as the catalyst the ratio was 8.4. This suggests that the presence of the dmp ligand somehow facilitates overoxidation of the alcohol to the ketone.

Table 3-8. Catalyst Variation for Cyclohexane Oxidation.

	Products[a] (%)	
Catalyst	Cyclohexanone	Cyclohexanol
none	--	--
NaY	--	--
Co^{2+}-Y	6.5	7.0
$Co^{2+}(dmp)_x$-Y	11.1	7.0
$V(O)^{2+}$-Y	15.5	4.8
$V(O)^{2+}(dmp)_x$-Y	21.8	2.6
$Ru(NH_3)_6^{3+}$-Y	7.4	7.0
Ru(dmp)-Y(1)	15.0	6.0
Ru(dmp)-Y(2)[b]	13.4	12.2

a: Based on starting moles of substrate.

b: 0.50 g of zeolite catalyst reused from Ru(dmp)-Y(1)

Reaction conditions: (absence of solvent)

cyclohexane: 0.185 moles

peroxide: 0.185 moles

catalyst: 1.00 g (5.0×10^{-4} mol M^{n+})

reaction time: 48 hours

Reactions monitored by GC.

Reaction at 50°C.

The third and final system used ruthenium as the metal catalyst. Ru^{3+} was exchanged into NaY as $Ru(NH_3)_6^{3+}$ so as to prevent polymerization of ruthenium within the zeolite and to prevent Ru^{3+} replacing Al^{3+} in the zeolite framework. Attempts were made in this study to form $Ru(dmp)_2^{2+}$ complexes within NaY.

The preparation of Ru(dmp)-Y was similar to that used by Lunsford for formation of $Ru(bpy)_3^{3+}$ within the α-cages of zeolite Y.[159] The dmp ligand was added to the $Ru(NH_3)_6^{3+}$-Y using absolute ethanol by slurrying the solution with the solid for 24 hours. Solvent was removed by vacuum. The reaction vessel was purged with N_2, then sealed and heated to 180°C for 24 hours. The reaction is believed to occur as shown in Equation 3-13:

$$6[Ru(NH_3)_6]^{3+} + 2dmp \xrightarrow{180^oC} 6[Ru(dmp)_2]^{2+} + N_2 + NH_3 + 6NH_4^+ \quad (3\text{-}13)$$

This reaction is expected, especially in view of the observations reported by Lunsford[160] that $[Ru(NH_3)_6]^{3+}$-Y zeolites undergo self-reduction in the absence of O_2 with concomitant formation of N_2.

The orange Ru(dmp)-Y solid prepared here was thought to be Ru^{2+}. Quayle and Lunsford[160] and Maruszewski et al.[154] both reported that ruthenium(II)-bipyridine complexes were orange in color, while the ruthenium(III) complexes were green. The UV/visible spectrum for the Ru(dmp)-Y sample is seen in Figure 3-6. This spectrum does not identically match up with $Ru(dmp)_2(H_2O)_2$ which according to Goldstein[161] had two absorption bands at 496 and 412 nm and is colored purple.

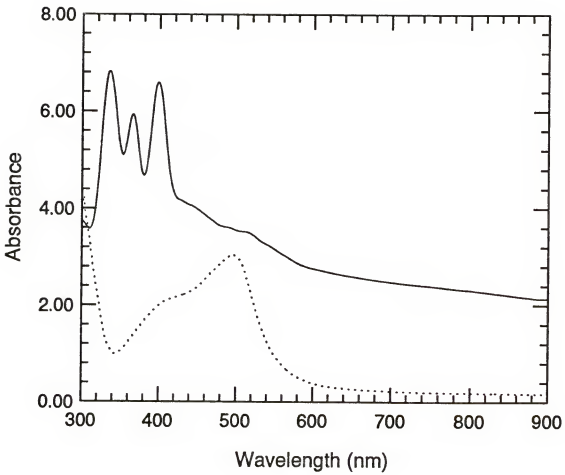

Figure 3-6. UV/Visible Spectra for $Ru(dmp)_2(H_2O)_2$ (dots) and Ru(dmp)-Y (solid).

Ru(dmp)-Y has a shoulder at 490 nm and an absorption band at 410 nm. Meyers[162] reported that the orange complex $(bpy)_2(py)Ru(OH_2)^{2+}$ in 1 M $HClO_4$ gave an absorption spectrum with bands at 470, 335, 290, and 243 nm. This would be similar to what is seen with Ru(dmp)-Y with bands at 410, 360, 336, and a shoulder at 273 nm.

Based on the ligand used, a $Ru(dmp)_3^{2+}$ is not possible due to the steric repulsions that would result from the methyl groups. Because the $Ru(dmp)_2^{2+}$ complex is a dark purple color, the only explanation is that the complex must be a mono Ru^{2+}(dmp) species with zeolitic oxygens occupying coordination sites.

When 1.00 g of the Ru(dmp)-Y catalyst (denoted Ru(dmp)-Y(1) in Table 3-8) was added to cyclohexane and t-ButOOH and heated to 50°C, after 48 hours 21% of the cyclohexane had been converted to products: 15% as the ketone, and 6.0% as the alcohol. When the reaction was terminated, the Ru(dmp)-Y catalyst was collected and washed with cyclohexane and then water, then dried. A 0.50 g sample of this used catalyst was run in a new reaction. These results are seen in Table 3-8 under Ru(dmp)-Y(2). After 48 hours, over 26% of the cyclohexane had been converted to product. This experiment demonstrated that the catalyst could be reused and that by decreasing the amount of catalyst by half the amount of cyclohexanol doubled. This data suggested that cyclohexanol was being overoxidized to the ketone in the presence of 5.0×10^{-4} moles of the ruthenium catalyst in the absence of solvent.

The peroxide efficiencies for the oxidation reactions involving $V(O)^{2+}$-Y and Ru(dmp)-Y were determined by iodometric titration. In each of these cases, the initial peroxide concentration was 4.5 M. After 48 hours reaction time, the $V(O)^{2+}$-Y catalyzed reaction had a final peroxide concentration of 1.7 M. Based on this and the products obtained, this reaction had a peroxide efficiency of 84%. The Ru(dmp)-Y catalyzed reaction had a final peroxide concentration of 0.8 M, and a peroxide efficiency of 54%. The Ru(dmp)-Y catalyst was perhaps one of the best catalysts in terms of products, but was lacking in terms of peroxide efficiency.

Oxidation of Cyclohexane at 50° C Using Mordenite

The study performed with Fe^{3+}-mordenite was extended to include cobalt and vanadium. Reactions were run at 50°C for 48 hours using a 1:1 mole ratio of cyclohexane to t-ButOOH in the absence of solvent. In each case, 1.00 g of zeolite catalyst was used (1.00×10^{-5} moles of M^{n+}). Product yields were based on moles of product formed relative to starting moles of cyclohexane. These results are seen in Table 3-9. Also included for comparison are the results obtained previously using Fe^{3+}-mordenite.

With Mn^{2+} as the catalyst, product yields were found to be 3.3% for the ketone and 1.0% for the alcohol. This catalyst stem gave the lowest product yields of any study using mordenite. $V(O)^{2+}$-mordenite product yields were found

Table 3-9. Cyclohexane Oxidation Using Metal Doped Mordenite.

	Products[a] (%)	
Catalyst	Cyclohexanone	Cyclohexanol
Fe^{3+}-Mord	9.4	4.1
Co^{2+}-Mord	6.0	4.2
$V(O)^{2+}$-Mord	9.0	7.8
Mn^{2+}-Mord	3.3	1.0

a: Based on starting moles of substrate.

Reaction conditions: (absence of solvent)

cyclohexane: 0.185 moles

peroxide: 0.185 moles

catalyst: 1.00 g ($1.0x10^{-5}$ mol M^{n+})

reaction time: 48 hours

Reactions monitored by GC.

Reaction at 50°C.

to be 9.0% to the ketone and 7.8% to the alcohol. The alcohol to ketone ratio of nearly one was very encouraging, while the total product yields were comparable to Fe^{3+}-mordenite. Co^{2+}-mordenite as the catalyst gave product yields found to be 6.0% to the ketone and 4.2% to the alcohol. Based on peroxide efficiency, the best catalyst system was Mn^{2+}-mordenite with a peroxide efficiency at 90%, while $V(O)^{2+}$-mordenite was the least efficient, with a peroxide efficiency of 79%.

Analysis for Cleavage Products

After establishing that these heterogeneous materials would catalyze the oxidation of cyclohexane, it became necessary to identify any cleavage products. Many times, as mentioned earlier in this chapter, catalytic decomposition of alkyl hydroperoxides is not selective to specific products. Overoxidation to undesired products usually results. For this reason, samples were submitted for independent analysis to Monsanto Fiber Technology. Cyclohexane oxidation reactions were catalyzed by Co^{2+}-Y, $Co^{2+}(dmp)_x$-Y, $V(O)^{2+}$-Y, and Ru(dmp)-Y with the reaction solutions after removal of the catalysts being submitted for analysis. Reactions were carried out using a 1:1 mole ratio of cyclohexane and t-ButOOH in the absence of solvent at 50°C. Reaction time was 48 hours.

Based on the data obtained, these zeolite catalysts appear to be selective to four products: cyclohexanol, cyclohexanone, cyclohexyl hydroperoxide, and adipic acid.

The results for each catalyst are given in terms of the percent conversion to adipic acid and cyclohexyl hydroperoxide. The results are summarized in Table 3-10.

With Ru(dmp)-Y, 0.2% of the cyclohexane was converted to cyclohexyl hydroperoxide and 0.7% to adipic acid. Based on these results coupled with the previous data, the Ru(dmp)-Y catalyst appears to be selective to the alcohol and ketone. With $V(O)^{2+}(dmp)_x$-Y as the catalyst, 6.9% of the cyclohexane was converted to adipic acid. The $Co^{2+}(dmp)_x$-Y catalyst system also had a significant amount of adipic acid formed with 3.7% of the cyclohexane being converted. The two cobalt catalysts give interesting results when compared to one another. The Co^{2+}-Y catalyzed reaction had 2.4% conversion to the hydroperoxide and 0.7% to adipic acid, with the $Co^{2+}(dmp)_x$-Y catalyzed reaction had 3.7% conversion to adipic acid and 0.9% conversion to the cyclohexyl hydroperoxide.

These results are significant and encouraging, but not unexpected. Homogeneous cobalt catalysts are typically used in industrial processes to catalyze the autoxidation of cyclohexane to the hydroperoxide. Patton[163] reported in the literature using Co-Y , N-methyl-2-pyrrolidinone (NMP), and molecular oxygen to form 5-hydroperoxy-1-methylpyrrolidin-2-one. The CoY eliminated the induction period in the autoxidation reaction and increased the hydroperoxide concentration relative to the uncatalyzed reaction.

The formation of adipic acid could be similar to what is seen when cobalt(II) octoate or cobalt(II) acetate are used in acetic acid to catalyze the conversion of cyclohexanone to adipic acid with molecular oxygen.[164] In the $Co^{2+}(dmp)_x$-Y case,

Table 3-10. Percent Conversion to Adipic Acid and Cyclohexyl Hydroperoxide.

	Co^{2+}-Y	$Co^{2+}(dmp)_x$-Y	$V(O)^{2+}(dmp)_x$-Y	Ru(dmp)-Y
adipic acid	0.7	3.7	6.9	0.7
CyOOH	2.4	0.9	--	0.2

All numbers are percent conversions from cyclohexane.

CyOOH: cyclohexyl hydroperoxide

the cyclohexyl hydroperoxide could be formed and is quickly oxidized to the ketone. The ketone reacts with $Co^{2+}(dmp)_x$-Y in the presence of the peroxide to yield adipic acid. This would account for the low amounts of cyclohexyl hydroperoxide seen also.

The fact that $V(O)^{2+}(dmp)_x$-Y produced significant amount of adipic acid (6.9% conversion) is very similar to what is observed in homogeneous solution. One of the ways that adipic acid is produced from cyclohexanol is through oxidation using nitric acid.[165] This reaction is typically catalyzed using vanadium(V) and copper(II) ions. In the uncatalyzed reaction, the major products are glutaric and succinic acid. Upon addition of the vanadium(V) and copper(II), the reaction is selective to adipic acid.

The advantages of forming adipic acid with $V(O)^{2+}(dmp)_x$-Y or $Co^{2+}(dmp)_x$-Y are that the catalyst is easily removed from the reaction. Furthermore, the reaction does not require corrosive acids such as nitric or acetic acid. Finally, the reaction conditions using these catalysts are much less severe than current processes for adipic acid production.

Autoxidation Reactions

The final studies with the zeolite catalysts were aimed at the autoxidation of hydrocarbons. Two substrates studied here were cumene and cyclohexane. Reactions were run with the neat substrate at 75°C under 50 psig of oxygen.

Using various zeolite catalysts, including $Fe^{3+}(dmp)_x$-Y, Co^{2+}-Y, $Co^{2+}(dmp)_x$-Y, and Ru(dmp)-Y attempts were made to autoxidize cyclohexane (see Table 3-11). No oxygen uptake, however, was observed after 72 hours and therefore no peroxide formed. Radical initiators were added to the cyclohexane to try and jump start the reaction. The catalysts used were Fe^{3+}-Y, Co^{2+}-Y, and $Co^{2+}(dmp)_x$-Y, with the radical initiator being 1 mL of acetaldehyde. Again, no oxygen uptake and no peroxide formation were observed after 72 hours. N-Methylpyrrolidinone (NMP), is both a radical initiator and hydroperoxide former.

In the third series of runs, with Co^{2+}-Y and $Co^{2+}(dmp)_x$-Y as the catalysts, 5 mL of NMP were added to the system. In the case of both catalysts, there was an initial oxygen pickup noted in the first 24 hours. However, no peroxide formation was noted by iodometric titration and no oxidation products were detected by GC. The NMP is most likely responsible for the initial oxygen pickup. The NMP does not initiate the autoxidation of cyclohexane.

Cumene was the next substrate studied. It is known to form cumene hydroperoxide at 50 psig and 75°C. This was confirmed by running a blank for 96 hours (see Table 3-12). Catalysis of cumene autoxidation was attempted using Co^{2+}-Y and Fe^{3+}-Y. In both cases, there was oxygen uptake, but no peroxide was noted by iodometric titration after 96 hours of reaction time. The oxygen uptake of the blank was significantly greater than the zeolite catalyzed reactions. The data suggest that Fe^{3+}-Y and Co^{2+}-Y are both decomposing cumene hydroperoxide.

Table 3-11. Autoxidation of Cyclohexane.

Catalyst	Initiator	Results
Fe^{3+}-Y	--	no O_2 pickup no peroxide
$Fe^{3+}(dmp)_x$-Y	--	no O_2 pickup no peroxide
Co^{2+}-Y	--	no O_2 pickup no peroxide
$Co^{2+}(dmp)_x$-Y	--	no O_2 pickup no peroxide
Ru(dmp)-Y	--	no O_2 pickup no peroxide
Co^{2+}-Y	CH_3CHO[a]	no O_2 pickup no peroxide
$Co^{2+}(dmp)_x$-Y	CH_3CHO	no O_2 pickup no peroxide
Fe^{3+}-Y	CH_3CHO	no O_2 pickup no peroxide
Co^{2+}-Y	NMP[b]	no peroxide
$Co^{2+}(dmp)_x$-Y	NMP	no peroxide

a: 1 mL
b: 5 mL

Reaction conditions: (absence of solvent)
cyclohexane: 0.453 moles (50 mL)
catalyst: 1.00 g (1.0×10^{-5} mol M^{n+})
reaction time: 72 hours

Reactions monitored by GC and iodometric titration.

Reaction at 75°C, 50 psig (3 atm) O_2.

Table 3-12. Autoxidation of Cumene.

Catalyst	Results
none	12 hrs- 0.03 M
	24hrs- 0.19 M
	48 hrs-0.62 M
	72 hrs- 0.95 M
	96 hrs- 1.22 M
Co^{2+}-Y	no peroxide formed
Fe^{3+}-Y	no peroxide formed

Reaction conditions: (absence of solvent)
cumene: 0.453 moles (65 mL)
catalyst: 1.00 g (5.0×10^{-4} mol M^{n+})
reaction time: 72 hours

Reactions monitored by GC and iodometric titration.

Reaction at 75°C, 50 psig (3 atm) O_2

The zeolite catalysts in this study including Fe3+-HSY, Fe3+-ZSM-5, Mn+-mordenite, Mn+-Y and Mn+(dmp)x-Y ($M^{n+} = Fe^{3+}, Mn^{2+}, V(O)^{2+}, Ru^{2+}$, (as well as Ru^{3+}), and Co^{2+}) favor the formation of ketone in the oxidation of cyclohexane with t-ButOOH in the absence of solvent at 50°C. This tendency toward forming the ketone is increased as reaction time increases and as the amount of t-ButOOH increases. Compared to analogous homogeneous reactions, the product yields are nearly identical, but reaction rates are greater for the zeolite catalyst example.

Saussine et al.[156] reported yields comparable to those seen in this work using macrocyclic cobalt(III) complexes with t-ButOOH in the absence of solvent to oxidize cyclohexane at 60°C. The reaction time was two hours, whereas the reaction time in this work was two days. This is to be expected for the heterogeneous system due to diffusion control limits within the zeolitic pore system. The zeolite catalyst has the added advantage of easy removal from the system for reuse.

The mechanism to account for the formation of the ketone with the $M^{n+}(dmp)_x$-Y catalysts is similar to the mechanism proposed by Mimoun[156] in the work previously mentioned. It explains the formation of the ketone as the major product and is shown in Figure 3-7.

The key is step B where the metal-dmp complex coordinates with the t-ButOO• radical. In step C, active catalytic species, $Z\text{-}(dmp)_xM^{n+}\text{-}O•$ is formed producing a t-ButO• radical. As seen in D and E, there is hydrogen atom

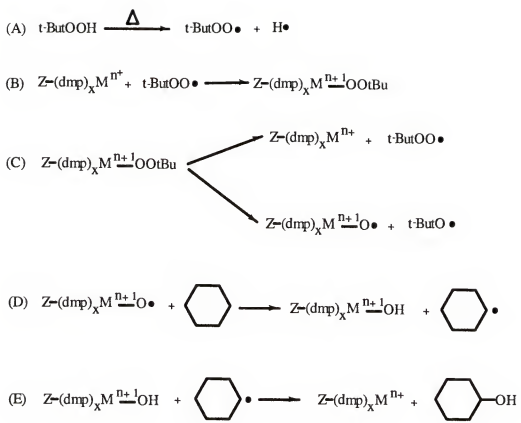

Figure 3-7. Cyclohexane Oxidation Mechanism Using Zeolite Catalysts.

abstraction from the substrate followed by coupling of the radical formed to yield the starting form of the catalyst and cyclohexanol. In step C, t-ButOO• radicals are generated after interaction with the zeolite encapsulated metal-complex. Large amounts of ketone are formed because the zeolite pores can concentrate t-ButO• and t-ButOO• radicals in the presence of the catalyst. This concentration effect tends to overoxidize the alcohol when formed to the ketone.

This mechanism is valid for M^{n+} where $M^{n+} = Co^{2+}$, Mn^{2+}, V^{4+}, and Ru^{3+} where one electron cycling would be possible. However, it is presently unclear whether it is valid whether this would be applicable to Ru^{2+}. This would involve a two electron reaction to achieve the Ru^{4+} oxidation state.

With $V(O)^{2+}(dmp)_x$-Y, $Co^{2+}(dmp)_x$-Y, Co^{2+}-Y, and $Ru(dmp)_x$-Y as the catalyst in the oxidation of cyclohexane using t-ButOOH in the absence of solvent at 50°C, selectivity to adipic acid as the cleavage product was observed. Of these catalysts, $V(O)^{2+}(dmp)_x$-Y and $Co^{2+}(dmp)_x$-Y had the largest yields. With further study and optimization of these catalysts, they could become industrially significant.

Autoxidation of cyclohexane using M^{n+}-Y and $M^{n+}(dmp)_x$-Y catalysts at 75°C and 50 psig of oxygen does not result in the formation of peroxide or in oxidation products. Oxygen does not appear to be a strong enough oxidant to oxidize the zeolite encapsulated metal or metal-complexes. Furthermore, these zeolite encapsulated transition metal complexes do not activate oxygen toward hydrogen atom abstraction from cyclohexane.

CHAPTER 4
CONCLUSIONS

A cobalt(II)-cyanide complex inside zeolite Y which has been identified by IR and EPR spectroscopy as $Co(CN)_5^{3-}$ has been prepared by reacting CsCoY and NaCN or KCN with methanol, water, CH_3CN or DMF as the solvent. This material has a high affinity for reversibly binding oxygen.

Solvent plays a vital role in determining the concentration of active cobalt(II)-cyanide complexes inside zeolite Y. When protic solvents such as water or methanol are used low concentrations of active cobalt complex result. This research has shown that using aprotic solvents is vital to forming large concentrations of active complex. Aprotic solvents should be used both in the zeolite metal exchanges and in the cyanide addition step. The $Co(CN)_5^{3-}$ complexes prepared in aprotic solvents have been shown to reversibly bind oxygen over many cycles. These samples are typically deoxygenated at 300°C under vacuum for one hour to remove the oxygen. Temperature studies have shown that the complexes are stabile to deoxygenation under vacuum at temperatures between 300-325°C.

Based on this research, to obtain the maximum amount of active cobalt complexes, the cyanide reaction should be performed in DMF using KCN as the salt. The zeolite should contain 8 Co^{2+} per unit cell and 24 Cs^+ per unit cell. The CsCoY material should be prepared by first exchanging in Cs^+ using the chloride salt

in aqueous solution, followed by extensive drying in a tube furnace to remove water. Then Co^{2+} addition is performed using CH_3CN or other aprotic solvents. The final purple solid should be reacted with a 10:1 mole ratio of cyanide to cobalt using DMF as the solvent at 130°C. A material using this preparation was found to chemisorb 5.12 cc O_2/g of material with an equilibrium constant for oxygen binding of 93.5 $torr^{-1}$.

Hydrogenation of the zeolite encapsulated cobalt(II)-cyanide complexes at elevated temperatures caused a significant increase in the amount of oxygen chemisorbed. However, not all of the oxygen chemisorbed was regenerable. Only after rehydrogenating at elevated temperatures did the material (prepared in CH_3CN) show enhanced affinity. It was experimentally shown that the material would eventually become inactive because cyanide was being removed from the zeolite as HCN. This hydrogenation process was determined to be interesting but not the answer to a high chemisorption material capable of continuous recycling.

Zeolite encapsulated transition metals and transition metal-dmp complexes were used as catalysts in the oxidation of cyclohexane at 50°C using t-ButOOH in the absence of solvent. Zeolite Y, high silica Y, ZSM-5, and large pore mordenite each were used in this study. The metals studied included: Mn^{2+}, Fe^{3+} V^{4+}, and Ru^{2+} (and Ru^{3+}). These catalysts are selective to cyclohexanone, cyclohexanol, cyclohexyl hydroperoxide, and adipic acid. The major product based on yields is cyclohexanone. The proposed mechanism suggests that the product alcohol is formed and then is

oxidizied further. The zeolite tends to concentrate the active t-butyl hydroperoxy radical in the pores leading to overoxidation and formation of the ketone.

Cyclohexane oxidation catalyzed by $Co^{2+}(dmp)_x$-Y and $V(O)^{2+}(dmp)_x$-Y both showed significant amount of adipic acid formed. With further studies and optimization, these catalysts could become significant industrially.

BIBLIOGRAPHY

1. Lee, H., in "Molecular Sieves," Meier, W. M. and Uytterhoeven, J. B., eds, Advances in Chemistry Series 121, American Chemical Society, Washington, DC 1973, p. 311.

2. Scherzer, J., "Octane Enhancing Zeolite FCC Catalysts," Marcel Dekker, Inc., New York, 1990.

3. Cronstedt, A. F., Akad. Handl. Stockholm, 1756, 18, 120.

4. Sand, L. B. and Mumpton, F. A., eds. "Natural Zeolites: Occurrence, Properties, and Uses," Pergamon Press, Oxford, 1978.

5. Bibby, D. M., Chang, C. D., Howe, R. F., and Yurchaki, S., eds. "Methane Conversion," Elsevier Science Publishers, Amsterdam, 1988.

6. Breck, D. W., "Zeolite Molecular Sieves," John Wiley and Sons, New York, 1974.

7. Deyer, A., "Introduction to Zeolite Molecular Sieves," John Wiley and Sons, New York, 1988.

8. Barrer, R. M., J. Chem. Soc., 1948, 2158.

9. Barrer, R. M., Discuss. Faraday Soc., 1944, 40, 206.

10. Barrer, R. M. and Ibbitson, D. A., Trans. Faraday Soc., 1944, 40, 195.

11. Breck, D. W., Eversole, W. G., and Milton, R. M., J. Amer. Chem. Soc., 1956, 78, 2338.

12. Milton, R. M., U.S. Patent 2882243 and 2882244, April 14, 1959.

13. Newsam, J. M., Science, 1986, 231, 1093.

14. Szostak, R., "Molecular Sieves: Principles of Synthesis and Identification," Van Nostrand Reinhold, New York, 1989.

15. Meier, W. M. and Olson, D. J., "Atlas of Zeolite Structure Types," Butterworth Scientific, Ltd., New York, 1988.

16. Lunsford, J. H., Rev. Inorg. Chem., 1987, 9, 1.

17. Sherry, H. S., Adv. Chem. Ser., 1971, 101, 350.

18. Lai, P. P. and Rees, L. C. V., Faraday Trans. I, 1976, 101, 350.

19. Greenwood, N. N. and Earnshaw, A., "Chemistry of the Elements," Pergamon Press, New York, 1984.

20. Heylin, M., ed. Chem. Eng. News, 1993, 71 (15), 10.

21. Heylin, M., ed. Chem. Eng. News, 1989, 67 (25), 38.

22. Isalski, W. H., "Separation of Gases," Clarendon Press, Oxford, 1989.

23. Stocchi, E., "Industrial Chemistry (vol. 1)," Ellis Horwood, New York, 1990.

24. Lee, B. S., "Synfuels from Coal," AIChE Series Volume 78, Number 14; American Institute of Chemical Engineers, New York, 1990.

25. White, H. L., "Introduction to Industrial Chemistry," John Wiley and Sons, New York, 1986.

26. Ozero, B. J. and Procelli, J. V., Hydrocarbon Process., 1984, 63 (3), 55-61.

27. Grayson, M. and Eckroth, D., eds. "Encyclopedia of Chemical Technology," Volume 9, John Wiley and Sons, New York, 1980.

28. De Maglie, B., Hydrocarbon Process., 1976, 55 (3), 78-81.

29. Gerhartz, W., ed. "Ulmann's Encyclopedia of Industrial Chemistry," Volume A10, VCH Publishers, New York, 1987.

30. Jira, R., Blau, W., and Grimm, D., Hydrocarbon Process., 1976, 55 (3), 97-100.

31. Petrochemical Handbook, Hydrocarbon Process., 1989, 68 (11), 90-115.

32. Wimwer, W. E. and Feathers, R. E., Hydrocarbon Process., 1976, 55 (3), 81-84.

33. Markeloff, R. G., Hydrocarbon Process., 1984, 63 (11), 91-94.

34. Veatch, F., Callahan, J. L., and Idol, J. D.; Chem. Eng. Prog., 1960, 56 (10), 65-67.

35. Petrochemical Handbook, Hydrocarbon Process., 1979, 58 (11), 124.

36. Petrochemical Handbook, Hydrocarbon Process., 1963, 42 (11), 138.

37. Stobaugh, R. B., Clark, S. G., and Camirand, G. D., Hydrocarbon Process.,1971, 50 (1), 109-113.

38. Pujado, P. R., Salazar, J. R., and Berger, C. V., Hydrocarbon Process., 1976, 55 (3), 91-96.

39. Chenier, P. J., "Survey of Industrial Chemistry," John Wiley and Sons, New York, 1986.

40. Speece, R. E. and Malina, J. V., "Applications of Molecular Oxygen to Water and Wastewater Systems," Center for Research in Water Resources, University of Texas at Austin, 1973.

41. Fresenius, W.; Schneider, W.; Bohnke, B.; and Poppinghaus, K.; eds."Wastewater Technology," Springer-Verlag, New York, 1991.

42. Samandi, G., Giles, K., and Fouhy, K., Chem. Eng., 1991, 98 (1), 37-43.

43. Roynoulik, S. K. and Brown, K. J., U.S. Patent 3832276, August 27, 1974.

44. Johnson, L. G., Chem. Eng., 1975, 82 (7), 66-70.

45. Basta, N., Kummant, I., Schabas, W., Frolich, G., Skole, R., and Tikkanen, T., Chem. Eng., 1984, 91 (10), 22-26.

46. Schelley, S., Chem. Eng., 1991, 98 (6), 30-39.

47. Schell, W. J., Hydrocarbon Process., 1983, 62 (8), 43-46.

48. Jenson, L. M., Chem. Eng., 1990, 97 (4), 37-43.

49. Rathbone, J., in "Gas Separation Technology;" Vansant, E. F. and Dewolfs, R., eds; Gas Separation Technology, Process Technology Proceedings No. 8, Elsevier Science Publishers B.V.; New York 1990; p. 149-160.

50. Barron, R. F., "Cryogenic Systems," Oxford University Press, New York, 1985.

51. Timmerhaus, K. D. and Flynn, L. M., "Cryogenic Process Engineering," Plenum Press, New York, 1989.

52. Yang, Ralph T., "Gas Separations by Adsorption Processes," Butterworth Publishers, New York, 1987.

53. Ausikaitis, J. P., Amer. Chem. Soc. Symp. Ser., 1977, 40, 681.

54. Stewart, H. A. and Heck, J. L., Chem. Eng. Prog., 1969, 65 (9), 78.

55. Symoniak, M. F., Hydrocarbon Process., 1980, 59 (11), 110.

56. Davis, John C., Chem. Eng., 1988, 95 (13), 26.

57. Ray, Martyn S., Sep. Science Tech., 1986, 21, 1.

58. Keller, George E. in "Industrial Gas Separations;"Comstock, M. Joan, ed; ACS Sympsium Series 223, ACS; Washington, D.C. 1983; p. 145-169.

59. Skarstrom, C. W., U.S. Patent 2944627, July 12, 1960.

60. Sircar, S., Sep. Science Tech., 1988, 23, 2379.

61. Knoblauch, K., Chem. Eng., 1978, 85 (25), 88.

62. Ruthven, D. M., Raghavan, N. S., and Hassan, M. M., Chem. Eng. Sci., 1986, 41, 1325.

63. Ruthven, D. M., Raghavan, N. S., and Hassan, M. M., Chem. Eng. Sci., 1987, 42, 2037.

64. Batta, L. B., U.S. Patent 3636679, January 25, 1972.

65. Sircar, S., U.S. Patent 4329158, May 11, 1982.

66. Sircar, S. and Kratz, W. C., Sep. Science Tech., 1989, 24, 429.

67. Martell, A. E., Acc. Chem. Res., 1982, 15, 155.

68. Lunsford, J. H. in "Molecular Sieves-II;" Katzer, J. R., ed.; American Chemical Society Symposium Series 40, American Chemical Society; Washington, DC 1977; p. 473.

69. Lunsford, J. H., Cat. Rev., 1975, 12, 137.

70. Woltermann, G. H. and Durante, V. A., Inorg. Chem., 1983, 22, 1954.

71. Ozin, G. A. and Gil, C., Chem. Rev., 1989, 89, 1749.

72. Seff, J., Acc. Chem. Res., 1976, 9, 121.

73. Herron, N., Inorg. Chem., 1986, 25, 4714.

74. Michalik, J., Narayana, M., and Kevan, L., J. Phys. Chem., 1984, 88, 5236.

75. Howe, R. F. and Lunsford, J. H., J. Phys. Chem., 1975, 79, 1836.

76. Vansant, E. F. and Lunsford, J. H., J. Chem. Soc., Fara. Trans., 1973, 69, 1028.

77. Howe, R. and Lunsford, J. H., J. Amer. Chem. Soc., 1975, 97, 5156.

78. Hoffman, B. M., Diemente, D. L., and Basolo, F., J. Amer. Chem. Soc., 1970, 92, 61.

79. Walker, F. A., J. Mag. Reson., 1974, 15, 201.

80. Bize, P. and DeVries, G., J. Chem. Soc., Dalton Trans., 1972, 303.

81. Imamura, S. and Lunsford, J. H., Langmuir, 1985, 1, 326.

82. Herron, N., Stucky, G. D., Tolman, C. A., Inorg. Chem. Acta, 1985, 100, 135.

83. Sharpe, A. G. "The Chemistry of Cyano Complexes of the Transition Metals," Academic Press, London, 1976, Chapter 8 and references therein.

84. Kwiatek, K., Catal. Rev., 1967, 1, 37.

85. Adamson, A. W., J. Amer. Chem. Soc., 1951, 73, 5710.

86. Bayston, J. H., Looney, F. D., and Winfield, M. E., Aust. J. Chem., 1963, 16, 557.

87. Brown, L. D. and Raymond, K. N., Inorg. Chem., 1975, 14, 2590.

88. Brown, L. D. and Raymond, K. N., Inorg. Chem., 1975, 14, 2595.

89. Drago, R. S., Bresinska, J., George, J. E., Balkus, K., Taylor, R. J., J. Amer.Chem. Soc., 1988, 110, 304.

90. Taylor, R. J., Drago, R. S., George, J. E., J. Amer. Chem. Soc., 1989, 111, 6610.

91. White, D. A., Solodar, A. J., Balzer, M .M., Inorg. Chem., 1972, 11, 2160.

92. Alexander, J. J. and Gray, H. B., J. Amer. Chem. Soc., 1967, 89, 3356.

93. Mizumo, K., Imamura, S., Lunsford, J. H., Inorg. Chem., 1984, 23, 3510.

94. Drago, R. S. and Corden, B. B., Acc. Chem. Res., 1980, 13, 353.

95. Wayland, B. B. and Abd-Elmageed, M. E., J. Amer. Chem. Soc., 1989, 111, 6610.

96. Booth, R. J. and and Lin, W. C., J. Chem. Phys., 1974, 61, 1226.

97. Taylor, R. J., Drago, R. S., and Hage, J. P., Inorg. Chem., 1992, 31, 253.

98. (a). Ward, J. W., J. Catal., 1970, 17, 355.
(b). Ward, J. W., J. Catal., 1972, 26, 470.
(c). Reschetilowski, W., Unger, B., Wendlandt, K. P., J. Chem. Soc., Fara. Trans. I, 1989. 85, 2941.
(d). Ozin, G. A., Ozkar, S., McMurray, L., J. Phys. Chem., 1990, 94, 8289.
(e). Ozin, G. A., Ozkar, S., McMurray, L., J. Phys. Chem., 1990, 94, 8297.

99. Cotton, F. A. and Wilkinson, G., "Advanced Inorganic Chemistry," John Wiley and Sons; New York, 1988.

100. Drago, R. S., Cannady, J. P., and Leslie, K. A., J. Amer. Chem. Soc., 1980, 102, 6014.

101. DeVries, B. J., J. Catal., 1962, 1, 489.

102. Roberts, H. L. and Symes, W. R., J. Chem. Soc. (A), 1968, 1450.

103. King, N.K. and Winfield, M. E., J. Amer. Chem. Soc., 1961, 83, 3363.

104. Carter, S. J., Foxman, B. M., Stuhl, L. S., J. Amer. Chem. Soc., 1984, 106, 265.

105. Carter, S. J., Foxman, B. M., Stuhl, L. S., Inorg. Chem., 1986, 25, 2888.

106. Ramprasad, D., Pez, G., Meier, I.K., US Patent, 5208335, May 4, 1993.

107. Jones, J. H., J. Chem. Phys., 1962, 36, 1204.

108. Swenson, B. I. and Jones, J. H., J. Chem. Phys., 1970, 53, 3761.

109. Banks, R. G. S. and Pratt, J. M., Chem. Commun., 1967, 776.

110. Shriver, D. and Brown, D. B., Inorg. Chem., 1968, 8, 42.

111. Simon, G. L., Adamson, A. W., Dohl, L. F., J. Amer. Chem. Soc., 1972, 94, 7654.

112. Haim, A. and Wilmarth, W. K., J. Amer. Chem. Soc., 1961, 83, 509.

113. Poskzozim, P. S., Inorg. Nucl. Chem. Lett., 1969, 5, 933.

114. Mosha, D. M. S. and Nicholls, D., Inorg. Chem. Acta, 1980, 38, 1980.

115. Nakamoto, Kazuo, "IR Spectra of Inorganic Coordination Compounds," John Wiley and Sons, Inc., 1963.

116. Gubelmann, M. H.,Ruttimann, S., Bocquet, B., and Williams, A. F., Helv. Chem. Acta, 1990, 73, 219.

117. Gerloch, M., "Magnetism and Ligand Field Analysis," Oxford University Press, Oxford, 1984.

118. (a) Pope, C. G. and Herd, A. C., Fara. Trans. I, 1973, 69, 833.
(b) Guilleux, M. F., Kermarec, M., and Delafosse, D., Chem. Commun., 1977, 102.

119. Sheldon, R. A. and Kochi, J. K., "Metal Catalyzed Oxidations of Organic Compounds," Academic Press, New York, 1981.

120. Criegee, R., Pilz, H., and Flygare, H., Chem. Ber., 1939, 72, 1799.

121. (a) Farmer, E. H., Sunndralingham, A., J. Chem. Soc., 1942, 121.
(b) Bolland, J. L., Q. Rev. Chem. Soc., 1949, 3, 1.
(c) Bateman, L., Q. Rev. Chem. Soc., 1954, 8, 147.
(d) Swern, D., Coleman, J. E., J. Am. Oil. Chem. Soc., 1955, 32, 700.
(e) Skellon, J. H., Chem. Ind. (London), 1951, 629; 1953, 1047.

122. Reich, L., Stivala, S. S., "Autoxidation of Hydrocarbons and Polyolefins-Kinetics and Mechanisms," Marcel Dekker, Inc., New York, 1969.

123. Benson, S. W., J. Amer. Chem. Soc., 1965, 87, 972.

124. (a) Ingold, K. U., Acct. Chem. Res., 1969, 2, 1.
(b) Barlett, P. D. and Traylor, T. G., J. Amer. Chem. Soc., 1963, 85, 2407.

125. Russell, G. A., J. Amer. Chem. Soc., 1957, 79, 3871.

126. Fenton, H. J. H., J. Chem. Soc., 1894, 65, 899.

127. Walling, C., Acct. Chem. Res., 1975, 8, 125.

128. Lee, W. A. and Bruice, L. C., J. Amer. Chem. Soc., 1985, 107, 513.

129. Yuan, L.-C. and Bruice, L. C., J. Amer. Chem. Soc., 1985, 107, 521.

130. Yuan, L.-C. and Bruice, L. C., Inorg. Chem., 1985, 24, 986.

131. Yuan, L.-C. and Bruice, L. C., Inorg. Chem., 1986, 25, 131.

132. Hill, C., ed., "Activation and Functionalization of Alkanes," John Wiley and Sons, New York, 1989.

133. Miller, S. A., Chem. Prog. Eng., 1969, 50 (6), 63.

134. Steeman, J. W. M., Kaarsemaker, S., and Hoftyzer, P. J., Chem. Eng. Sci., 1961, 14, 139.

135. Druliner, J. D., Ittel, S. D., Krusic, P. J., and Tolman, C. A., U.S. Patent 4326084, May 8, 1982.

136. Parshall, G. W., J. Mol. Catal., 1978, 4, 243.

137. Lindsay, A. F., Chem. Eng. Sci., 1954, 3 (1), 78.

138. Prengle, H. W. and Hatch, L. F., Hydrocarbon Process., 1970, 49 (3), 106.

139. Parlant, C., Seree de Roch, I., and Balanceanu, Bull. Soc. Chim. France, 1963, 11, 2452.

140. Onopchenko, A and Schulz, J. G. D., J. Org. Chem., 1973, 38, 3729.

141. Tanaka, K., Hydrocarbon Process., 1974, 53 (11), 114.

142. Tanaka, K., Chemtech, 1974, 4, 555.

143. Naacade, C. and Taarit, Y. B., Pure Appl. Chem., 1980, 52, 2175.

144. Jacobs, P. A., Chantillon, R., DeLaet, P., Verdonck, J., and Tielmem, M., ACS Symp. Ser., 1983, 218, 439.

145. Auroux, A., Bolis, V., Wierzchowski, P., Gravelle, P., and Vedrine, J., J. Chem. Soc., Fara. Trans., 2, 1979, 75, 2544.

146. Iwamoto, M., Kusano, H., and Kugawa, S., Inorg. Chem., 1983, 22, 3366.

147. White, R. E., Coon, M. J., Annu. Rev. Biochem., 1980, 49, 315.

148. Hamberg, M., Samuelsson, B., Bjorkhem, I., and Danielsson, N., "Molecular Mechanisms of Oxygen Activation," Haijaishi, O., ed., Academic Press: New York, 1974, p. 29.

149. Herron, N., Stuckey, G. D., and Tolman, C. A., J. Chem. Soc., Chem. Commun., 1986, 1521.

150. Herron, N., J. Coord. Chem., 1988, 19, 25.

151. Herron, N. and Tolman, C. A., J. Amer. Chem. Soc., 1987, 109, 2837.

152. Herron, N., New J. Chem., 1989, 13, 761.

153. Cook, B. R., Reinert, T. J., Suslick, K. S., J. Amer. Chem. Soc., 1986, 108, 7281.

154. Maruszewski, K., Strommen, D. P., Handrich, K., and Kincaid, J. R., Inorg. Chem., 1991, 30, 4579.

155. Sharpless, K. B., Gao, Y., Hanson, R. M., Klunder, J. M., Soo, Y. K., Masamune, H. J., J. Amer. Chem. Soc., 1987, 109, 5765.

156. Saussine, L., Brazi, E., Rabine, A., Mimoun, H., Fischer, J., and Weiss, R., J. Amer. Chem. Soc., 1985, 107, 3534.

157. Mimoun, H., Saussine, L., Daire, E., Pastel, M., Fischer, J., Weiss, R., J. Amer. Chem. Soc., 1983, 105, 3701.

158. Leung, L., James, B. R., and Dolhin, D., Inorg. Chem. Acta, 1983, 79, 180.

159. DeWilde, P. G., Lunsford, J. H., J. Phys. Chem., 1980, 84, 2306.

160. Quayle, W. H. and Lunsford, J. H., Inorg. Chem., 1982, 21, 97.

161. Goldstein, A., Ph. D. Dissertation, University of Florida, 1991.

162. Meyer, T. J. and Moyer, B. A., Inorg. Chem., 1981, 20, 436.

163. Patton, D. E. and Drago, R. S., Perkin Trans. I, 1993, 1611.

164. Rao, D. G. and Ragunathan, L. S., J. Chem. Tech. Biotechnol., 1984, 34A, 381.

165. Smith, L. and Richard, D. I., Thomas, D. I., Thomas, C. B., and Whittacker, M., Perkin Trans. II, 1985, 1677.

BIOGRAPHICAL SKETCH

John Phillip Hage was born in Orlando, Florida, on December 20, 1966, to Roxann and Thomas Hage. He is the eldest of five children, the eldest grandson of Helen and John Hage, and Alice and Phillip Grossi. He is also the eldest great grandson of Catherine Skaff who immigrated to the United States in 1919 from Hums, a suburb of Damascus, Syria.

He attended Bishop Moore High School and graduated in May of 1984, 2nd in his class of 150 students. In September, 1984, he entered Rollins College. He graduated summa cum laude with a Bachelor of Arts degree (chemistry) in May of 1988. He entered graduate school in chemistry at the University of Florida in August, 1988, working under Professor Russell S. Drago. In January, 1994, he will be working as a postdoctoral fellow at Texas A&M University in College Station, Texas, with Dr. Donald T. Sawyer.

I certify that I have read this study and that in my opinion it conforms to acceptable standards of scholarly presentation and is fully adequate, in scope and quality, as a dissertation for the degree of Doctor of Philosophy.

Russell S. Drago, Chairman
Graduate Research Professor of Chemistry

I certify that I have read this study and that in my opinion it conforms to acceptable standards of scholarly presentation and is fully adequate, in scope and quality, as a dissertation for the degree of Doctor of Philosophy.

Robert C. Stoufer
Associate Professor of Chemistry

I certify that I have read this study and that in my opinion it conforms to acceptable standards of scholarly presentation and is fully adequate, in scope and quality, as a dissertation for the degree of Doctor of Philosophy.

James M. Boncella
Associate Professor of Chemistry

I certify that I have read this study and that in my opinion it conforms to acceptable standards of scholarly presentation and is fully adequate, in scope and quality, as a dissertation for the degree of Doctor of Philosophy.

Martin T. Vala
Professor of Chemistry

I certify that I have read this study and that in my opinion it conforms to acceptable standards of scholarly presentation and is fully adequate, in scope and quality, as a dissertation for the degree of Doctor of Philosophy.

Ellsworth D. Whitney
Professor of Materials Science and Engineering

This dissertation was submitted to the Graduate Faculty of the College of Liberal Arts and Sciences and to the Graduate School and was accepted as partial fulfillment of the requirements for the degree of Doctor of Philosophy.

April, 1994

Dean, Graduate School